

Dissertation zur Erlangung des Doktorgrades
der Fakultät für Chemie und Pharmazie
der Ludwig-Maximilians-Universität München

**Biochemical studies of a *NOD2* sequence variant identified in a
patient with primary immunodeficiency**

Maryam Ghalandary

aus

Tehran, Iran

2021

Erklärung

Diese Dissertation wurde im Sinne von § 7 der Promotionsordnung vom 28. November 2011 von Herrn Prof. Dr. Christoph Klein betreut und von Herrn Prof. Dr. Horst Domdey von der Fakultät für Chemie und Pharmazie vertreten.

Eidesstattliche Versicherung

Diese Dissertation wurde eigenständig und ohne unerlaubte Hilfe erarbeitet.

München, den 03.05.2021

(Maryam Ghalandary)

Dissertation eingereicht am	03.05.2021
1. Gutachter:	Prof. Dr. Horst Domdey
2. Gutachter:	Prof. Dr. Christoph Klein
Mündliche Prüfung am	23.06.2021

Table of Contents

1. Introduction	1
1.1. The immune system	1
1.2. Pattern recognition receptors	1
1.3. NOD2 structure, expression and cellular localization.....	3
1.4. NOD2-mediated signaling.....	4
1.4.1 NOD2 peptidoglycan-dependent activation and signaling.....	4
1.4.2 NOD2 peptidoglycan-independent activation and signaling	7
1.6. Regulation of NOD2 signaling.....	9
1.7. <i>NOD2</i> mutations and Crohn's disease (CD)	10
1.8. NOD2 involvement in diseases other than CD	12
1.9. An introduction to the main NOD2 interacting proteins identified by immunoprecipitation-coupled mass spectrometry.....	13
1.9.1. VCP	13
1.9.2. ATAD3A	15
2. The aim of this study	17
3. Material and Methods.....	19
3.1. Materials.....	19
3.1.1. Chemicals and Reagents.....	19
3.1.2. Media and supplements	19
3.1.3. Plasmids	21
3.1.4. Cloning, mutagenesis and qPCR primers.....	23
3.1.5. siRNAs and sgRNA target sequences	26
3.1.6. Antibodies	26
3.1.7. Restriction enzymes	29
3.1.8. Buffers and solutions.....	30
3.2. Methods	31
3.2.1. Isolation of PBMCs and neutrophils	31
3.2.2. DNA sequencing	31
3.2.3. Molecular biology	32
3.2.4. Cell culture	40
3.2.5. Protein analysis	45
3.2.6. Flow Cytometry.....	49

3.2.7. Nano-LC MS/MS analysis	51
3.2.8. Statistics	52
4. Results	53
4.1. Identification of a patient with biallelic mutation in the first CARD domain of NOD2	53
4.2. Immunophenotyping of Peripheral Blood Mononuclear Cells revealed impaired B cell activation and proliferation in the index patient.....	54
4.3. Evaluating NOD2 mediated signaling in patient primary cells.....	57
4.3.1. Impaired L18-MDP-induced TNF α production in patient's PBMC-derived monocytes.....	57
4.3.2. Abrogated nuclear factor-kB (NF-kB) and mitogen-activated protein kinase (MAPK) signaling in patient 's primary cells upon stimulation with MDP	58
4.3.3. Impaired CD62L shedding on Patient's neutrophils upon MDP stimulation	59
4.4. Evaluating NOD2-mediated signaling in <i>NOD2</i> -deficient heterologous cell lines	60
4.4.1. Impaired NF-kB activity in HEK293T cells overexpressing mutant NOD2	60
4.4.2. Impaired NOD2-mediated signaling in colon carcinoma-derived HCT116 cells overexpressing E54K variant	61
4.5. Evaluating NOD2 interacting proteins	63
4.5.1. Impaired interaction of the NOD2 variant E54K with RIPK2.....	63
4.5.2. Abrogated RIPK2 ubiquitination in HCT116 cells overexpressing mutant NOD2 upon L18-MDP stimulation	64
4.5.3. Immunoprecipitation-coupled mass spectrometry unveiled novel NOD2-interacting proteins	65
4.5.4. Evaluating NOD2-mediated signaling in HCT116 cells with <i>ATAD3A</i> KO	67
4.5.5. Evaluating NOD2-mediated signaling in VCP knockdown HCT116 cells	70
5. Discussion	80
5.1. NOD2, a key player in intestinal homeostasis	80
5.2. Identification of biallelic missense mutation in <i>NOD2</i>	81
5.3. Characterization of a biallelic missense mutation in <i>NOD2</i>	82
5.3.1. PGN- dependent signaling	82
5.3.2. PGN-independent signaling	84
5.3.3 Investigating RIPK2 interaction and post-translational modification.....	85
5.4. Investigating interaction network of mutated NOD2 protein (E54K).....	86
5.5. The role of <i>ATAD3A</i> in the NOD2 signaling pathway	87
5.6. The role of VCP in NOD2 signaling pathway	89
5.7. Perspectives.....	92
6. Summary	94
7. References	96
8. List of Figures	111

9. List of Tables.....	114
10. Abbreviations	115

1. Introduction

1.1. The immune system

The immune system comprises a collection of cells and molecules that provide the host protection against infections. In vertebrates, the immune system can be classified into two different defense systems, innate immunity and adaptive immunity. As the first line of defense against pathogens, innate immunity is antigen-independent and recruits various means to respond rapidly to an intruding pathogen. The defensive barriers employed by the innate immune system to protect the host can be divided into four different types: anatomic, physiologic, phagocytic, and inflammatory barriers [1]. The immune responses mediated by the innate immune system have limited specificity with no immunological memory. However, innate immunity directs adaptive immune responses that are antigen-dependent and antigen-specific. Other features of adaptive immunity include the ability to recognize self from non-self and the establishment of immunological memory. Innate and adaptive immunity are complementary mechanisms and defects in either system may see the host prone to many diseases such as recurrent infections, autoimmunity, immunodeficiency disorders and hypersensitivity reactions [2].

1.2. Pattern recognition receptors

Pattern recognition receptors (PRRs) are specialized groups of proteins that recognize structurally conserved molecular patterns derived either from pathogens, referred to as pathogen-associated molecular patterns (PAMPs), or from damaged cells, known as damage-associated molecular patterns (DAMPs). PRRs enable the innate immune

system to recognize general microbial fingerprints and promote defense mechanisms [3]. According to the homology of protein domains, PRRs can be classified into five categories: Toll-like receptors (TLRs), C-type lectin receptors (CLRs), nucleotide-binding domain, leucine-rich repeat (LRR)-containing (or NOD-like) receptors (NLRs), RIG-I-like receptors (RLRs), and the AIM2-like receptors (ALRs) [4, 5].

PRR	Members	Localization
TLR	1-10 in human	Plasma membrane, endolysosome
CLR	Dectin-1, Dectin-2 and MNCLE	Plasma membrane
NLR	NOD1(NLRC1), NOD2(NLRC2), NLRC3-5, NLRP1-9 and 11-14, NAIP1, -2, -5, -6	Cytoplasm, Plasma and endosomal membrane
RLR	RIG-I, MDA5 and LGP2	Cytoplasm
ALR	AIM2 and IFI16	Cytoplasm, nucleus

Table 1-1 Pattern-recognition receptor families

PRRs are expressed predominantly by antigen-presenting cells such as macrophages and dendritic cells but expression by non-immune cells is also observed [3]. Innate immune responses triggered by PRRs can be classified as transcriptional responses, which lead to the transcription of proinflammatory cytokines, type I interferon (IFNs), chemokines and other proteins involved in inflammatory responses, or non-transcriptional responses such as induction of cell death, phagocytosis, cytokine processing and autophagy [6].

1.3. NOD2 structure, expression and cellular localization

Nucleotide-binding oligomerization domain 2 (NOD2) is an intracellular pattern recognition receptor that belongs to the NLR family of proteins [7-9]. NLR proteins composed of an N-terminal domain which varies between different proteins as the caspase recruitment domain (CARD), pyrin domain (PYD), acidic trans activating domain, or baculovirus inhibitor repeat (BIR); a nucleotide-binding oligomerization (NBD) domain located at the center of the protein and C-terminal leucine-rich repeats (LRR) [10]. After ligand detection by the LRR domain, the NBD module mediates self-oligomerization which induces protein-protein interaction through the CARD domain and generation of a complex referred to as Nodosome [11, 12]. NOD2 has two CARD domains that interact with downstream adaptor receptor-interacting protein 2 (RIPK2) through homotypic CARD–CARD interactions [13-16].

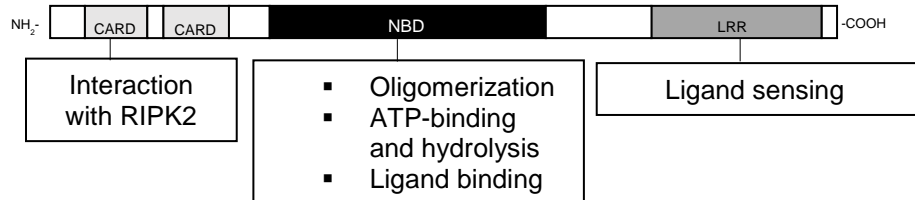


Figure 1-1 Schematic illustration of NOD2 protein domains. This model has been adapted from reference [17].

NOD2 is expressed in many types of both hematopoietic (T cells, B cells, neutrophils, macrophages, dendritic cells, mast cells) and non-hematopoietic cells such as Paneth cells, goblet cells, intestinal epithelial, and stem cells [18-27]. It has been reported that different stimuli including members of the tumor necrosis factor (TNF) family, interferon γ (IFN- γ), 1,25-dihydroxylvitamin D3, or butyrate can induce expression of NOD2 and increase response to muramyl dipeptide (MDP) treatment in intestinal epithelial cells

[28-30]. Accordingly, stimulation of macrophages with $\text{TNF}\alpha$, lipopolysaccharide (LPS), or type I IFN has been shown to increase NOD2 expression [31, 32].

NOD2 is a cytoplasmic protein lacking transmembrane domains, however, it has been shown that the NOD2 complex can be formed at the plasma membrane to detect invasive bacteria at their entry site and mediate activation of the NF- κ B pathway [33].

Correspondingly, Lipinski et al. have shown that NOD2 assembles into a complex with FRMPD2 and membrane-associated ERBB2IP proteins which mediates its localization to the basolateral compartment of polarized intestinal epithelial cells [34]. FRMPD2 is a scaffolding protein residing in the basolateral membrane of epithelia cells where it mediates basolateral targeting of peripheral proteins [35]. ERBB2IP (ERBIN) is a member of the LRR and PDZ domain family which has been previously reported as a negative regulator of the NOD2-induced NF- κ B signaling pathway [36].

1.4. NOD2-mediated signaling

1.4.1 NOD2 peptidoglycan-dependent activation and signaling

NOD2 senses muramyl dipeptide (MDP), a peptidoglycan (PGN) motif derived from the cell wall of both gram-positive and gram-negative bacteria [8]. As NOD2 is a cytosolic receptor and MDP is an extracellular bacterial component, several models have been proposed and documented for the mechanism by which MDP enters the cell; through phagocytosis of bacteria or through oligopeptide transporters like hPepT1, solute carrier family 15 member 3 (SLC15A3), and SLC15A4, bacterial secretion system, endocytosis, and PGN fragments from bacteria-derived OMVs (Figure 1-2) [37-41].

Upon MDP binding, NOD2 undergoes conformational changes leading to its self-oligomerization and recruitment of RIPK2. RIPK2 activation is marked by conjugation of K63- and M1-linked ubiquitin and autophosphorylation on Y474 [42-44]. Several E3 ubiquitin ligases have been reported to be involved in RIPK2 K63-polyubiquitination, including cellular inhibitor of apoptosis 1 (cIAP1), cIAP2, ITCH, Pellino3, and X-linked inhibitor of apoptosis protein (XIAP) [45-48]. M1- polyubiquitination is mediated by the linear ubiquitin chain assembly complex (LUBAC) [48].

K63- and M1-ubiquitinated RIPK2 serves as a platform to recruit and activate TAK1, TAB1, TAB2/3 [42, 43, 48, 49]. Activated TAK1 drives the I κ B kinase (IKK) complex and induces the MAPK pathway. The IKK complex subsequently phosphorylates NF- κ B inhibitor I κ B α leading to its proteasomal degradation and activation of the NF- κ B pathway [50]. Activated NF- κ B and MAPK signaling regulate the production of several proinflammatory cytokines such as TNF α , *IL6*, the neutrophil chemoattractant CXC-chemokine ligand 8 (CXCL8; also known as IL-8), and various antimicrobial components including defensins and mucins [17].

Prolonged stimulation with MDP has been reported to induce non-responsiveness. A possible mechanism for a putative negative regulatory pathway could be the ligand-stimulation-dependent degradation of NOD2 and RIPK2 [21, 51, 52]. However, the mechanism attenuating NOD2 signaling during both acute and chronic stimulation needs to be addressed in more detail in further studies.

In addition to triggering NF- κ B and MAPK pathways, NOD2 stimulation has been linked to autophagy and inflammasome activation through interaction with ATG16L1 and caspase-1 respectively [53, 54]. Autophagy is a bulk catabolic process for the

degradation of damaged organelles, long-lived proteins and/or intracellular pathogens. Stress conditions like nutritional starvation can trigger autophagy in which the cargo is sequestered into double-membraned compartments, known as autophagosome [55, 56]. NOD2 has been shown to target bacteria at the entry site to autophagy machinery through interaction with ATG16L1. The targeting function of NOD2 to deliver bacteria to the autophagy system has been reported to be RIPK2-independent [53]. However, NOD2 function in inducing the formation of autophagosomes in epithelial and dendritic cells has been shown to require RIPK2 as well as the autophagy-related proteins (ATG) 5, ATG7, and ATG16L1 [22].

The inflammasome is a multi-protein complex mediating activation of caspase1 that subsequently cleaves inactive precursors of IL-1 β and IL-18 [57]. Previous studies demonstrated that NOD2 functions in the regulation of transcription and activation of IL-1 β . Human mononuclear cells of patients with the NOD2 3020insC germline mutation showed decreased production of IL-1 β in response to MDP [58, 59]. Moreover, activated NOD2 forms a complex with NALP1 and caspase1 which leads to caspase1 activation [60].

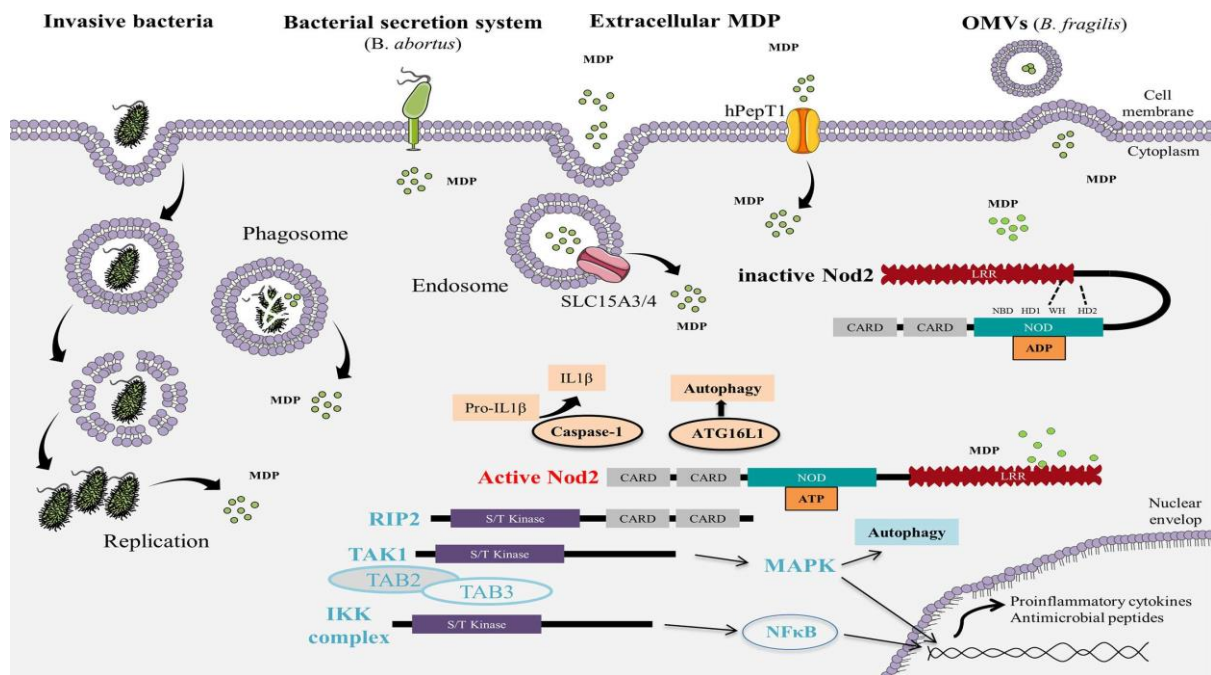


Figure 1-2 Mechanisms of bacterial recognition by NOD2 and downstream signaling. MDP can be internalized through several pathways including endocytosis, phagocytosis, transporters like hPrepT1, bacterial secretion system or can be released from outer membrane vesicle (OMVs). Upon MDP binding to LRR domain, NOD2 undergoes conformational changes and interacts with RIPK2. Subsequently, recruitment of TAK1, TAB2 and TAB3 to the complex leads to activation of NF- κ B and MAPK pathways and production of several proinflammatory cytokines and antimicrobial peptides. Emerging evidences linked NOD2 to autophagy and inflammasome activation through interaction with ATG16L1 and caspase-1, respectively (the scheme was published by Al Nabhani, Z., et al. 2017) [41].

1.4.2 NOD2 peptidoglycan-independent activation and signaling

In parallel to the recognition of bacterial PGN, some studies are suggesting that the NOD2 signaling pathway can be activated independent of PGN [61]. Murine NOD2 (Nod2) has been implicated in establishing immune responses against some ssRNA viruses such as respiratory syncytial virus, vesicular stomatitis virus, and influenza virus through interaction with Mitochondrial Antiviral Signaling (MAVS) protein [62]. This interaction leads to type I IFNs expression via activation of regulatory factor-3 (IRF3) [62].

Protozoan parasites are the second group of pathogens lacking PGN but are able to activate Murine NOD2 (Nod2) signaling however the exact underlying molecular mechanism is not clearly understood [63].

Recently, NOD2 has been shown to be involved in sensing endoplasmic reticulum (ER) stress and the establishment of proinflammatory responses [64]. The ER in eukaryotic cells is an organelle that regulates important cellular events such as calcium storage/release and translation of secretory and transmembrane proteins [65]. ER homeostasis is a result of the balance between ER protein load and the folding and processing of loaded proteins. Disturbance of this balance due to different physiological and pathological events trigger ER stress response, known as the unfolded protein response (UPR). Inositol-requiring enzyme 1 (IRE1 α), PKR-like ER kinase (PERK), and Activating Transcription Factor 6 (ATF6) are the key transmembrane proteins triggering UPR upon ER stress [66]. IRE1 α activation during ER stress leads to TRAF2-dependent activation of NOD2 and subsequently the NF- κ B pathway [64].

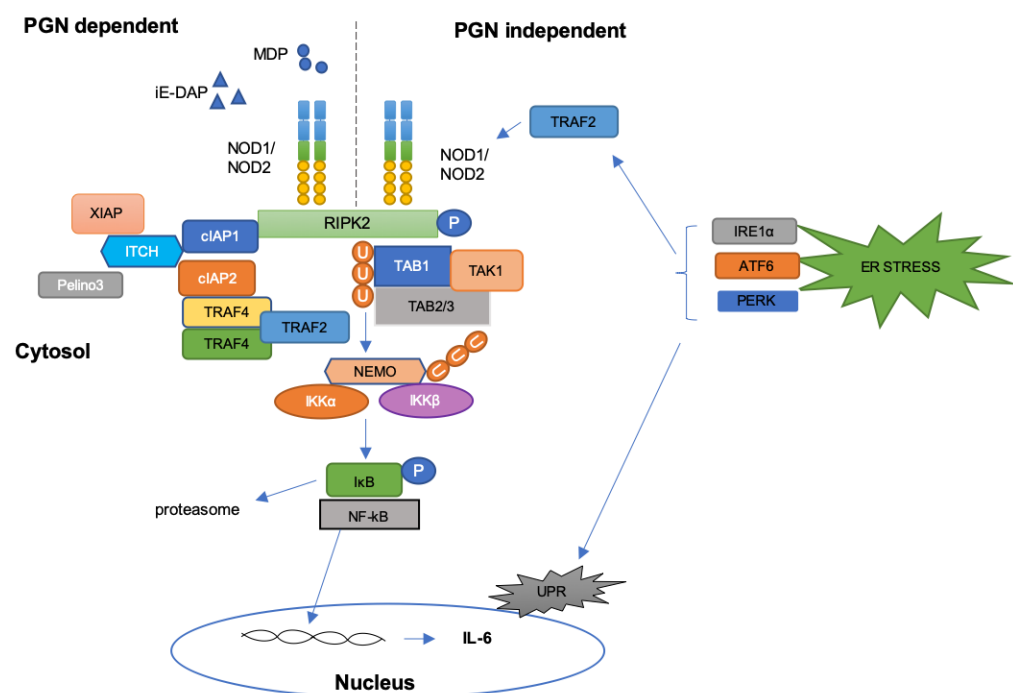


Figure 1-3 NOD1/NOD2-mediated signaling. Peptidoglycan-dependent signaling of NOD1/NOD2 leads to NF- κ B activation. However, ER stress has been demonstrated to induce NOD1/NOD2 signaling and proinflammatory responses through TRAF2. This model has been adapted from reference [67].

1.6. Regulation of NOD2 signaling

Given the relevant function of NOD2 in innate immunity, understanding the underlying regulatory mechanism and its interaction partners has been of great interest. Several positive and negative regulators of NOD2 signaling have been identified through different screening approaches. However, many questions of the NOD2 regulation mechanism remain unanswered.

Post-translational modifications such as ubiquitination, are critical regulators of protein localization, activity, stability and interactions with other proteins [68]. NOD2-mediated signaling is partly regulated by ubiquitination of the Nodosom complex [11]. For example, the Suppressor of cytokine signaling-3 protein is among NOD2 interacting proteins that has been reported to recruit the ubiquitin machinery to NOD2 and promote its proteasomal degradation [52]. ZNRF4 is an E3-ubiquitin ligase that negatively regulates NOD2 signaling through mediating K48-linked ubiquitination and subsequent degradation of RIPK2 [69]. Both ZNRF4 and Suppressor of cytokine signaling-3 proteins have been proposed to be involved in the tolerance mechanism induced by MDP. Ubiquitin-mediated regulation of NOD2 signaling is not restricted to RIPK2. It has been reported that ubiquitin can compete with RIPK2 in binding to the CARDs domain of NOD2 and lead to reduced activation [70].

Cytoskeletal factors are also known to regulate NOD2 signaling. Employing actin-disrupting compounds such as cytochalasin D (Cyt D) on macrophages enhances MDP-induced signaling [71]. In addition, the intermediate filament protein vimentin is interacting with NOD2 and regulates NOD2-induced NF- κ B activation, autophagy, and bacterial handling [72].

In addition, non-coding microRNAs (miRNAs) have also been shown to play a key role in the regulation of NOD2 function [73]. In the context of Inflammatory bowel diseases (IBD) miRNAs including mir-320, miR-192, miR-122, miR-512, miR-671, and miR-495 have been shown to post-transcriptionally regulate NOD2 expression by targeting NOD2 mRNA [74]. Mir-320 exhibits diminished expression in inflamed tissue of IBD patients associated with increased expression of NOD2 [75].

1.7. *NOD2* mutations and Crohn's disease (CD)

IBD encompasses a group of complex and multifactorial diseases consisting of two major types, Crohn's disease (CD) and ulcerative colitis (UC) [76, 77]. The most common symptoms of IBD include abdominal pain, diarrhea, hematochezia, weight loss and fever [78]. Twin studies revealed that genetic factors may have a stronger contribution in the development of CD rather than in UC [79]. *NOD2* is the strongest genetic susceptibility factor associated with CD that has been first identified using genome-wide linkage strategies [80]. Further studies later led to the identification of three main CD-associated *NOD2* polymorphisms, R702W, G908R and 1007fs. Individuals harboring one of these three polymorphisms have a two- to four-fold increased risk for developing CD; however, for homozygous or compound heterozygous carriers the risk increases to 15-40 fold [80-82]. In addition, other

investigations unraveled more NOD2 variants in association with CD [83-85]. The presence of *NOD2* variants in many individuals does not lead to the development of intestinal inflammation, indicating that other elements participate in triggering the disease [20]. The CD-associated *NOD2* variants are mainly located within or close to the LRR domain of the protein which is involved in ligand recognition [80, 81, 86, 87].

The pathomechanism of *NOD2* variants in the development of CD and the main cell types regulated by NOD2 is yet to be clearly defined, however an increasing number of studies in mouse and humans cells have led to the description of several different cellular mechanisms. One such mechanism suggests that the impaired response of NOD2 variants to MDP underpins the disease; this is supported by data that has shown impaired production of proinflammatory cytokine IL-8 in monocytes isolated from CD patients carrying the 1007fsinsC variant upon stimulation with MDP [9, 88]. According to this hypothesis, the impaired capacity of NOD2 variants to induce inflammation leads to aberrant inflammation mediated by other inflammatory mechanisms, unrelated to NOD2. The other hypothesis suggests a role for a defective epithelial defense mechanism. It has been shown that only transfection of WT NOD2, but not mutant NOD2, can restrict survival of *S. typhimurium* in intestinal epithelial cells [26]. A key component of this hypothesis is the reduced capacity of NOD2 variants to activate NF- κ B and see the production of antimicrobial components such as α -defensins in Paneth cells [89]. Additionally, impairment in the capacity of NOD2 to direct autophagy and thus the uptake and trafficking of bacteria through has been implicated in disease progression [22, 90, 91]. In accordance with this notion, patients with CD-associated NOD2 variants showed decreased expression of two α -defensins [89].

Dysbiosis or alteration of the community of gut microbiome has been reported in *Nod2*^{-/-} mice compared with WT one which results in the proinflammatory microenvironment,

however this finding was not confirmed by the other studies on gut microbiome in *Nod2*^{-/-} mice [92-95].

Another hypothesis regarding NOD2 contribution in the development of CD implicates dysregulated IL-12 production. NOD2 has been shown to negatively regulate TLR-induced IL-12 production [96, 97]. Increased levels of IL-12 have been observed in *Nod2*-deficient antigen-presenting cells (APCs) in mice upon treatment with ovalbumin (OVA) peptide and peptidoglycan or recombinant *E. coli* expressing OVA peptide (ECOVA) [97]. However, another group working on *Nod2* KO mice did not observe the same phenotype. Further studies on human CD-associated NOD2 variants revealed reduced production of cytokines after TLR stimulation [91, 98, 99].

Interestingly, loss of *Nod2* in mice neither leads to spontaneous colitis nor increased susceptibility to DSS-induced colitis. However, *Nod2* KO mice show an increased susceptibility to bacterial infections [91, 100].

1.8. NOD2 involvement in diseases other than CD

NOD2 polymorphisms have been associated with other inflammatory diseases including Blau syndrome, early-onset sarcoidosis, allergies, asthma, and autoimmunity [101-108]. In contrast to loss-of-function *NOD2* polymorphisms associated with CD, *NOD2* variants that are linked to Blau syndrome, located in the NBD domain, are considered to mediate gain-of-function [108, 109].

There have been some studies suggesting the involvement of NOD2 in cancer development. *Nod2* knockout mice are characterized by a proinflammatory intestinal microenvironment which consequently results in enhanced epithelial dysplasia upon challenging with dextran sulfate sodium [110]. The proinflammatory microenvironment

in mice is due to the Nod2-dependent dysbiosis. Since dysbiosis is not a confirmed phenotype in *Nod2* KO mice, the contribution of NOD2 to the development of intestinal dysplasia requires further studies. *NOD2* polymorphisms have also been associated with *H. pylori*-induced noncardia gastric carcinoma and gastric lymphoma [111, 112].

1.9. An introduction to the main NOD2 interacting proteins identified by immunoprecipitation-coupled mass spectrometry

1.9.1. VCP

Valosin-containing protein (VCP, also called p97) is a highly conserved AAA+-type ATPase that has been linked to a myriad of cellular processes [113]. The VCP protein comprises four domains, the N-terminal domain, two ATPase domains (D1 and D2), and the C-terminal domain [114]. The energy generated through ATP hydrolysis leads to VCP conformational changes which allow it to structurally remodel or unfold the client molecules [115-117]. VCP is a cytosolic and nuclear protein that also localizes in Golgi apparatus, ER, and mitochondria [118-122]. It is widely expressed and can be found in the brain, skeletal muscle, ovary, testis, kidney, liver, heart, lung, lymph nodes, and whole blood [123].

VCP binds to a large number of cofactors and interacting proteins which facilitate its various functions [124-126]. VCP has been associated with diverse cellular activities such as ubiquitin-mediated protein degradation, autophagy, apoptosis, DNA damage responses, membrane fusion, and vesicular trafficking [127-134]. In general, VCP has been shown to directly or indirectly bind to several ubiquitinated proteins and mediate downstream steps of ubiquitination. It can liberate ubiquitinated proteins from macromolecular structures or membranes. It also facilitates proteasomal elimination of

damaged or misfolded proteins in different compartments including the ER (termed ER-associated degradation or ERAD), the outer mitochondrial membrane, on ribosomes (in a process termed ribosome-associated degradation) and in the nucleus [113]. The degradative function of VCP has also been shown to be important in regulating some crucial signaling pathways like degradation of I κ B α in canonical NF- κ B pathway or degradation of HIF1 α , leading to the downregulation of the hypoxic response [135, 136]. VCP has been shown to have a similar role in the non-canonical NF- κ B pathway by regulating proteolysis of p100 and p105 and generation of p50 and p52 [137, 138].

In addition to VCP function as a chaperone in proteasome degradation system, recent studies link it to autophagy which is the other critical cellular degradative system. In mammals, VCP regulates autophagosome maturation. Muscle tissue from patients with p97-associated disease Paget disease of bone and frontotemporal dementia (IBMPFD), showed LC3 and p62-enriched vacuoles [139]. The data was reproduced in a transgenic mice model expressing a disease-associated variant of Vcp [140, 141]. Accumulation of ubiquitinated proteins in cells overexpressing VCP mutant (K251A/K524A or E578Q) induces apoptotic cell death [130]. The VCP orthologue in yeast, Cdc48, together with its cofactor Shp1 are mediating the formation of autophagosomes through direct interaction of Shp1 with ATG8 (homolog of the mammalian LC3) [142].

Vcp/p97 knockout mice are not viable and die at a peri-implantation stage; however, the heterozygous *Vcp*^{+/-} mice are identical to wild-type animals [143]. In human *VCP* mutation cause inclusion body myopathy associated with Paget disease of bone, frontotemporal dementia, amyotrophic lateral sclerosis, and Huntington's disease [121,

144, 145]. In line with VCP function in maintaining genome stability, its overexpression in mammalian cells triggers anti-apoptotic signaling and increases the metastatic ability of these cells [146]. VCP expression is a prognostic marker for many cancers [147-149].

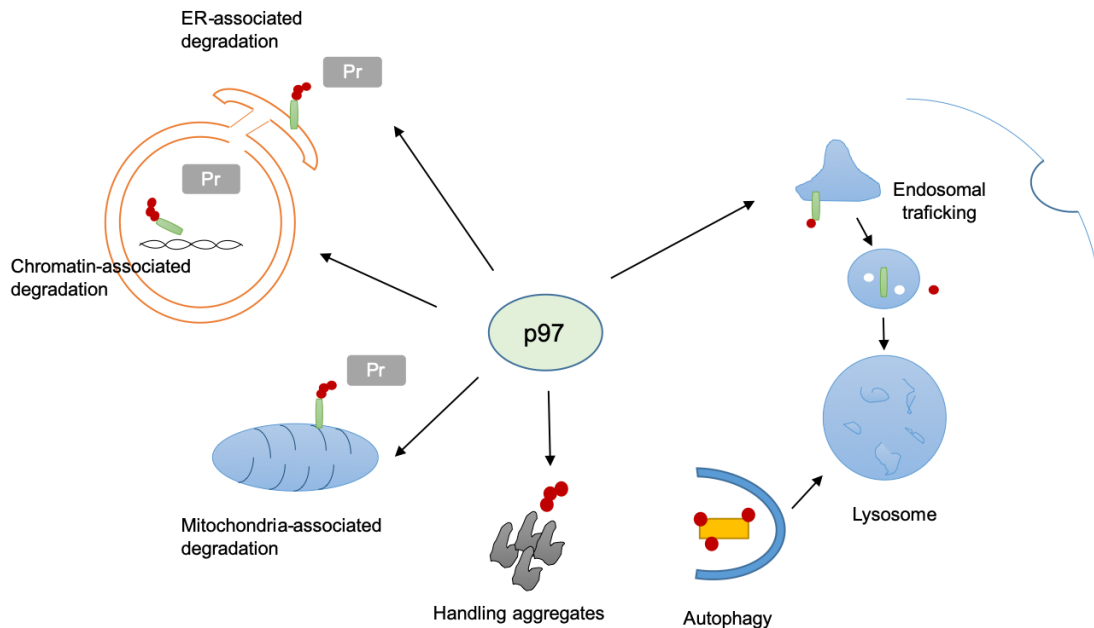


Figure 1-4 VCP cellular functions. VCP has been associated with several ubiquitin-dependent cellular processes such as chromatin-associated degradation, mitochondria-associated degradation, ER-associated degradation, clearance of protein aggregates, autophagy, and endosomal trafficking. This model has been adapted from reference [127].

1.9.2. ATAD3A

ATPase family AAA-domain containing protein 3A (ATAD3A) is a mitochondrial protein that belongs to the AAA-ATPases (ATPases associated with diverse cellular activities) family of proteins [150]. The mouse genome contains one copy of the gene (*Atad3*) and its knockout has been reported to be embryonic lethal [151, 152]. Primates and human have three paralogs of ATAD3 (ATAD3A, ATAD3B, and ATAD3C) [153, 154]. AAA+ proteins govern numerous cellular functions such as protein unfolding and

degradation, mitochondrial activity and dynamics, vesicular transport, DNA recombination, replication, and repair [155, 156]. ATAD3A is ubiquitously expressed and involved in the maintenance of mitochondrial nucleoid, mitochondrial dynamics regulation, and cholesterol metabolism [150, 157-159]. A *de novo* missense c.1582C>T (p.Arg528Trp) variant in the *ATAD3A* gene has been reported in patients presenting with developmental delay, hypotonia, optic atrophy, peripheral neuropathy, and hypertrophic cardiomyopathy [160]. Fibroblasts of the patients showed a higher level of mitophagy leading to decreased mitochondrial content of the cells. Another study linked a dominantly inherited heterozygous variant c.1064G>A (p.G355D) in *ATAD3A* with hereditary spastic paraplegia and dyskinetic cerebral palsy. Fibroblasts of patients harboring p.G355D exhibited reduced ATAD3A ATPase activity and disturbed mitochondrial morphology. However, the authors did not observe any differences in the content of mitochondrial DNA [161]. ATAD3A is involved in many cancers and has also been implicated in resistance to cancer treatment [162-166].

2. The aim of this study

My thesis aimed to better understand NOD2 signaling by investigating the functional consequences of a rare missense mutation in the first CARD domain of the protein identified in a pediatric patient suffering from IBD. This is deemed to be of importance since NOD2 has critical implications in the development of Crohn's disease, a chronic debilitating inflammatory disorder of the digestive tract.

In this context, initially, the NOD2-mediated signaling induced by peptidoglycan or non-peptidoglycan stimulus were elucidated. Furthermore, it was dissected whether the mutation influenced the interaction and post-translational modification of RIPK2, a direct interaction partner of NOD2 that is recruited to the complex upon NOD2 activation. Due to the observed effect of the mutation in the NOD2-mediated signaling pathway, we were interested to gain molecular insights into the NOD2 interaction networks. Immunoprecipitation-coupled mass spectrometry unveiled VCP and ATAD3A as novel interacting proteins. Therefore, evaluating their relevant function in NOD2-mediated signaling became another goal of this study.

The main aims of this study were as follows:

- _ Investigating the pathomechanism of the identified mutation in:
 - MDP-induced signaling
 - ER-induced inflammation
 - interaction with RIPK2 and its MDP-induced ubiquitination
 - NOD2 interaction network

- _ Investigating the relevant function of newly identified interacting proteins in NOD2-mediated signaling pathways

3. Material and Methods

3.1. Materials

3.1.1. Chemicals and Reagents

All common chemicals were purchased from Roth (Karlsruhe, Germany), Sigma (Deisenhofen, Germany), and PanReac AppliChem (Darmstadt, Germany), unless stated otherwise. DNA oligonucleotides used in this study were procured from Eurofins MWG (Munich, Germany). The list of the reagents used in this thesis is provided in Table 1 or mentioned in the methods part.

Name	Company	Cat. #
Agarose TUBE 2	Lifesensors	UM402
Anti-FLAG M2 Affinity Gel	Sigma-Aldrich	A2220
BD GolgiStop™ Protein Transport Inhibitor	BD Biosciences	51-2092kz
L18-MDP	Invivogen	t1rl-lmdp
Lipopolysaccharide (LPS)	Sigma-Aldrich	L2654
Lipofectamine 2000	Thermo-Scientific	11668019
Lipofectamine™ 3000	Thermo-Scientific	L3000015
Tunicamycin Streptomyces sp.	Sigma-Aldrich	T7765

Table 3-1The list of reagents

3.1.2. Media and supplements

Name	Company	Cat. #
-------------	----------------	---------------

Materials and Methods

DMEM Medium	Thermo Fisher Scientific (Gibco)	11960-044
Fetal Bovine Serum	Thermo Fisher Scientific (Gibco)	10270106
HEPES 1M, 100ml	Thermo Fisher Scientific (Gibco)	15630-056
IMDM Medium	Thermo Fisher Scientific (Gibco)	12440061
L-glutamine	Thermo Fisher Scientific	25030123
Luria Broth (LB) liquid media	ROTH	X968.4
Opti-MEM Medium	Thermo Fisher Scientific (Gibco)	11058021
Penicillin-Streptomycin	Thermo Fisher Scientific (Gibco)	15070063
RPMI 1640 Medium, GlutaMAX™ Supplement	Thermo Fisher Scientific (Gibco)	61870-044
Sodium Pyruvate (100 mM)	Thermo Fisher Scientific	11360088

Table 3-2 The list of mediums and supplements

RPMI-1640 medium was supplemented with 1% L-glutamine, 10% v/v fetal bovine serum (FBS), 1% penicillin-streptomycin, 1 mM Sodium Pyruvate, and 10 mM HEPES. RPMI-1640 medium was used for culturing PBMCs and neutrophils. DMEM medium supplemented with 1% L-glutamine, 10% v/v FBS, and 1% penicillin/streptomycin and was utilized for culturing HEK293T and HCT116 cells. IMDM medium supplemented

with 10% fetal bovine serum (FBS) was used to enrich for human primary monocytes from PBMCs.

3.1.3. Plasmids

Vector	Description
pRRL-hNOD2-IRES-RFP	Lentiviral expression vector, containing human wildtype NOD2 plus an RFP reporter
pRRL-hNOD2(E54K) - IRES-RFP	Lentiviral expression vector, containing a patient specific variant (c.160G>A) of human NOD2 plus an RFP reporter
pRRL-hNOD2(L1007fsinsC)- IRES-RFP	Lentiviral expression vector, containing a patient specific variant (L1007fsinsC) of human NOD2 plus an RFP reporter
pRRL-Flag-hNOD2-IRES-RFP	Lentiviral expression vector, containing N-terminal Flag Tagged human wildtype NOD2 plus an RFP reporter
pRRL-Flag-hNOD2(E54K) - IRES-RFP	Lentiviral expression vector, containing an N-terminal Flag Tagged patient specific variant (c.160G>A) of human NOD2 plus an RFP reporter
pRRL-Flag-hNOD2(L1007fsinsC)- IRES-RFP	Lentiviral expression vector, containing an N-terminal Flag Tagged patient specific variant (L1007fsinsC) of human NOD2 plus an RFP reporter
pRRL-Flag-hNOD2.IRES-GFP	Lentiviral expression vector, containing N-terminal Flag Tagged human wildtype NOD2 plus a GFP reporter

Materials and Methods

pRRL-Flag-hNOD2(E54K) -IRES-GFP	Lentiviral expression vector, containing an N-terminal Flag Tagged patient specific variant (c.160G>A) of human NOD2 plus a GFP reporter
pRRL-Flag-hNOD2 (L1007fsinsC) -IRES-GFP	Lentiviral expression vector, containing an N-terminal Flag Tagged patient specific variant (L1007fsinsC) of human NOD2 plus a GFP reporter
pRRL-Flag-hNOD2-IRES- mCD24	Lentiviral expression vector, containing N-terminal Flag Tagged human wildtype NOD2 plus a mCD24 reporter
pRRL-Flag-hNOD2(E54K) -IRES-mCD24	Lentiviral expression vector, containing an N-terminal Flag Tagged patient specific variant (c.160G>A) of human NOD2 plus a mCD24 reporter
pRRL-Flag-hNOD2 (L1007fsinsC)-IRES- mCD24	Lentiviral expression vector, containing an N-terminal Flag Tagged patient specific variant (L1007fsinsC) of human NOD2 plus a mCD24 reporter
pRRL-hRIPK2-IRES-RFP	Lentiviral expression vector, containing human wildtype RIPK2 plus an RFP reporter
pRRL-hVCP-IRES-GFP	Lentiviral expression vector, containing human wildtype VCP plus a GFP reporter
pRRL-hATAD3-IRES-GFP	Lentiviral expression vector, containing human wildtype ATAD3A plus a GFP reporter
pENT1RA-hATAD3	Gateway Entry vector, containing human wildtype

ATAD3A	
PB-TAC-ERP2-ATAD3A-IRES-mCHERRY	PiggyBac transposon Destination vector for dox-inducible expression of Gateway cloned elements (inducible mCherry and constitutive rtTA and puromycin resistance), containing human wildtype ATAD3A plus a mCherry reporter

Table 3-3 The list of constructs generated in this thesis

3.1.4. Cloning, mutagenesis and qPCR primers

Name	Sequence of primers used (5'-3')
CHOP forward	ATGAACGGCTCAAGCAGGAA
CHOP reverse	GGGAAAGGTGGGTAGTGTGG
GAPDH forward	TGATGACATCAAGAAGGTGGTGAAG
GAPDH reverse	TCCTTGGAGGCCATGTGGGCCAT
IL-8 forward	ACTCCAAACCTTTCCACCCCAAAT
IL-8 reverse	ACAACCCTCTGCACCCAGTTTT
VCP forward	ATCCGTGAATCCATCGAGAG
VCP reverse	GGAATCTGAAGCTGCCAAAG

Table 3-4 The list of the qPCR primers

Name	Sequence	comments
NOD2-c.160g>A-F	TGCCTTCTCTGGGTCTCAAT	For sanger sequencing
NOD2-c.160g>A-R	TTCTGACAGGCCCAAGTACC	For sanger sequencing
STXBP2-F	CCCTCGTGTGACTCCAGACT	For sanger sequencing
STXBP2-R	TCTCAGTCCAGGCTCGAAAT	For sanger sequencing

Materials and Methods

NOD2-F	ctACCGGTgccaccatgggggaagagggtg g	With Age I cut site, binds beginning of longer variant of NOD2(NM-022162:2)
NOD2-R	ctACTAGT tcaaagcaagagtctggtgtcc	With Spe I cut site
NOD2-F2	cctggaattccttcacatcactttc	EcoR I cut site
NOD2-R2	gaaagtgatgtgaaggaattccaggg	EcoR I cut site
NOD2-F-N	ATGTGCTCGCAGGAGGCTTTTC	Binds beginning of shorter NOD2 variant (NM-001293557.1)
NOD2 extend F1	aagagcaagtgtcctcctcggacattctccgggtt gtgaaatgtgctcgcaggaggc	
NOD2 extend F2	ctACCGGTgccaccatgggggaagagggtg gttcagcctctcacgatgaggaggaaagagcaa gtgtcctcc	With Age I cut site
NOD2-c.802t>c-F	catggctggacccccgcagaagagcccagc	
NOD2-c.802t>c-R	Gtccagccatgccacatctgcccag	
NOD2-IBD244-F	ggaaggcttcAagagtgtcctggactggctgctgt c	Site directed mutagenesis primer for c.160G>A
NOD2-IBD244-R	tgaagcctccagggaccctgagaccagcagct c	Site directed mutagenesis primer for c.160G>A

Materials and Methods

NOD2-3020insC-F	ctgcaggcccCttgaaaggaatgacaccatcct ggaagtctgg	Site directed mutagenesis primer for 3020insC
NOD2-3020insC-R	Ggggcctgcaggagggtcttctgccctagg	Site directed mutagenesis primer for 3020insC
N-flag-NOD2-v1-F	CtACCGGTgccaccatgGACTACAAAG ACGATGACGACAAGggggaagagggt ggttc	to make fusion construct with an N-terminal FLAG tag
RIP2-F	ctACCGGTgccaccatgaacggggaggcca t	With Age I cut site
RIP2-R	ctACTAGTcagtcacttacatgctttatittgaag taa	With Spe I cut site
ATAD3A-ager-F	ctACCGGTgccaccatgtcgtggctcttcggca ttaac	With Age I cut site
atad3a-SpeI-R	ctACTAGT tcaggatggggagggtcgtc	With Spe I cut site
atad3a-bamhi-F	ctGGATCCgccaccatgtcgtggctcttcggca ttaac	
atad3a-xhoi-R	ctCTCGAGtcaggatggggagggtcgtc	
pGEMT_F	TGTAAAACGACGGCCAGT	Sequencing primer
pGEMT_R	CAGGAAACAGCTATGAC	Sequencing primer
pRRL_F	GCTTCTGCTTCCCGAGCTCTA	Sequencing primer
pRRL_IRES_R	GCCTTATTCCAAGCGGCTTC	Sequencing primer

Table 3-5 The list of Primers used for Sanger sequencing, cloning and site directed mutagenesis

3.1.5. siRNAs and sgRNA target sequences

Name	Sequence of siRNAs and sgRNA targets (5'-3')
sg-NOD2-T1	CGGGACCTAACCAGACAAT
sg-NOD2-T2	GCTTCCTCAGTACCTATGA
sg-NOD2-T3	GTGCCAAAGGTGTCGTGCCA
sg-NOD2-T4	GAGGCCTGGATGCACATCGT
sg-ATAD3A-T1	GAATGAGATGCTGCGAGTGG
sg-ATAD3A-T2	CCTTCAGGCGGATCTGCTCG
sg-VCP-T1	GGATGAGACCATTGATGCCG
sg-VCP-T2	GTAACCTGGGAAGACATCGG
sg-VCP-T3	GCTGCCCATTTGATGACACAG
sg-VCP-T4	GCGTATCGACCCATCCGGAA
VCP-si1	GAAUAGAGUUGUUCGGAAU
VCP-si2	GGAGGUAGAUUUGGAAUU
Nontargeting (NT) siRNA	UGGUUUACAUGUCGACUAA

Table 3-6 the list of the siRNA and sgRNA target sequences**3.1.6. Antibodies**

Antibody	Clone	Company	Cat.#
phospho- NF- κ B (p65) (Ser536)	93H1	Cell signaling technology	3033
NF- κ B (p65)	D14E12	Cell signaling technology	8242
phospho-p44/42 MAPK (Erk1/2) (Thr202/Tyr204)	D13.14.4E	Cell signaling technology	4370

Materials and Methods

p44/42 MAPK (Erk1/2)		Cell signaling technology	9102
Phospho-p38 MAPK (Thr180/Tyr182)	D3F9	Cell signaling technology	4511
Phospho-IkBa (Ser32)	14D4	Cell signaling technology	2859
IkBa	L35A5	Cell signaling technology	4814
RIP2	D10B11	Cell signaling technology	4142
VCP		Cell signaling technology	2648
HRP-conjugated anti-rabbit IgG		Cell signaling technology	7074
Beta-Actin-HRP	c4	Santa Cruz Biotechnology	sc-47778
GAPDH	0411	Santa Cruz Biotechnology	sc-47724
ATAD3A		Novus Biologicals	H00055210- D01P
RASGRP1	A-7	Santa Cruz Biotechnology	Sc-365358

Table 3-7 The list of antibodies used for immunoblotting

Antibody	Fluorochrome	Clone	Company	Cat.#
CD19	BUV395	SJ25C1	BD	563549
CD20	PE-Cy7	2H7	BD	560735
IgD	BB515	IA6-2	BD	565243
IgM	BV421	G20-127	BD	747878
CD21	BUV737	B-Ly4	BD	564437
CD27	BV786	L128	BD	563327
CD10	PE	HI10a	BD	555375
CD38	APC	HB-7	BD	345807

Materials and Methods

Anti-human TNF α	PE	MAb11	BD	559321
CD3	BUV395	SK7	BD	564000
CD14	FITC	M5E2	BD	557153
CD14	BV786	M5E2	BD	563698
CD62L	APC	DREG-56	BD	56916
CD62L	BV650	DREG-56	BD	563808
CD3	pacific blue	SK7	Biologend	344823
CD3	BUV496	UCHT-1	BD	564809
CD8	BUV737	SK1	BD	564629
CD56	PE-CF594	NCAM16.2	BD	564849
CD57	BB515	NK-1	BD	565285
CD14	BB700	M5E2	Biologend	301806
CD16	APC	3G8	Biologend	302012
HLA-DR	BV711	G46-6	BD	563696
CD123	BV785	6H6	Biologend	306032
CD11c	BV421	B-ly6	BD	562561
CD33	PE-Cy7	P67.6	Biologend	366618
TCR g-d	PE		BD	555717
TCR a-b	APC-Fire750		BD	306736
CD45	BV480	HI30	BD	566115
CD3	APC-Fire750	SK7	Biologend	344840
CD4	BUV395	RPAT4	BD	564724
CD8	BUV496	RPAT8	BD	564804
CD45RA	BUV737	HI100	BD	564442
CD45RO	BB515	UCHL1	BD	564529

CD127	APC	A019D5	Biolegend	351316
CD25	PE	M-A251	BD	555432
CD27	APC-R700	M-T271	BD	565116
CD28	BB700	L293	Biolegend	302922
HLA-DR	BV711	G46-6	BD	563696
CCR7	BV421	G043H7	Biolegend	353208
CCR6	BV785	G034E3	Biolegend	353422
CXCR3	PE-CF594	1C6	BD	562451
CCR4	PE-Cy7	L291H4	Biolegend	359410
CD38	BV650	HB-7	Biolegend	356620

Table 3-8 The list of antibodies used for Flow cytometry

3.1.7. Restriction enzymes

Enzymes	Company
BamHI FastDigest	All from Thermo Scientific, USA
BcuI (SpeI) FastDigest	
BshTI (AgeI) FastDigest	
DpnI FastDigest	
EcoRI FastDigest	
HincII FastDigest	
NcoI FastDigest	
NdeI FastDigest	
PvuI FastDigest	
SacI FastDigest	
XagI (EcoNI) FastDigest	

XhoI FastDigest

Table 3-9 The list of the restriction enzymes used in this study

3.1.8. Buffers and solutions

All solutions were made using high pure deionized water (Millipore).

DNA loading dye (6X)

30% (v/v) Glycerol

0.01% (w/v) Bromophenol blue

Laemmli buffer (6X)

750 mM Tris pH 6.8

6% (w/v) SDS

25% (v/v) Glycerol

0.05% (w/v) Bromophenol blue

Tris-Borate-EDTA (TBE) buffer

90 mM Tris

90 mM Boric acid

2 mM EDTA

Stripping buffer

200 mM Glycine

1% (w/v) SDS

0.01% (v/v) Tween 20

pH 2.2

Western blot running buffer

25 mM Tris

190 mM Glycine

0.1% (w/v) SDS

Western blot transfer buffer

25 mM Tris

190 mM Glycine

LB agar plates

25 g/L LB broth

17 g/L Agar-Agar

LB medium

25 g/L LB broth

RIPA buffer

10mM Tris-HCl, pH 7.5

150mM NaCl

5mM EDTA

1% NP-40

10 % glycerol

30mM sodium pyrophosphate

50mM sodium fluoride

1 mM phenylmethylsulfonyl fluoride

1x protease inhibitors cocktail

Tube assay lysis buffer

50mM Tris-HCl, pH 7.5

150mM NaCl

1mM EDTA

1% NP-40

10% glycerol

1 mM phenylmethylsulfonyl fluoride

1xprotease inhibitors cocktails

1mM Nethylmaleimide

3.2. Methods

3.2.1. Isolation of PBMCs and neutrophils

PBMCs and neutrophils were isolated from heparinized blood by density gradient centrifugation over Ficoll paque plus (GE healthcare) following the manufacturer's protocols. PBMCs were either cultured immediately or cryopreserved for later use. Neutrophils were immediately used for further experiments.

3.2.2. DNA sequencing

Isolation of genomic DNA from peripheral blood samples was conducted using the QIAamp DNA Blood Mini Kit according to the provided instructions by the manufacturer. Enrichment for all coding exons was performed using the SureSelect Human All Exon kit followed by sequencing on the NextSeq 500 platform (Illumina) to an average coverage depth of 90x. Burrows-Wheeler Aligner (BWA 0.7.15), Genome

Analysis ToolKit (GATK 3.6), and Variant Effect Predictor (VEP 89) used for Bioinformatical analysis [167, 168]. Public (e.g. ExAC, GnomAD, and GME) and in-house databases used for frequency filtering [169, 170].

Segregation of *NOD2* (ENST00000300589; c.160G>A, p.E54K) and *STXBP2* (ENST00000441779; c.949C>G, p.L317V) variants in the family were confirmed by Sanger sequencing using primers listed in table 3-5.

PCR amplification was performed the same way as described in part 3.2.3.1. using OneTaq® DNA Polymerase master mix. The PCR product was cleaned using ExoSAP as follows:

DNA 20µl

ExoSAP-IT 2µl

- Mixed and incubated at 37 °C for 15 minutes
- ExoSAP-IT inactivated by heating to 80 °C for 15 minutes

Cleaned fragments were Sanger sequenced by GATC (Biotech, Konstanz, Germany) and Eurofins MWG (Munich, Germany) and sequence traces were aligned with CodonCode Aligner (CodonCode Corporation, Dedham, MA.)

3.2.3. Molecular biology

3.2.3.1. Polymerase chain reaction (PCR)

PCR conditions were adjusted for different polymerases according to the manufacturer's instructions. 4 different polymerases used in this project: Q5 (NEB), PFU (Promega), OneTaq® DNA Polymerase (NEB), and HIFI polymerase (ROCHE). Standard PCR was done to amplify a certain DNA sequence using the following components:

polymerase 0.5-1 µl

10x polymerase buffer	2.5 μ l
dNTP mix(10mM)	0.5 μ l
Forward primer (10 μ M)	1.5 μ l
Reverse primer (10 μ M)	1.5 μ l
Template	Variable(100ng)
H ₂ O	Up to 25 μ l

For Q5 polymerase the buffer is 5x and the amount taken was adjusted accordingly. 5 μ l/reaction 5X Q5 High GC Enhancer also included. OneTaq® DNA polymerase is a 2x master mix which just mixed with primers and DNA templates. PCR reaction was performed in a thermocycler using the following general method for each polymerase:

Cycle Step	Temperature	Time	Cycles
Initial denaturation	98 °C	30 s	1
Denaturation	98 °C	30 s	25 – 40
Annealing	52 – 68 °C	30 s	
Extension	72 °C	1 min / kb	
Final extension	72 °C	10 min	1
Hold	4 °C	∞	

Table 3-10 Standard PCR program

3.2.3.2. Agarose gel electrophoresis and DNA fragment isolation

PCR product was analyzed on 0.8 % (W/V) agarose melted in TBE-Buffer. The gels were stained with ethidium bromide. 1 kb DNA-ladder (peqlab) or Mid-Range DNA Ladder (100bp - 3000bp) (JenaBioscience) were used as DNA size reference. Samples were mixed with 6X DNA loading dye and gels were run in TBE buffer on a Mini-Sub® Cell GT device for 40 min at 120 V. DNA was detected on a GelDoc XR+ Imager. Purification of desired band performed using QIAquick Gel Extraction Kit

(Qiagen) or Zymoclean™ Gel DNA Recovery Kit - Uncapped columns (Zymo) according to the manufacture's instruction.

3.2.3.3. Site-directed mutagenesis

Mutations were introduced into PCR products using primers that contain the desired point mutations, at 3' end of one of the primers and one somewhere in the middle of the second primer sequence. After PCR amplification, methylated wild type (WT) template plasmid digested with 1 µL FastDigest DpnI enzyme (Thermo) for 1 h at 37 °C and 10 µL transformed into chemically competent XL-10 Gold E. coli cells.

3.2.3.4. Transformation

For transformation, 20 µL chemically competent XL-10 Gold E. coli cells thawed on ice. 10 µL of ligation mixed add to the bacteria and incubated on ice for 30min. heat shock was performed at 42 °C for 45 sec and kept on ice for another 2 min. 500 µL LB medium added and bacteria left on a shaking incubator for 1 h at 37 °C. Transformation mixture plated on a 10 cm LB agar plate containing ampicillin (amp) and incubated overnight at 37 °C.

3.2.3.5. Inoculation of bacteria and plasmid purification

To obtain pure plasmid DNA, single colonies were picked from the agar plate and inoculated into 3-5 ml fresh LB medium supplemented with 100 µg/ml ampicillin and kept overnight on shaking incubator at 37 °C shaking at 200 rpm. Plasmid purification was performed from overnight grown bacteria using Zyppy Plasmid Miniprep Kit (Zymo) or NucleoSpin Plasmid kit (Machery-Nagel) according to the manufacturer's protocol. Plasmid integrity was verified by restriction digestion and sequencing at Eurofins Genomics (Ebersberg, Germany). All obtained plasmid preparations were stored in nuclease-free water at -25 °C.

3.2.3.6. Restriction digestion

All Restriction digestions performed in this work were done using FastDigest restriction enzymes from Thermo Fisher Scientific according to the manufacturer's instructions. New ligated constructs were analyzed by restriction digestion. The list of restriction enzymes used in this study and corresponding constructs is given in table 3-9.

3.2.3.7. Ligation

For ligation T4 DNA Ligase (Thermo Fisher Scientific) was used according to the manufacturer's protocol. The molar ratios between vector and insert ranged from 1:3 to 1:5.

3.2.3.8. RNA isolation and cDNA synthesis

RNA isolation was conducted using RNEasy Plus Mini Kit (Qiagen) according to the manufacturer's instructions. 1 μ L RiboLock RNase Inhibitor (Thermo Scientific) added per reaction. RNA concentration and purity were evaluated by Nanodrop. Subsequently, reverse transcription was performed using High-Capacity cDNA Reverse Transcription Kit (ThermoFischer) as follows:

Oligo dT	3 μ L
dNTP(10Mm)	2 μ L
Random primer (10x)	2 μ L
RT buffer (10x)	5 μ L
MultiScribe™ Reverse Transcriptase	2 μ L
Nuclease-free H ₂ O	Up to 50 μ L
RNA	1 μ g

After mixing the components on ice, reverse transcription was performed on a thermocycler according to the protocol provided by the manufacturer.

3.2.3.9. Cloning of *NOD2* gene

To generate full-length human *NOD2* (*ENST00000300589.6*), first, the shorter *NOD2* variant (NM-001293557.1) was amplified using a 2 fragment strategy, then the 81 bp sequence added to the 5' end of the shorter variant to generate the longer variant of *NOD2* (NM-022162.2).

There is a unique *EcoRI* site in the middle of the *NOD2* sequence which was used for the two fragment strategy with overlapping primers. *NOD2* was amplified in two fragments, a first amplicon from the start codon to the *EcoRI* site and a second one, from the *EcoRI* site to the stop codon. Amplification was performed using Pfu polymerase on cDNA prepared from EBV-LCLs.

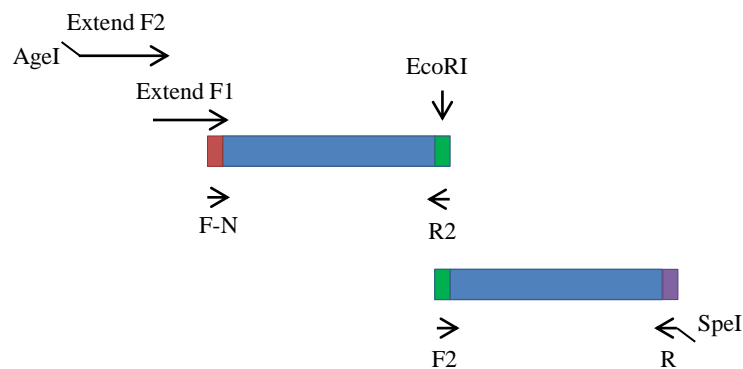


Figure 3-1 Schematic representation of *NOD2* cloning strategy

2 amplicons digested with *EcoRI* enzyme and ligation performed as follows:

Amplicon1	10 μ L
Amplicon2	10 μ L
10x T4 ligase buffer	2.5 μ L
T4 ligase	1 μ L
Nuclease-free H ₂ O	Up to 25 μ L

Ligation reaction was performed at 16 °C overnight.

Ligated fragments were purified from the mixture by using QIAquick Gel Extraction Kit (Qiagen) just by adding 300µL of the first QF buffer to the mixture. The remaining parts of the procedure were performed according to the manufacturer's protocol.

To obtain full-length *NOD2*, the purified ligated fragments were amplified using FN and R primers. Poly-A tail was added to the amplified PCR product using Hifi polymerase as follows:

Eluted DNA	35µL
dNTP(10mM)	1µL
10x Hifi buffer 2	4 µL
Polymerase	1 µL

The reaction was performed at 72 °C for 30 min. The A-overhang fragments were separated on agarose gel and purified and then ligated into pGEM®-T Easy Vector (Promega) as follows:

Eluted DNA	10µL
pGEM®-T Vector	1µL
10x T4 ligase buffer	2 µL
T4 ligase	1 µL
Nuclease-free H ₂ O	6 µL

Ligation was performed at 16 °C overnight.

Transformation, inoculation of bacteria and plasmid purification were performed in the same way as outlined before. The recombinant plasmid construction was verified by restriction digestion (NcoI) and sequencing.

To generate the *NOD2* variant (NM-022162.2) which is 81 bp longer, two long forward primers were designed (NOD2 extend F1 and NOD2 extend F2) to cover the whole

81bp. Amplification was performed first with the NOD2 extend F1 and the reverse primer binding at 5' end of the gene this amplicon then served as a template for generating full-length *NOD2* by using NOD2 extend F2 and the reverse primer binding at 5' end of the gene.

Sequencing of the plasmid revealed unwanted polymorphism at c.802 C>T which converted to WT sequence by Site-directed mutagenesis PCR. Patient-specific mutations (encoding E54K and L1007fsinsC) were also introduced into the WT sequence using site-directed mutagenesis PCR.

WT and mutated *NOD2* fragments also amplified with forward primer including FLAG sequence to generate a fusion construct with an N-terminal FLAG tag.

For the expression of target proteins, the 3rd generation bicistronic lentiviral vector backbone pRRL.cPPT.SF was used. The multiple cloning site of the pRRL.cPPT.SF vector was altered by insertion of a small oligonucleotide, introducing a few additional restriction sites (5' to 3': BamHI, AgeI, SpeI, MluI, BsiWI, ApaI, NdeI, NsiI, Sall). WT and mutated *NOD2* cDNAs were amplified using primers with appropriate restriction site added to their 5' end (AgeI and SpeI). Lentiviral cloning performed into IRES-EGFP, IRES-RFP, and IRES-mCD24 bicistronic lentiviral pRRL.cPPT.SF vectors.

The sequence of primers used in this part is described in table 3-5.

3.2.3.10. Cloning of *RIPK2* gene

Human WT *RIPK2* was amplified from the verified cDNA sequence clone (GE Dharmacon, cat.no. MHS6278-202830678). The PCR product was subcloned into pGEM-T and subsequently cloned into IRES-RFP bicistronic lentiviral pRRL.cPPT.SF vector. Restriction sites were AgeI and SpeI.

3.2.3.11. Cloning of *VCP* gene

Human WT *VCP* was amplified from the verified cDNA sequence clone (GE Dharmacon, cat.no. MHS6278-202760239) introducing 5' *AgeI* and 3' *SpeI* cleavage sites via primers. After subcloning into pGEM-T, the desired fragment was excised by restriction digestion and subsequently ligated into the bicistronic lentiviral pRRL vector harboring IRES-EGFP as a reporter.

3.2.3.12. Cloning of *ATAD3A* gene

Human WT *ATAD3A* was amplified from the verified cDNA sequence clone (Dharmacon, cat.no. MHS6278-202758359) and cloned into IRES-GFP bicistronic lentiviral pRRL.cPPT.SF vector using *AgeI* and *SpeI* cut sites. To obtain *ATAD3A* in a doxycycline-inducible expression system, The Gateway® Technology from Invitrogen was employed. First, *ATAD3A* was amplified with primers having *Bam*HI and *SpeI* cut sites. The amplified fragments were cloned into the pENTR1A noCCDB (w48.1) plasmid using the mentioned cut sites. *ATAD3A* was transferred to destination vector PB-TAC-ERP2 by using LR recombination reaction as follows:

PB-TAC-ERP2	10µL
ATAD3A- pENTR1A	4.5µL
5X BP Clonase™ reaction buffer	2 µL
TE Buffer, pH 8.0	1.5 µL

- The components above were mixed well and incubated at 25 °C.

- 2 µL Proteinase K solution was added and incubation was performed for 10 min at 37 °C.

Transformation and the rest of the cloning procedure performed as stated before.

3.2.3.13. Quantitative real-time PCR (qPCR)

qPCR was conducted with the SYBR Green PCR Master Mix (FAST SYBR Green Master mix from ABI or PowerUp SYBR Mastermix from ThermoFischer). All gene expressions were normalized to GAPDH. Relative quantification was measured according to the $2^{-\Delta\Delta CT}$ method. The primer information is given in table 3-4.

3.2.4. Cell culture

3.2.4.1. Cell cultivation

Human embryonic kidney HEK293T cells (ATCC, CRL3216) and HCT116 cells (ATCC, CCL247) were cultured in DMEM medium (Thermo Fisher Scientific) supplemented with 1 % L-glutamine, 10 % v/v FBS, and 1 % penicillin/streptomycin. All the cells were cultivated at 37 °C and 10 % CO₂. For passaging of cells, cells were washed with PBS then trypsinized for about 3 min followed by the addition of complete medium. Cells were centrifuged for 10 min at 1200 rpm, 4 °C, and resuspended in fresh medium. The appropriate number of cells were seeded in a fresh cell culture flask. Cells were routinely tested for Mycoplasma contamination.

3.2.4.2. Transfection

Transient transfection was performed at 70% confluency using PEI or lipofectamine 2000 or lipofectamine 3000.

Culture vessel	Number of adherent cells to seed	Amount of DNA (Plasmid)- μ g
10cm plate	2,000,000-4,000,000	10
6-well	200,000-400,000	3
12-well	80,000-200,000	2
24-well	50,000-100,000	0.5- 1

Table 3-11 recommended number of cells and DNA amount for different cell culture plates

3.2.4.2.1. Polyethylenimine (PEI; Polysciences) transfection

DNA and PEI (1 mg/mL) were diluted in DMEM medium in separate eppies in a 1:2 ratio. PEI mixture was added to DNA mix, pipetted well, and incubated at RT for 30 min. Then, the mixture was added dropwise to the cells. The medium was changed after 12-18 h.

3.2.4.2.2. Lipofectamine 2000 transfection

To transfect cells in a 24-well plate, Lipofectamine® 2000 DNA Transfection Reagent (ThermoFisher Scientific), was used and the two mixtures were prepared as follows:

(A) Opti-MEM 25 μ l + Lipofectamine 2000 1.5 μ l

(B) Opti-MEM 25 μ l + plasmids

(A) added to (B) and mixed well by pipetting gently. After 15 min incubation at RT, the mixture was added dropwise to the cells.

3.2.4.2.3. Lipofectamine 3000 transfection

Lipofectamine™ 3000 Transfection Reagent (ThermoFisher Scientific) was used for transfection of DNA and of siRNA. Transfection was conducted according to the manufacturer's instructions.

3.2.4.3. NF- κ B luciferase reporter gene assays

To assess NF- κ B activation upon MDP stimulation, HEK293T cells were transfected with 0.5 ng *NOD2* or RFP control plasmid, 100 ng p55-A2-Luc luciferase reporter plasmid containing the NF- κ B binding sites, and 5 ng pTK-Green Renilla plasmid as an internal control for 18 h. L18-MDP stimulation was performed for 7-8 h and cells were lysed in 1x passive lysis buffer (Biotium) and incubated 15 min at RT before

storage at -80 °C. NF- κ B activity was measured by using Dual Luciferase Assay Kit (Biotium). First, lysates were cleared by centrifugation at 15000 RPM, 4 °C, 5 min, and transferred into new tubes. Firefly and Renilla luciferase working solution was prepared according to the manufacturer's protocol. 80 μ l of luciferase solutions was added to 20 μ l lysates in a white F96 Microwell plate. Experiments were performed in duplicates and luminescence signal was measured on a luminometer. Firefly luciferase activities were normalized to Renilla luciferase activities.

3.2.4.4. Production of lentiviral particles and cellular transduction

To produce lentiviral particles, HEK293T cells were seeded in 10 cm petri dishes and transfected with viral packaging plasmids psPAX2 (10 μ g) and pMD2.G (2.5 μ g) and lentiviral vectors (15 μ g) using polyethyleneimine (PEI; Polysciences) as a transfection agent. After 12 h cell medium changed and the supernatant was collected every 24 h for 3 days, filtered through a 0.45 μ m syringe filter, and used for transducing cells.

Cell transduction was performed using the virus supernatant in the presence of 8 μ g/ml polybrene (Sigma-Aldrich) for 6-12 h. 72 h post virus transduction, transduced cells were sorted on the BD FACSAria cell sorter (BD Bioscience) based on RFP or EGFP mean fluorescence intensity (MFI). In the case of different mean fluorescence intensities, sorting was repeated to obtain the same MFI between cell lines. *NOD2* KO HCT116 cells were transduced with viruses carrying WT and mutated *NOD2* fragments with or without an N-terminal FLAG tag cloned into IRES-EGFP, IRES-RFP, and IRES-mCD24 bicistronic lentiviral pRRL vectors. *ATAD3A* KO HCT116 cells were transduced with viruses carrying WT *NOD2* fragments with an N-terminal FLAG tag cloned into IRES-EGFP bicistronic lentiviral pRRL vectors.

3.2.4.5. generating *NOD2* and *ATAD3A* knock-out HCT116 cell lines

HCT116 cells were engineered by Alt-R® CRISPR-Cas9 (IDT technology, Belgium) genome editing system for generating *NOD2* or *ATAD3A* knock-out (KO) cells according to the manufacturer's instructions. Two different pairs of sgRNAs were electroporated using SE Cell Line 4D-Nucleofector® X Kit and the 4DNucleofector™ System (Lonza, Switzerland). Cells were single sorted into 96-well plates on a BD FACSAria (BD Bioscience, USA) 48 h after electroporation. Expanded *NOD2* KO clones were investigated using NF-κB luciferase reporter gene assays to functionally evaluate *NOD2* activity upon MDP stimulation. NF-κB luciferase reporter gene assay performed the same way as described in part 3.2.4.3. and transfection performed for p55-A2-Luc luciferase reporter plasmid together with pTK-Green Renilla plasmid. For *ATAD3A* KO clones, *ATAD3A* protein level was evaluated by immunoblotting. The sequence of sgRNAs are provided in table 3-6.

3.2.4.6. Generating stable cell line overexpressing *ATAD3A* under DOX control

For stable genomic integration of *ATAD3A*, HEK293T cells (3×10^5 cells/well seeded in 6 well plate) were cotransfected with PiggyBac transposon vector PB-TAC-ERP2-*ATAD3A*-IRES-mCHERRY (3µg) and a piggyBac transposase plasmid (1µg) using Lipofectamine™ 3000. 48 h post-transfection, puromycin treatment started at 1 µg/ml concentration. Growing colonies had integrated *ATAD3A* into their genome.

3.2.4.7. VCP knockdown

VCP targeting siRNAs and non-targeting (NT) siRNA oligonucleotides were designed as described by Paola Magnaghi et al [171]. For identification of optimal concentration of oligonucleotides, HCT116 cells were transfected with different concentrations of VCP siRNAs (1, 2.5, and 5 nM) using Lipofectamine 3000 (Thermo Fisher Scientific). 72 h after transfection, samples were harvested in cell lysis buffer and analyzed by

immunoblotting. To investigate the effect of VCP knockdown on cellular processes using qPCR or immunoblotting, 8×10^4 HCT116 cells per well were grown in DMEM complete medium in 24 well plate overnight. siRNAs transfection performed using 5 nM of siRNA oligonucleotides using Lipofectamine 3000 (Thermo Fisher Scientific). 72 h post siRNA transfection, stimulation performed with MDP or tunicamycin for indicated time points. For evaluating NF- κ B activity by NF- κ B luciferase reporter assay, 24 h after siRNA transfection cells were transfected with 100 ng p55-A2-Luc luciferase reporter plasmid together with 5 ng pTK-Green Renilla plasmid by lipofectamine 3000 (Thermo Fisher Scientific). 72 h post siRNA transfection, MDP stimulation was performed for 4 and 8 h. Cells were lysed in 1x passive lysis buffer (Biotium) and lysates either stored $-80\text{ }^{\circ}\text{C}$ for later use or processed for evaluating luciferase activity the same way as described in part 3.2.4.3.

3.2.4.8. L18-MDP stimulation of NOD2 reconstituted, *ATAD3A* KO or VCP

knockdown HCT116 cells

HCT116 cells were reconstituted with NOD2 (WT, E54K, or L1007fsinsC variants). Reconstituted HCT116 (1.7×10^5 cells per well) were stimulated with $1\text{ }\mu\text{g/ml}$ L18-MDP for 2, 4, and 8 h. Then lysis performed in $350\text{ }\mu\text{l}$ RNA lysis buffer supplemented with β -mercaptoethanol (β -ME) according to the manufacturer's instructions. Lysates stored at $-80\text{ }^{\circ}\text{C}$ or RNA isolation performed as described in 3.2.3.8. *ATAD3A* KO HCT116 cells (1.7×10^5 cells per well) stimulated for 2 and 8 h with $1\text{ }\mu\text{g/ml}$ L18-MDP and lysis was performed as described before. HCT116 cells were transfected with si-NT or si-VCP for 72 h, followed by stimulation with $1\text{ }\mu\text{g/ml}$ MDP for 2, 4, and 8 h and lysed in $350\text{ }\mu\text{l}$ RNA lysis buffer or $60\text{ }\mu\text{l}$ cell lysis buffers for immunoblotting.

3.2.4.9. Tunicamycin stimulation of NOD2 reconstituted, WT NOD2 overexpressing ATAD3A KO or VCP knockdown HCT116 cells

HCT116 cells deficient of NOD2 that were reconstituted with NOD2 (WT, E54K, or L1007fsinsC variants) or HCT116 cells deficient of ATAD3A that were overexpressing WT NOD2 (1.7x10⁵ cells per well) were stimulated with 5 µg/ml tunicamycin for 8 and 24 h then lysis performed in 350 µl RNA lysis buffer supplemented with β-ME according to the manufacturer's instructions. Lysates were stored at -80 °C or RNA isolation performed according to part 3.2.3.8. HCT116 cells were transfected with si-NT or si-VCP for 72 h, followed by stimulation with 5 µg/ml tunicamycin for 8 and 24 h and lysed in 350 µl RNA lysis buffer supplemented with β-ME. For immunoblotting of VCP-silenced cells, tunicamycin stimulation was performed for 4, 8, and 24 h, and cells were lysed in 60 µl lysis buffer.

3.2.5. Protein analysis

3.2.5.1. Protein isolation and normalization

Cells lysis was performed in 1x cell lysis buffer (Cell Signaling) supplemented with 1 mM phenylmethylsulfonyl fluoride and 1x protease inhibitors and stored on ice for 30 min. Centrifugation was performed for 15000 RPM at 4 °C for 10 min and the supernatants were transferred into a new 1.5 ml tube. Normalization of protein amount was conducted by performing a Bradford assay. Appropriate amounts of protein were mixed with 6x Laemmli buffer supplemented with 3 % β-mercaptoethanol and boiled 10 min at 95 °C.

3.2.5.2. SDS- polyacrylamide gel electrophoresis (PAGE) and Immunoblotting

Equal amounts of protein lysate were subjected to 10% SDS-PAGE. Gels were prepared using a mini-protean electrophoresis system (Biorad). As a molecular weight

solution. Primary antibody incubations were performed overnight at 4 °C and secondary antibody incubations for 1 h at room temperature. After each antibody incubation, washing was performed 3x for 10 min in PBS-T buffer. The list of antibodies used in this work is provided in table 3-7.

SuperSignal West Dura detection kit (Thermo-Scientific) was used for Chemiluminescence signals detection. Images were analyzed with ImageLab™ software (Bio-Rad).

3.2.5.3. Silver staining

SDS PAGE silver staining was conducted using silverQuest™ kit (Invitrogen) according to the instructions provided by the manufacturer.

3.2.5.4. Co-immunoprecipitation assays

HEK293t cells were transfected at 70% confluency in 10 cm petri dishes with 10 µg FLAG-NOD2 WT and mutants alone or together with RIPK2 using polyethyleneimine (PEI; Polysciences). 72 h after transfection, cells were washed in PBS and harvested in RIPA buffer. Lysates were kept for 30 min on ice and then harvested by centrifugation at 15000 rpm for 20 min. Supernatants were transferred to fresh eppies. 10 % of the lysates were kept as input and the lysate was incubated with Anti-FLAG M2 Affinity Gel (Sigma-Aldrich) for 7 h at 4 °C on the rocker platform. Beads were washed with 3x in RIPA buffer 2000rpm, 2 min, 4 °C. To elute bound proteins, beads resuspended in 1x Laemeli buffer (supplemented with 3% β-mercaptoethanol and diluted in RIPA buffer) and boiled at 95 °C for 10 min. After a short centrifugation step, the supernatant was transferred to fresh eppies.

3.2.5.5. Purification of endogenous Ub conjugates

5 x 10⁵ NOD2 KO HCT116 cells reconstituted with WT or mutant NOD2 variants were seeded in 6 well plates in DMEM complete medium. The day after, stimulation was

performed with 200 ng/ml L18-MDP for 1 and 2 h. Cells were washed in PBS and harvested in 500 μ L cell lysis buffer. Pull down of ubiquitinated proteins was conducted using Tandem Ubiquitin Binding Entities (TUBEs, LifeSensors) according to the manufacturer's instructions.

3.2.5.6. Evaluating NF- κ B and MAPK signaling on PBMCs and neutrophils by immunoblotting

Serum starvation was performed by incubating cells in RPMI medium without FBS in 96 well plates for 1-2 h. Stimulation was conducted using L18-MDP (10 μ g/ml) or LPS (1 μ g/ml) for 10 and 30 min. Cell lysis was performed the same way as described in part 3.2.5.1.

3.2.5.7. Investigating the effect of ATAD3A on NOD2 protein level

HEK293T seeded in 12 well plates (2×10^5), were transfected with 2 μ g of the following constructs using PEI as described in part 3.2.4.2.1:

- _ pRRL-Flag-hNOD2-IRES-mCD24
- _ pRRL-hRIPK2-IRES-RFP
- _ pRRL-hATAD3-IRES-GFP

Constructs were transfected either alone or two together or all together. 72 h post-transfection, cells were incubated with medium alone or supplemented with (20 μ M) MG-132 for 8 h. Cells were harvested and lysed in lysis buffer prepared as follows: 10 Mm Tris-HCL PH-7.5, 150 Mm NaCl, 0.5 mM EDTA, 0.5 % NP-40, 1 mM phenylmethylsulfonyl fluoride, 1x protease inhibitors cocktail.

HEK293T cells constitutively expressing ATAD3A upon doxycycline were transfected with 500 ng pRRL-Flag-hNOD2-IRES-GFP or pRRL- hVCP-IRES-GFP or pRRL-h RASGRP1-IRES-RFP. 24 h after transfection, cells were incubated in medium alone

or supplemented with 200 ng/ml or 1 µg/ml doxycycline for 24 h. Samples were harvested in cell lysis buffer for immunoblotting.

3.2.6. Flow Cytometry

Quantitative and qualitative sample acquisition was conducted on an LSRFortessa flow cytometer and analysis of raw data was done using FlowJo v9.

3.2.6.1. Cell sorting

Lentivirally transduced cell lines were harvested and washed once with ice-cold PBS. Cell pellets were resuspended in 400-700 µl PBS containing 2% FCS. Samples were filtered through a 35 µm nylon mesh. Cells were analyzed and sorted on a FACSAria™ III sorter using a 100 µm nozzle and flushed into 15 ml falcons containing cell culture medium. Sorted cells were centrifuged (10 min, 1200 RPM, RT) and resuspended in a fresh medium.

3.2.6.2. Immunophenotyping of peripheral blood mononuclear cells

For immunophenotypical analysis, blood samples were washed with PBS, and cells were collected by centrifugation (10 min, 300 g, RT). 150 µl of blood was mixed with 50 µl brilliant stain buffer containing monoclonal antibodies as indicated in table 3-8 and incubated for 20 min at RT light protected. Next, red blood cells were removed using 1x FACS lysing solution according to the manufacturer's instructions. Cells were washed twice with ice-cold PBS, resuspended in 500 µl PBS containing 2% FCS and FACS analyzed.

3.2.6.3. In vitro activation and proliferation analysis of B cells

PBMCs were labeled with 0.5 µM Carboxyfluorescein succinimidyl ester (CFSE) (ThermoFisher/ebioscience) and cultured in the absence or presence of recombinant human CD40 ligand/TNFSF5 (200 ng/ml) (R&D), Hemagglutinin/HA peptide antibody

(R&D Systems) alone or together with IL-4 (200 ng/ml) (PeproTech) and IL-21 (50 ng/ml) (PeproTech) or CpG (1 µg/ml) (InvivoGen) for 5-9 days. B cell proliferation was assessed by analyzing CFSE dilution after 4-6 days. Cells were harvested and were stained with BD Horizon Fixable Viability Stain 450 (BD), CD19 (BD), CD27 (BD), and CD38 (BD) antibodies to investigate plasmablast differentiation. Cells were acquired using an LSRFortessa™ flow cytometer (BD Biosciences) and analyzed with Flowjo V9 software (TreeStar).

3.2.6.4. Analysis of CD62L shedding on neutrophils upon L18-MDP stimulation

Isolated neutrophils were cultured in RPMI medium without FBS in the absence or presence of 10 µg/ml L18-MDP. At each time point, cells were harvested in ice-cold PBS and kept on ice. Staining of cells was performed for all the time points at the same time using CD62L antibody diluted in PBS for 20 min, on ice, light protected. Cells were washed and resuspended in PBS. Acquisition was performed using an LSRFortessa Flow Cytometer (BD Bioscience), and data were analyzed with FlowJo Software (TreeStar).

3.2.6.5. In vitro T cell activation

2×10^5 cells/well freshly isolated PBMCs were stained with 0.5 µM CFSE and stimulated with 0.1 µg/ml anti-CD3 with and without 1 µg/ml soluble anti-CD28 in a 96-well plate. Medium was changed the day after and cells were kept in culture for 5 days. Consequently, cells were washed with PBS and incubated on ice with anti-CD3, anti-CD4, and anti-CD28 for 20 min, light-protected. After washing with PBS, cells were resuspended in 300 µl PBS containing 2% FCS and analyzed by flow cytometry

3.2.6.6. Intracellular flow cytometry to measure TNF α

1–1.5 $\times 10^6$ PBMCs/well were seeded in Iscove's modified Eagle's medium (IMDM) (Gibco, Life Technologies), 10% fetal bovine serum (FBS) in a 24-well plate and rested overnight. The next day, non-adherent cells were washed away and the remaining adherent cells were incubated with the medium alone or supplemented with either 200 ng/ml L18-MDP or 200 ng/ml LPS (Sigma-Aldrich) in the presence of Golgistop (BD Biosciences) for 2.5 h. Cells were washed with PBS and surface staining was performed for CD3 and CD14 by incubating the cells resuspended in PBS/2% FCS with antibodies for 20 min on ice, light protected. Subsequently, cells were fixed and permeabilized using Cytofix/Cytoperm Kit (BD Bioscience) and stained for intracytoplasmic TNF α according to the manufacturer's protocol.

3.2.6.7. Cell death analysis

NOD2 WT reconstituted and *NOD2* KO HCT116 cells were transfected with VCP siRNA oligonucleotides and stimulated with tunicamycin for 24 h as described under 3.2.4.9. Cells were washed with PBS and stained with Annexin V (Thermo Fisher Scientific) and DAPI according to the provided protocol by the company.

HEK293T cells constitutively expressing ATAD3A upon doxycycline treatment were seeded (1×10^5 cells per well) in a 24 well plate in a complete DMEM medium. The day after, cells were treated with 0.5 or 1 $\mu\text{g/ml}$ doxycycline for 24 h and subsequently stained with Annexin V/Dapi and analyzed by flow cytometry.

3.2.7. Nano-LC MS/MS analysis

Samples were briefly separated on an SDS gel (SERVAGel TG PRiME 4-20%, Serva, Heidelberg, Germany). Gels were stained with Coomassie (Simply Blue, Expedeon, San Diego, USA) and the part containing proteins was cut out. After destaining with (50 % acetonitril, 50 mM NH₄HCO₃), gel slices were subjected to in-gel digestion

conducted as follows: first gel slices were incubated in 45 mM DTE/50 mM NH₄HCO₃ for 30 min at 55 °C followed by incubation for 30 min in 100 mM iodoacetamide/50 mM NH₄HCO₃. For In-gel digestion, incubation with 0.7 µg Trypsin was performed at 37 °C overnight. Analysis of samples was conducted by nano-LC MS/MS Ultimate 3000 nano liquid chromatography system (ThermoFisher Scientific,) coupled to a TripleTOF 5600+ instrument (Sciex). Solvent A composed of 0.1% formic acid and solvent B, acetonitrile with 0.1% formic acid. Peptides separation was performed on an Acclaim PepMap RSLC C18 column (75 µm x 50 cm, Thermo Fisher Scientific) at a flow rate of 200 nL/min using the following gradient: from 2 % B to 25 % B in 120 min followed by 25 % B to 50 % B in 10 min. The ion source was performed at a needle voltage of 2.3 kV. Mass spectra were obtained in cycles of one MS scan from 400 m/z to 1250 m/z and up to 40 data dependent MS/MS scans of the most intensive peptide signals. MaxQuant software platform [172] together with the Human subset of the UniProt database were employed for protein identification (FDR < 1 %) and label-free quantification.

3.2.8. Statistics

Statistical evaluation of experimental data was performed using GraphPad Prism v6. To analyze quantitative data sets two-way repeated measures ANOVA was employed. P values < 0.05 were considered statistically significant. Sample numbers are referred to as n unless indicated otherwise.

4. Results

4.1. Identification of a patient with biallelic mutation in the first CARD domain of NOD2

The index patient (II-1) who was born to consanguineous parents from Afghanistan presented with intractable diarrhea, recurrent perianal candida dermatitis responsive to topical antifungal treatment, hemophagocytic lymphohistiocytosis (HLH), and prolonged Norovirus infection. Whole exome sequencing was conducted to investigate the genetic etiology of the disease. A rare missense mutation was identified in *NOD2* (ENST00000300589) (c.160G>A, p.Glu54Lys) and in *STXBP2* (ENST00000441779) (c.949C>G, p.Leu317Val). Sanger sequencing confirmed the segregation of both mutations in the family. *In silico* analysis was performed using PolyPhen-2 and SIFT to assess the predicted effect of the variants on the function of both proteins [173, 174]. While the missense mutation in *NOD2* is predicted to be probably damaging and deleterious (Polyphen 0.996, Sift 0), the *STXBP2* variant is considered as a benign and tolerated variant (Polyphen 0.326, Sift 0.56).

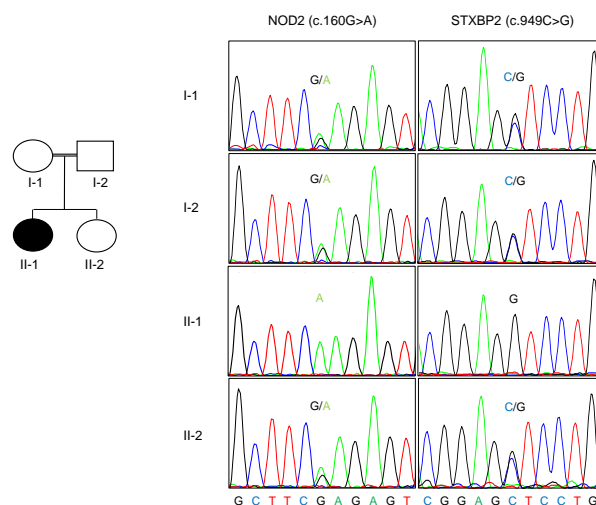


Figure 4-1 Confirmation of *NOD2* and *STXBP2* variants segregation in the family. Sanger sequencing of the amplified PCR product. Both variants showed a homozygous pattern in the index patient and a heterozygous pattern in parents.

4.2. Immunophenotyping of Peripheral Blood Mononuclear Cells revealed impaired B cell activation and proliferation in the index patient

Immunophenotypic analysis of PBMCs revealed markedly reduced peripheral CD19⁺ and class-switched (CD19⁺IgD⁻CD27⁺) B cell counts in the index patient as compared with healthy donors. Furthermore, the patient showed increased frequencies of immature CD19⁺CD38^{Hi}CD10^{Hi} B cells accompanied by decreased expression of CD21 in (CD19⁺CD38⁺) cells, also increased level of IgM as depicted in (CD19⁺IgM⁺IgD⁺) B cell subsets and higher frequency of transitional (CD19⁺CD38^{Hi}IgM^{Hi}) B cells. Further analysis of the B-cell compartment revealed an increased number of germinal center founder (CD19⁺CD38^{Hi}IgD^{Hi}) population in our index patient (Fig 4-2). To investigate the B cell proliferative capacity, CFSE dilution was assessed in PBMCs that were cultured in medium alone or supplemented with CD40L and CpG or CD40L, *IL21*, and *IL4*. In line with impaired B cell maturation, PBMC-derived B cells from the index patient were characterized by reduced proliferation and decreased differentiation of plasmablasts (CD19⁺CD38^{Hi}CD27^{Hi}) upon stimulation with CD40L in combination with *IL4* and *IL21*. However, no obvious differentiation was observed in cells stimulated with CD40L together with CpG in all samples (Fig 4-3). The observed B cell deficiency in our index patient could be attributed to the STXBP2 variant that has previously been shown to be associated with reduced percentages of IgM⁺ CD27⁺ marginal zone-like B cells and IgM⁻CD27⁺ class-switched memory B cells [175].

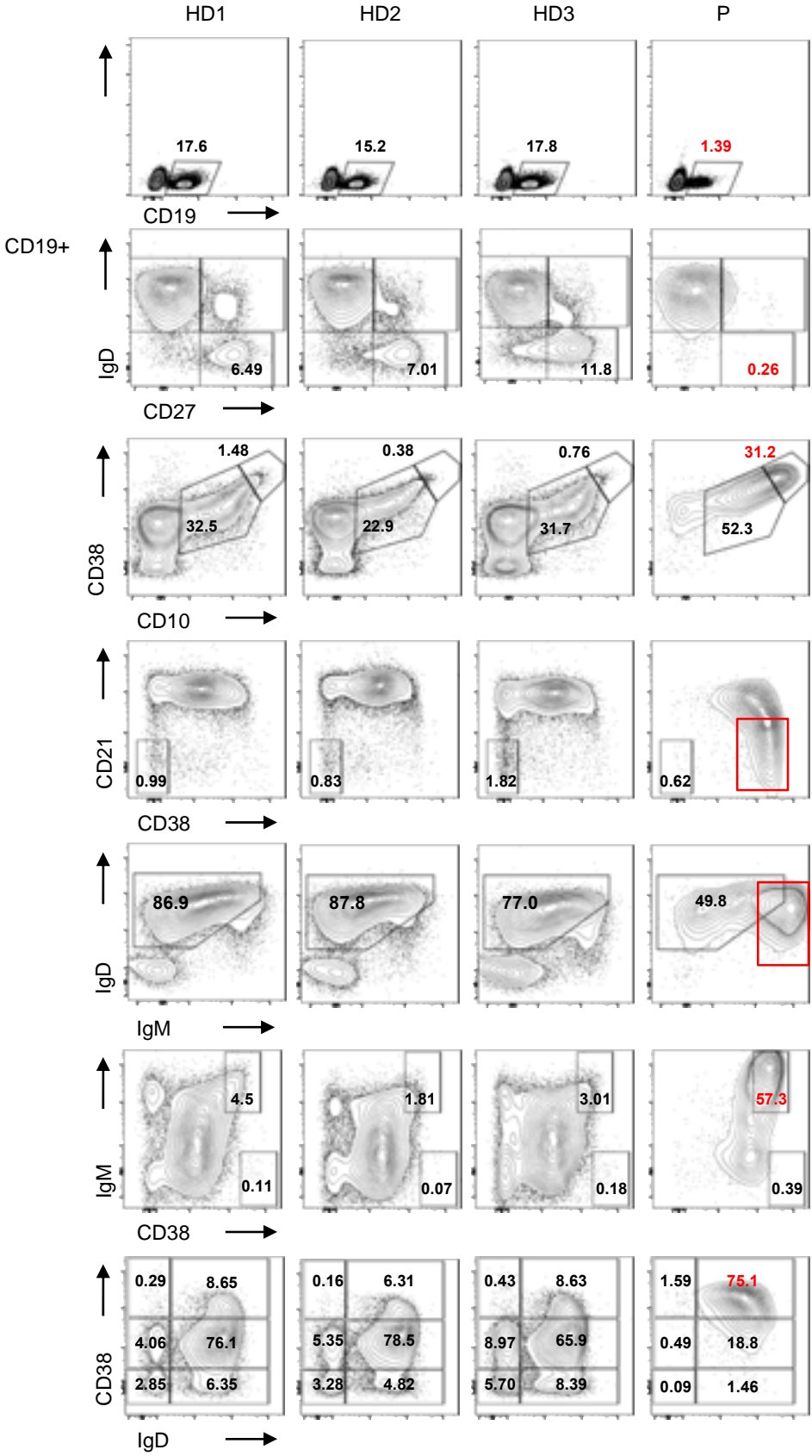


Figure 4-2 Immunophenotyping of B cells. Representative FACS analysis of B cell subset immunophenotyping. HD, healthy donor; P, patient.

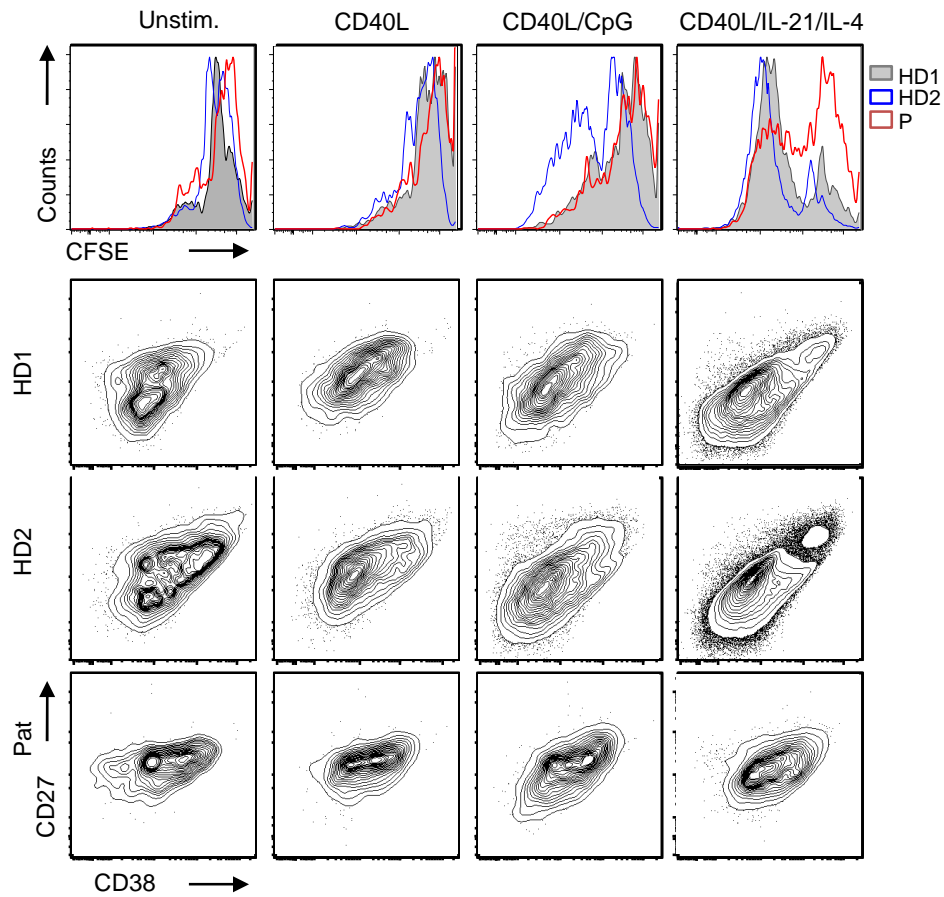


Figure 4-3 B cell proliferation and plasmablasts differentiation. Representative FACS of PBMCs treated with CD40L (200 ng/ml) alone or together with CpG (1 μ g/ml) or IL-4 (200 ng/ml) and IL-21 (50 ng/ml). In the upper panel, B cell proliferation was assessed by measuring CFSE dilution in different conditions. In the lower panel, plasmablast differentiation was determined by staining for CD38 and CD27 in CD19⁺ cells. HD, healthy donor; Pat, patient.

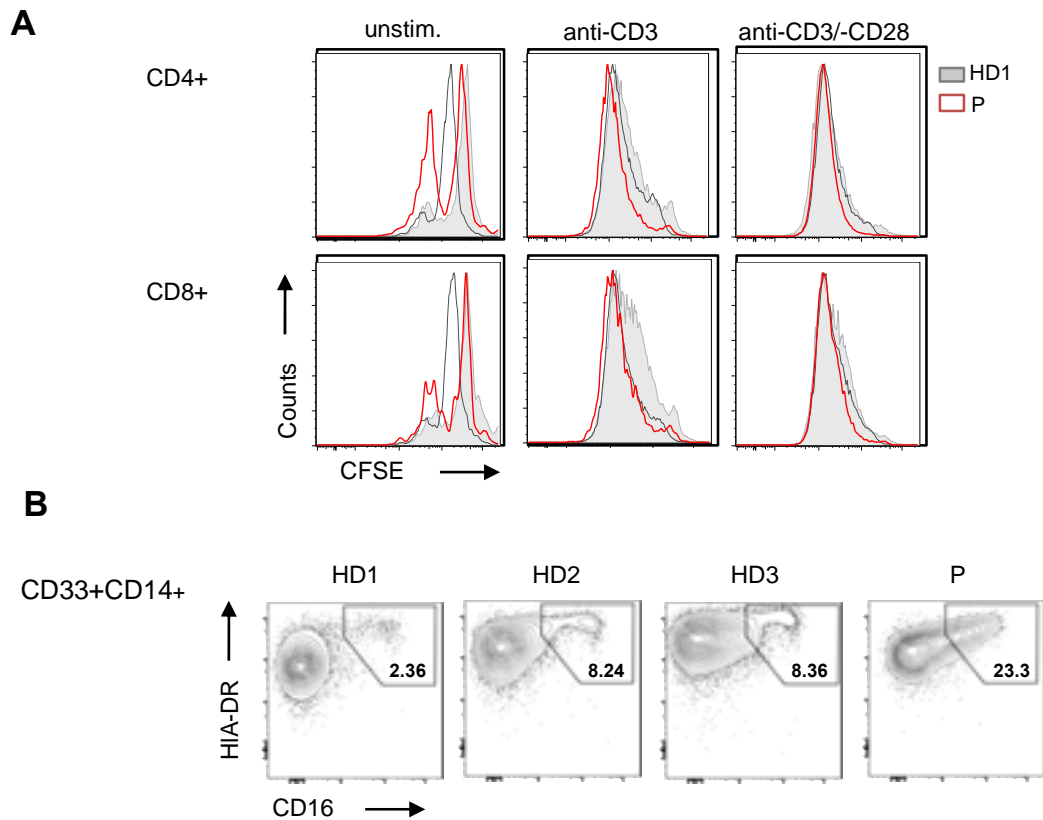


Figure 4-4 Immune phenotyping of T cells and monocytes. (A) T cell proliferation assay upon anti-CD3, anti-CD3, and anti-CD28 stimulation. (B) Immunophenotyping of monocytes (CD33⁺CD14⁺). HD, healthy donor; P, patient.

In addition to B cell subsets, patient T cell proliferation was next. T cell proliferation upon stimulation with anti-CD3 alone or in combination with anti-CD28 did not reveal any differences as compared with healthy donor and father, (Fig 4-4, A). Further flow cytometric analysis revealed an increased proportion of proinflammatory monocytes (CD33⁺CD14⁺CD16⁺ HLA-DR⁺) (Fig 4-4, B).

4.3. Evaluating NOD2 mediated signaling in patient primary cells

4.3.1. Impaired L18-MDP-induced TNF α production in patient's PBMC-derived monocytes

MDP challenge has been shown to trigger nuclear factor-kB (NF-kB) and MAPK signaling cascade and subsequently production of proinflammatory cytokines such as

TNF α , IL-6, and IL-8 [33]. To ascertain whether the NOD2 mutation E54K influenced L18-MDP-mediated signaling, the intracytoplasmic level of TNF α was elucidated in PBMC-derived monocytes from the index patient and healthy controls by FACS. As a control, cells were stimulated with LPS which can induce NF- κ B pathway activation and subsequent TNF α production independent of NOD2. Whereas all samples responded comparably to LPS, MDP-induced TNF α production was impaired in patient-derived cells as compared with healthy donors (Fig 4-5).

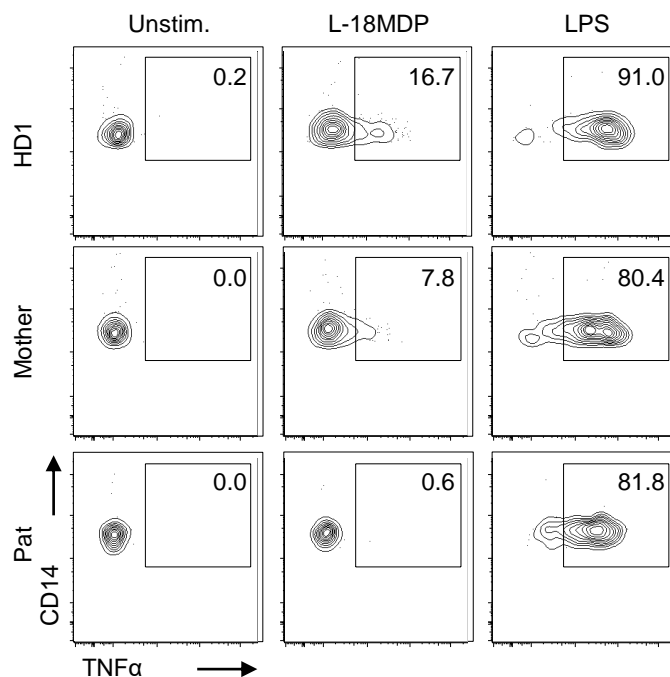


Figure 4-5 Impaired MDP responses of patient-derived monocytes. Representative FACS analysis of intracytoplasmic TNF α staining on PBMC-derived monocytes stimulated with L18-MDP (200 ng/ml) and LPS (200 ng/ml) for 2-3 h in the presence of Golgi stop (n=3). HD, healthy donor; Pat, patient.

4.3.2. Abrogated nuclear factor- κ B (NF- κ B) and mitogen-activated protein

kinase (MAPK) signaling in patient 's primary cells upon stimulation with MDP

To investigate NF- κ B and MAPK activation triggered by MDP in greater detail, the patient's PBMCs and neutrophils were serum starved for 2-3 h then stimulated with L18-MDP and LPS for indicated time points and NF- κ B and MAPK signaling were

analyzed by Western immunoblotting. Immunoblotting revealed impaired phosphorylation of the NF- κ B p65 subunit (Ser536), ERK1/2 (Thr202/Tyr204), and p38 (Thr180/Tyr182) in PBMCs (Fig 4-6, A) and reduced phosphorylation of ERK1/2 and p38 in neutrophils of the patient upon L18-MDP treatment compared with healthy donors (Fig 4-6, B).

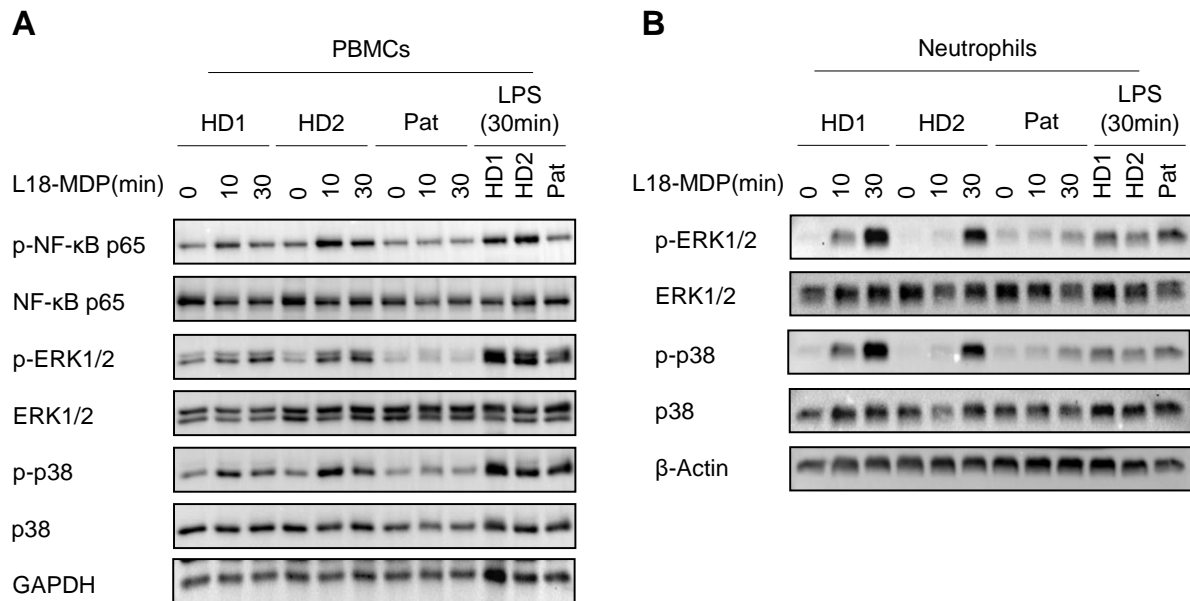


Figure 4-6 Impaired nuclear factor- κ B (NF- κ B) and mitogen-activated protein kinase (MAPK) signaling in patient's primary cells upon stimulation with MDP. (A) Representative immunoblotting (n = 3) of serum starved PBMCs from patient (pat) and two healthy donors (HD) stimulated with L18-MDP (10 μ g/ml) and LPS (1 μ g/ml) for 0, 10, and 30 min. (B) Representative immunoblotting (n = 2) of serum starved neutrophils from patient (pat) and two healthy donors (HD) stimulated with L18-MDP (10 μ g/ml) and LPS (1 μ g/ml) for 0, 10, and 30 min.

4.3.3. Impaired CD62L shedding on Patient's neutrophils upon MDP stimulation

Given the impaired MDP-induced NF- κ B activation observed in patient's neutrophils, it was interesting to test whether activation of neutrophils upon MDP treatment was affected as well. To examine this, CD62L shedding was investigated from neutrophils upon L18-MDP stimulation. CD62L is an adhesion molecule that is constitutively expressed in resting neutrophils. When neutrophils are activated, CD62L is

enzymatically cleaved [176-178]. Neutrophils from the index patient and two healthy donors were isolated using Ficoll and stimulated with L18-MDP for indicated time points. Samples were stained for CD62L and acquisition of CD62L stained cells was performed on the LSRFortessa™ flow cytometer. Even though all samples responded to MDP, patient cells showed a substantially reduced shedding based on the mean fluorescence signal (Fig 4-7).

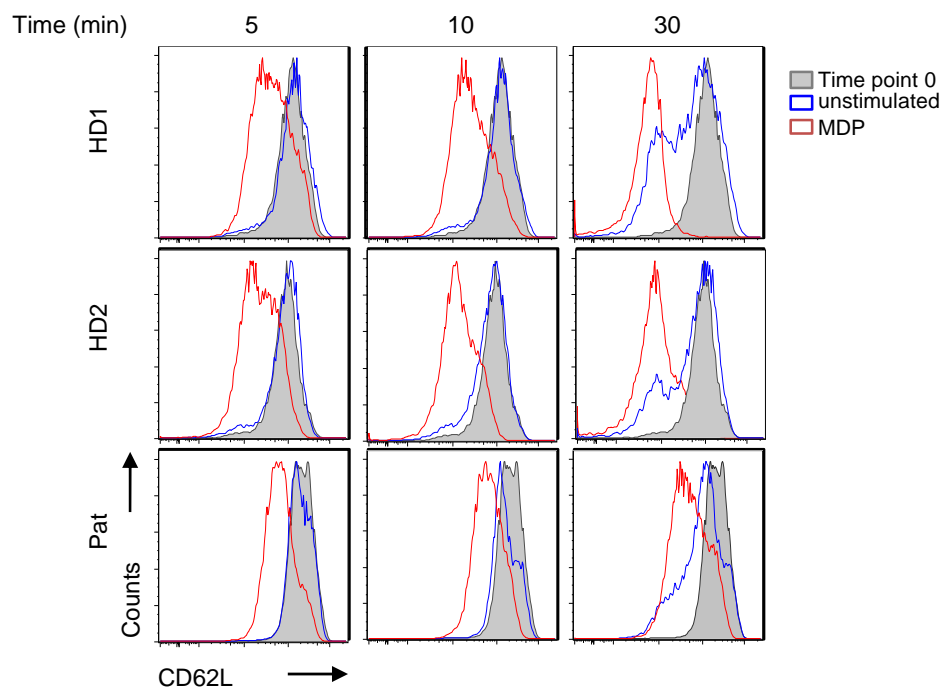


Figure 4-7 impaired CD62L shedding on neutrophils upon MDP stimulation. Neutrophils from the patient and two healthy donors were stimulated with L18-MDP (10 $\mu\text{g}/\text{ml}$) for 0, 5, 10, and 30 min. For each time point unstimulated sample was measured as CD62L is spontaneously shed from cultured cells without stimulation (n=3). HD, healthy donor; Pat, patient.

4.4. Evaluating NOD2-mediated signaling in *NOD2*-deficient heterologous cell lines

4.4.1. Impaired NF- κ B activity in HEK293T cells overexpressing mutant NOD2

To gain insights into the effect of identified NOD2 variant in transcriptional activity of NF- κ B, luciferase-based reporter assays were employed. Cells were co-transfected

with p55-A2-luciferase reporter plasmid containing the NF- κ B binding sites upstream of the firefly luciferase and pTK-Green Renilla plasmid as an internal control to normalize for transfection efficiency. HEK293T cells were transiently transfected with a construct encoding IRES-RFP control or NOD2 WT or the E54K variant. As a positive control, CD-associated NOD2 variant L1007fsinsC was also included in this study which encodes for a truncated NOD2 protein that has been previously shown to abrogate MDP-mediated NF- κ B activation [81]. While MDP stimulation significantly increased NF- κ B activity in cells overexpressing WT NOD2, for both mutant variants the relative luciferase signal was comparable to the RFP control indicating impaired response to MDP (Fig 4-8).

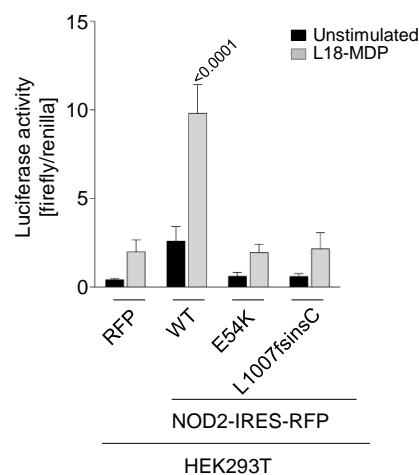


Figure 4-8 Impaired NF- κ B activation upon L18-MDP stimulation. NF- κ B luciferase reporter assay in HEK293T cells overexpressing NOD2 WT or variants stimulated with 200 ng/ml L18-MDP. Data represent mean \pm SEM of three independent experiments.

4.4.2. Impaired NOD2-mediated signaling in colon carcinoma-derived HCT116 cells overexpressing E54K variant

NOD2 protein has been shown to be expressed in immune cells as well as intestinal epithelial cells. To investigate the pathomechanism of the mutation in the context of intestinal inflammation, colon carcinoma-derived HCT116 were engineered with

CRISPR-Cas9 to delete endogenous NOD2 and subsequently reconstituted by lentiviral overexpression of NOD2 WT and mutants (E54K and L1007fsinsC). Due to the lack of a NOD2 specific antibody, putative knock-out (KO) clones were screened and confirmed functionally by determining defective MDP-mediated signaling using the NF- κ B luciferase reporter system (Fig 4-9).

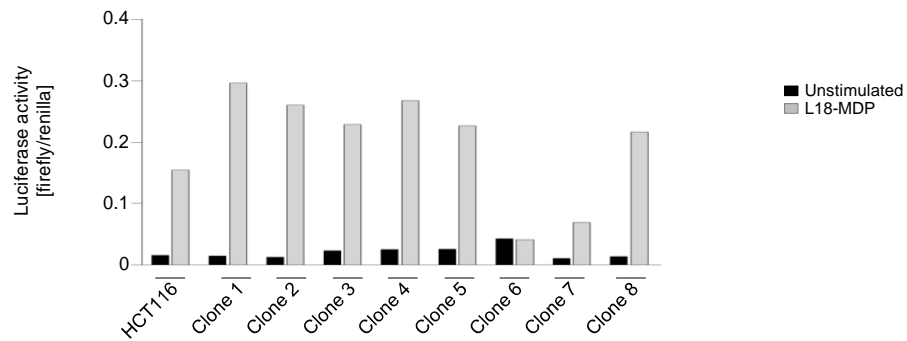


Figure 4-9 Screening NOD2 KO HCT116 cells using NF- κ B luciferase reporter assay. Putative KO clones were stimulated with MDP (200 ng/ml) and NF- κ B activity was investigated using luciferase signal. Unmodified HCT116 cells were included as a control.

Subsequently, these cells were stimulated with L18-MDP and the level of the proinflammatory cytokine IL-8 was measured using quantitative PCR (q-PCR). MDP treatment significantly (p -value <0.0001) increased IL-8 mRNA level in NOD2 WT cells but not in both variants E54K and L1007fsinsC (Fig 4-10, A). Afterward, considering the NOD2 function in driving inflammation induced by ER stress, the reconstituted HCT116 cells were stimulated with tunicamycin. Tunicamycin is a drug derived from *Streptomyces sp.* inducing ER stress through inhibition of N-linked protein glycosylation. Analyzing IL-8 mRNA level by qPCR revealed, while cells overexpressing WT and L1007fsinsC variant displayed increased IL-8 transcriptional level upon tunicamycin challenge, E54K overexpressing cells showed abrogated response (Fig 4-10, B).

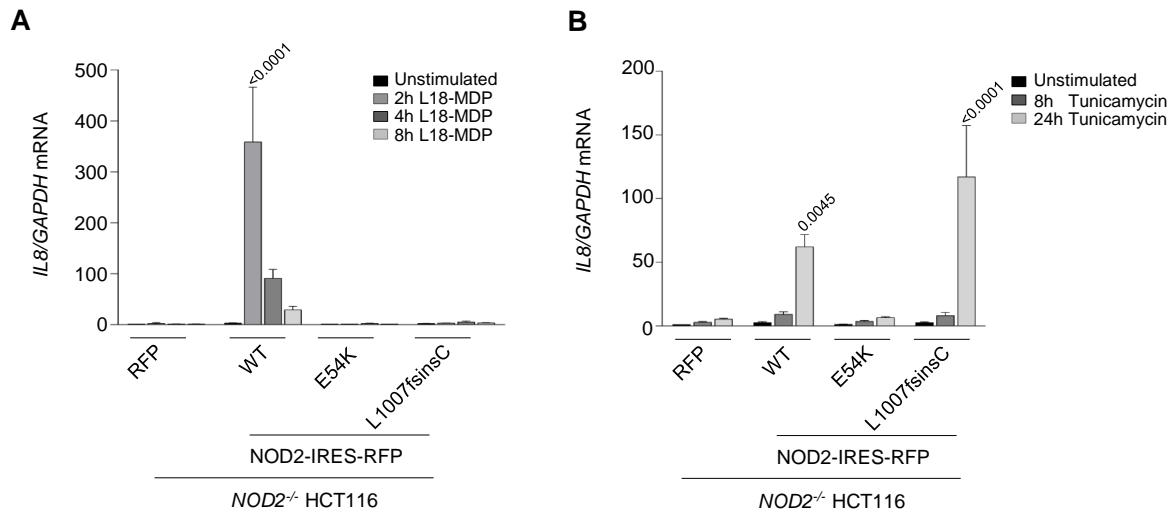


Figure 4-10 Impaired NOD2-mediated signaling upon MDP or tunicamycin stimulation. (A) Quantitative RT-PCR analysis of IL-8 transcriptional level upon L18-MDP stimulation (1 μ g/ml) on heterologous HCT116 cells for 0 h, 2 h, 4 h, and 8 h (n=3). (B) quantitative RT-PCR analysis of IL-8 transcriptional level upon tunicamycin stimulation (5 μ g/ml) on heterologous HCT116 cells for 0 h, 8 h, and 24 h (n=5). Data represent mean \pm SEM.

4.5. Evaluating NOD2 interacting proteins

4.5.1. Impaired interaction of the NOD2 variant E54K with RIPK2

Upon MDP treatment, NOD2 oligomerizes and interacts with RIPK2 through its CARD domains leading to activation of NF- κ B and MAPK signaling [17]. As the identified mutation E54K resides in the first CARD domain, NOD2 and RIPK2 interaction was investigated in HEK293T cells ectopically overexpressing FLAG-tagged NOD2 WT or mutants (E54K and L1007fsinsC) along with WT RIPK2. NOD2 pull-down was performed using agarose beads conjugated with anti-Flag antibodies. Immunoblotting revealed that NOD2 WT and L1007fsinsC variant interacted with RIPK2 however, E54K showed impaired interaction (Fig 4-11). These data are consistent with previous studies demonstrating the interaction of L1007fsinsC NOD2 variant with RIPK2 [179].

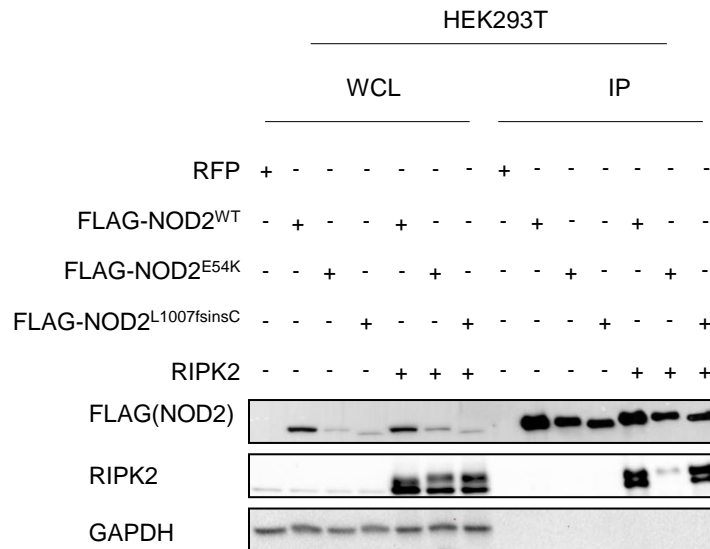


Figure 4-11 Impaired RIPK2 interaction. Representative immunoblotting of NOD2 pull down on HEK293T transiently transfected with Flag-NOD2 WT or mutants alone or along with RIPK2 (n=3). RIPK2 immunoblotting revealed interaction with WT and L1007fsinsC NOD2 but no interaction with the E54K variant.

4.5.2. Abrogated RIPK2 ubiquitination in HCT116 cells overexpressing mutant NOD2 upon L18-MDP stimulation

Upon stimulation, oligomerized NOD2 recruits a complex including RIPK2 and different E3-ubiquitin ligases including cIAP1/2, XIAP, OTULIN, and Pellino3 leading to K63- or M1-linked ubiquitination of RIPK2 [45, 47, 48, 180, 181]. To assess the effect of the identified mutation on RIPK2 ubiquitination, tandem ubiquitin-binding entities (TUBEs) were employed to affinity purify endogenous ubiquitin conjugates in heterologous HCT116 cells reconstituted with NOD2 WT, E54K, or L1007fsinsC variant upon MDP stimulation. While stimulation of HCT116 cells overexpressing WT NOD2 induced RIPK2 ubiquitination, HCT116 cells overexpressing NOD2 E54K and L1007fsinsC variants exhibited impaired ubiquitination of RIPK2 (Fig 4-12). These data suggest that the RIPK2 interaction is necessary but not sufficient for signal transduction and disclose ubiquitination as possibly a critical step for signal propagation upon NOD2

activation. Ligand-dependent degradation of NOD2 and RIPK2 has been reported as a possible underlying mechanism mediating tolerance to bacterial cell wall components. A reduced level of RIPK2 was observed only in HCT116 cells overexpressing WT NOD2 might be due to the tolerance mechanism activated upon NOD2 overexpression and MDP stimulation.

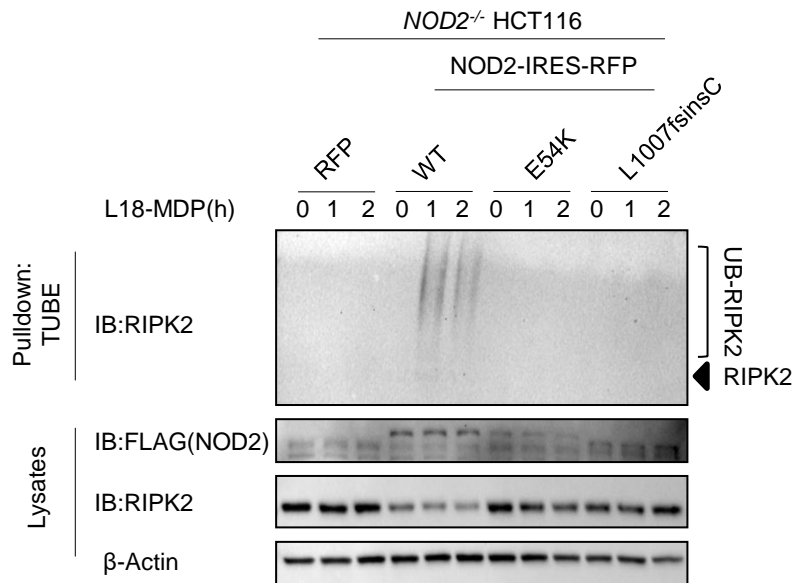


Figure 4-12 Impaired RIPK2 ubiquitination upon MDP stimulation. Representative immunoblotting of TUBE pull-downs from heterologous HCT116 cells treated with L18-MDP (200 ng/ml) for 0 h, 1 h, and 2 h (n=2). Ubiquitin-conjugated proteins were purified from whole cell lysates. Immunoblotting on pulled down samples using RIPK2 antibody showed a band in cells overexpressing WT NOD2 at RIPK2 size plus smear at higher molecular weight indicating of RIPK2 ubiquitination upon MDP stimulation.

4.5.3. Immunoprecipitation-coupled mass spectrometry unveiled novel NOD2-interacting proteins

Based on the effect of NOD2 E54K in abrogating NOD2 PGN-dependent and independent signaling, the NOD2 interactome was studied by immunoblotting of cell lysates from immunoprecipitation (IP) experiments on HEK293 cells with ectopic expression of wild-type or mutant NOD2 alone or together with RIPK2. Silver staining of the SDS-page revealed different bands in the IP part comparing WT and NOD2

variants. In particular, we could detect a band with a molecular weight at around 100 KDa in WT samples that was absent in both variants (Fig 4-13). To gain a better understanding of the differences in the interactome of WT NOD2 compared with the two mutant variants E54K and L1007fsinsC, IP samples were analyzed using a nano liquid chromatography tandem mass spectrometry (LC-MS/MS). Among the identified NOD2 interacting proteins, VCP and ATAD3A were chosen based on the function and the size of the proteins that corresponded to the silver staining bands.

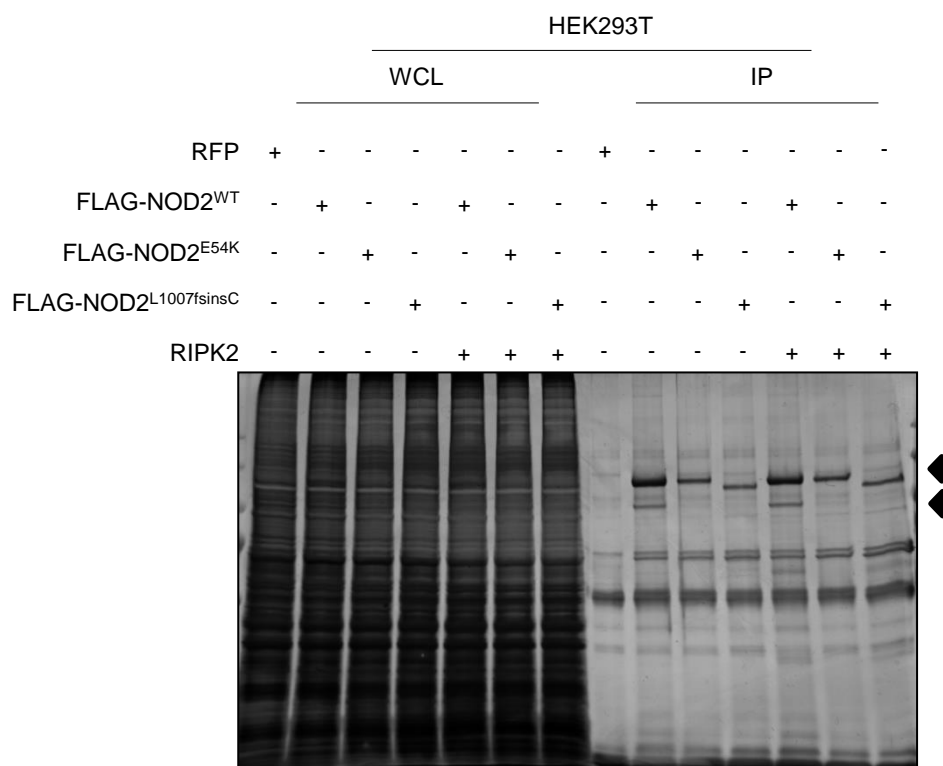


Figure 4-13 Different pattern of protein bands in cells overexpressing WT NOD2 compared with E54K variant. Representative SDS-Page and silver staining (n = 3) of cell lysates from immunoprecipitation experiments on HEK293T cells transiently transfected with NOD2 WT or mutants (E54K and L1007fsinsC) alone or together with RIPK2.

Immunoblotting confirmed the interaction of the identified proteins with NOD2 (Fig 4-14, A and B). VCP is a 97 KD protein that showed compromised interaction with E54K and L1007fsinsC variants. ATAD3A exhibited reduced interaction with both variants.

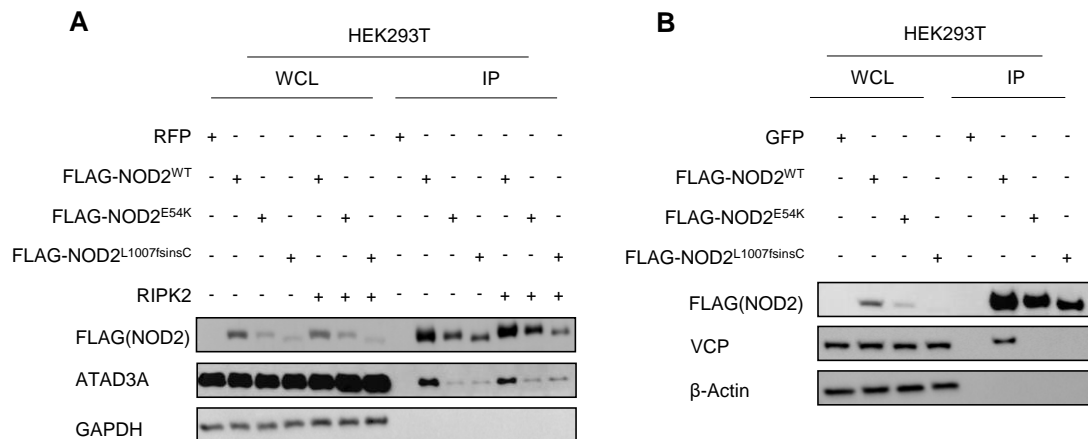


Figure 4-14 Identification of VCP and ATAD3A as novel NOD2 interacting proteins. (A and B) representative immunoblotting of NOD2 pull down on HEK293T cells transiently transfected with Flag-NOD2 WT or mutants along with RIPK2 (n=3). Samples were immunoprecipitated using anti-Flag beads. ATAD3A and VCP immunoblotting on precipitates (IP) revealed interaction of WT NOD2 with ATAD3A and VCP.

4.5.4. Evaluating NOD2-mediated signaling in HCT116 cells with *ATAD3A* KO

4.5.4.1 Increased MDP-triggered NOD2 signaling in *ATAD3A* KO HCT116 cells

To assess the function of the newly identified interaction partners in NOD2-mediated signaling, guide RNAs were designed that target *ATAD3A*. Alt-R® CRISPR-Cas9 genome editing system was used for generating KOs. After electroporation, cells were single-sorted into 96-well plates on a BD FACSAria, and screening was performed on growing colonies. Immunoblotting revealed 3 *ATAD3A* KO clones as the *ATAD3A* protein could not be detected using *ATAD3A* specific antibody (Fig 4-15).

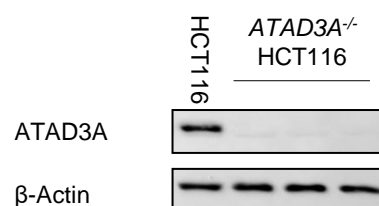


Figure 4-15 Confirmation of *ATAD3A* Knock out in HCT116 cells. Immunoblotting of HCT116 cells and *ATAD3A* KO HCT116 (3 different clones). CRISPR-Cas9 genome

editing system together with two specific sgRNAs targeting different regions of the gene were used for generating *ATAD3A* KO cells.

To elucidate the putative role of *ATAD3A* in the NOD2 signaling pathway, first *ATAD3A* KO HCT116 cells were stimulated with canonical NOD2 stimuli, L18-MDP and the transcriptional level of IL-8 was measured using qPCR. MDP stimulation induced a significantly higher level of IL-8 mRNA in *ATAD3A* KO HCT116 cells as compared with unedited cells (Fig 4-16, A). Next, the NOD2 function in mediating inflammation during ER stress was examined by stimulating *ATAD3A* KO HCT116 cells overexpressing WT-NOD2 with the ER stress inducer tunicamycin. HCT116 cells stimulation with tunicamycin did not significantly induce IL-8 expression. It has been speculated that this might be overcome by overexpressing of NOD2 in these cells. For that reason, tunicamycin response was measured in HCT116 WT and *ATAD3A* deficient cells that were lentivirally transduced with the NOD2 WT construct. No difference was observed between NOD2 overexpressing *ATAD3A* KO and WT HCT116 cells in the mRNA level of proinflammatory cytokine IL-8 after tunicamycin stimulation (Fig 4-16, B).

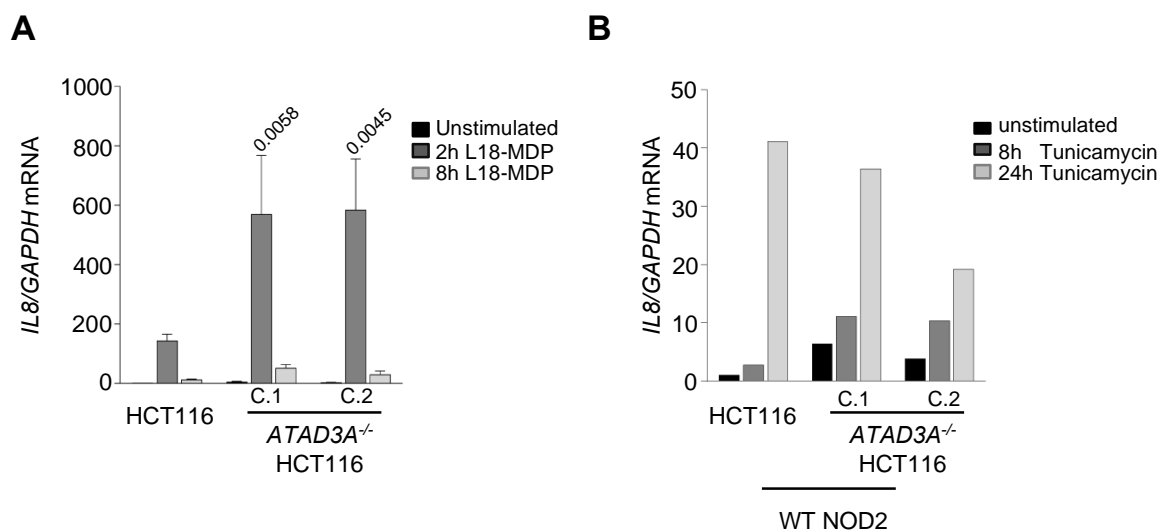


Figure 4-16 *ATAD3A* Knockout resulted in enhanced interleukin-8 production in HCT116 cells upon MDP stimulation. (A) IL-8 qPCR in *ATAD3A* KO HCT116 upon MDP stimulation (1 μ g/ml) for 0 h, 2 h, and 8 h (B) IL-8 qPCR in NOD2 overexpressing *ATAD3A* KO HCT116 cells upon tunicamycin stimulation (5 μ g/ml) for

0 h, 8 h, and 24 h (B). A is representative of three independent experiments and data are represented as mean \pm SEM. C.1 is clone 1 and C.2 is clone 2.

4.5.4.2. ATAD3A overexpression induced degradation of NOD2 associated with higher rate of cell death

Given the significant higher level of IL-8 mRNA level in *ATAD3A* KO cells upon MDP stimulation, it has been speculated that ATAD3A might negatively regulate NOD2 signaling by controlling the turnover of NOD2 or its direct interaction partner RIPK2. To test the hypothesis, HEK293T cells were transiently transfected with ATAD3A, NOD2, and/or RIPK2. 72 h after transfection, cells were treated with the proteasome inhibitor MG132. ATAD3A co-overexpression with NOD2 and RIPK2 reduced the protein levels of NOD2 and RIPK2 which could not be rescued by blocking proteasomal degradation (Fig 4-17).

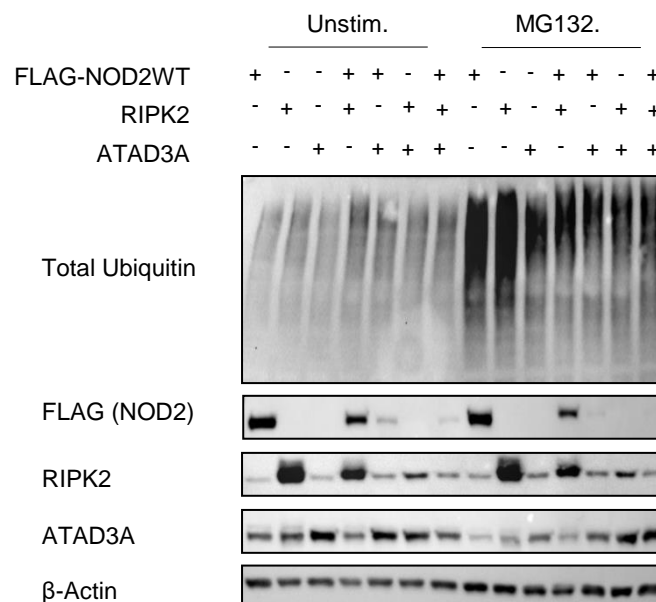


Figure 4-17 ATAD3A overexpression promoted NOD2 and RIPK2 degradation in HEK293T cells. Representative immunoblotting (n = 2) of HEK293T cells ectopically overexpressing Flag-NOD2, RIPK2 and ATAD3A, untreated or treated with MG132 (20 μ M) for 8 h.

To confirm this finding, HEK293T cells were generated to express ATAD3A under the control of a doxycycline (Dox) inducible promoter. These cells were transfected with NOD2 followed by doxycycline stimulation with two different concentrations. To test if the degradation effect of ATAD3A is specifically affecting NOD2, cells were transfected with other constructs encoding for VCP and RASGRP1. ATAD3A overexpression upon doxycycline treatment resulted in reduced protein levels of NOD2, VCP, and RASGRP1 indicating that the effects are not NOD2 specific (Fig 4-18, A). One potential explanation for the general effect of ATAD3A overexpression can be due to the higher rate of cellular death. Flow cytometry revealed an increased frequency of Annexin V-positive cells in cells treated with doxycycline (Fig 4-18, B).

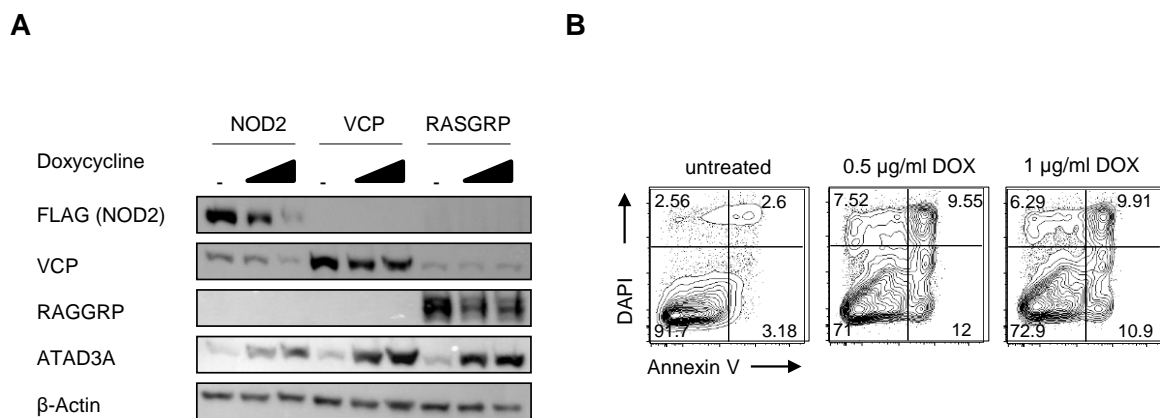


Figure 4-18 ATAD3A overexpression promoted NOD2, VCP, and RASGRP1 degradation in HEK293T cells. (A) Immunoblotting of HEK293T cells overexpressing ATAD3A under the control of doxycycline ectopically expressing NOD2, VCP, or RASGRP1 upon treatment with 200 ng/ml or 1 µg/ml doxycycline for 24 h. (B) Annexin V /DAPI staining of HEK293T cells overexpressing ATAD3A upon doxycycline treatment.

4.5.5. Evaluating NOD2-mediated signaling in VCP knockdown HCT116 cells

Generation of VCP KO HCT116 cells was performed as described in 4.5.5.1 for ATAD3A. Targeting of VCP with four different sgRNAs did not yield any KOs after screening >150 clones using immunoblotting with a VCP specific antibody (Fig 4-19, A). Due to the failure in generating VCP KO HCT116 cells, 2 different siRNAs targeting

the coding region of VCP plus non-targeting siRNAs were used to deplete VCP from HCT116 cells. To optimize the siRNA conditions, HCT116 cells were transfected with different concentrations (1, 2.5, and 5nM). The 5nM concentration efficiently reduced VCP protein level without affecting cellular viability (data not shown). Thus, further experiments were conducted using the VCP siRNA at a final concentration of 5nM. The non-targeting siRNA was transfected at 5nM concentration (Fig 4-19, B).

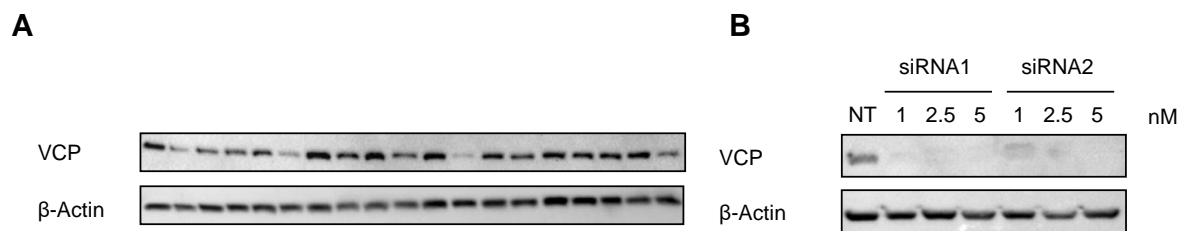


Figure 4-19 Screening putative VCP KO clones and optimizing VCP-targeting siRNAs concentrations in HCT116 cells. (A) Representative Immunoblotting for screening of possible VCP KO HCT116. (B) Immunoblotting of HCT116 cells transfected with non-targeting (5nM) or two VCP-targeting siRNAs (different concentrations) 72 h post-transfection.

4.5.5.1. Evaluating MDP-induced NOD2 signaling in VCP knockdown HCT116 cells

To investigate the relevant function of VCP in the NOD2-mediated signaling pathway, HCT116 cells were transfected with VCP targeting siRNAs or non-targeting siRNA as a control. NOD2 PGN-dependent signaling was assessed by evaluating IL-8 transcriptional level and NF- κ B luciferase activity upon MDP treatment. qPCR confirmed VCP knockdown at the mRNA level (Fig 4-20, C). VCP knock-down significantly decreased IL-8 mRNA levels and NF- κ B activity upon L18-MDP stimulation (Fig 4-20, A and B).

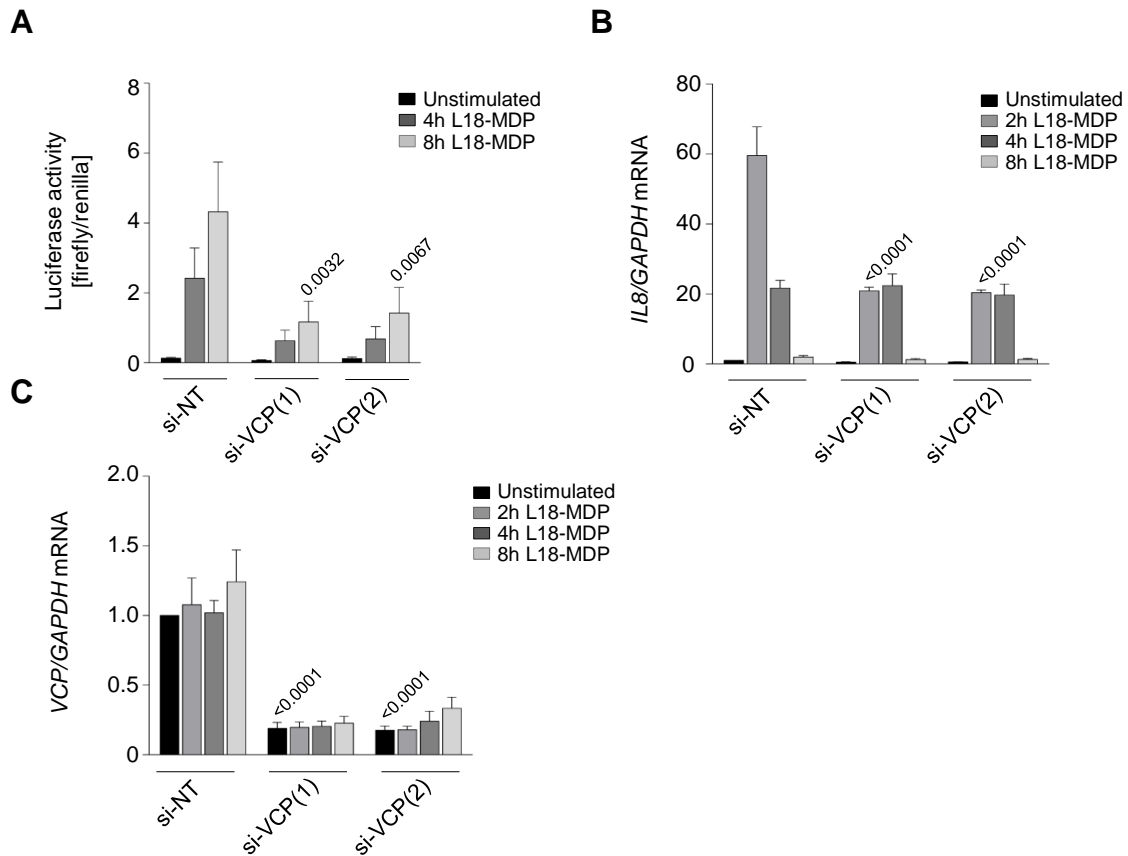


Figure 4-20 Impaired MDP-mediated NOD2 signaling in VCP knockdown cells. (A) NF- κ B reporter assay (n=5) or (B) IL-8 quantitative RT-PCR in HCT116 cells transfected with non-targeting or VCP siRNAs upon MDP stimulation. (C) qRT-PCR analysis to measure VCP transcriptional level in L18-MDP treated HCT116 cells transfected with si-NT or si-VCP. B and C are representative of three independent experiments and data are represented as mean \pm SEM.

VCP has been previously implicated in inflammation and regulation of NF- κ B signaling by promoting degradation of I κ B α [135]. Li et al. reported reduced TNF α and IL-1 β -induced NF- κ B activation in VCP knockdown cells due to impaired turnover of I κ B α [135]. To investigate whether the reduced IL-8 mRNA level and NF- κ B activity observed upon L18-MDP stimulation is due to the impaired degradation of I κ B α , immunoblotting was conducted in VCP knockdown HCT116 cells upon MDP stimulation. The experiment revealed altered kinetics of I κ B α activity with sustained phosphorylation of (Ser32) after four hours but no accumulation was observed. VCP

knockdown was confirmed on protein level. Consistent with the result observed in the NF- κ B luciferase assay (Fig 4-20, A), immunoblotting of phospho-NF- κ B p65 subunit (Ser536) showed diminished phosphorylation in VCP knockdown cells (Fig 4-21).

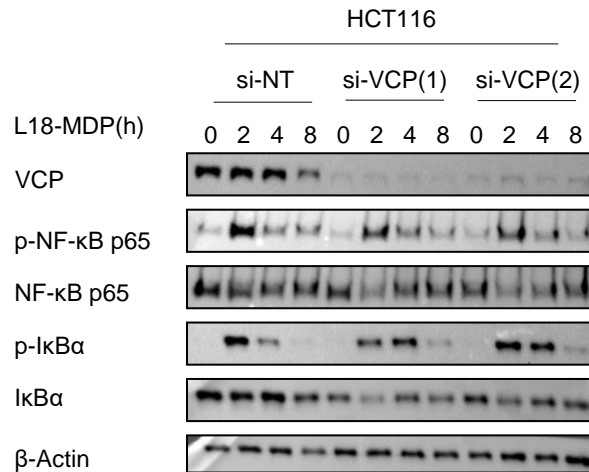


Figure 4-21 Normal turnover of I κ B α in VCP knockdown HCT116 cells upon MDP stimulation. Representative immunoblotting (n = 3) of HCT116 cells transfected with si-NT or si-VCP and stimulated with L18-MDP (1 μ g/ml) for 0 h, 2 h, 4 h, and 8 h.

VCP is known to be involved in quality control and structurally remodeling of several ubiquitinated client proteins and regulating a myriad of ubiquitin-mediated processes [127]. To elucidate the mechanism of impaired MDP-induced NF- κ B activation in VCP-silenced HCT116 cells, RIPK2 ubiquitination was tested by pulldown of total polyubiquitinated proteins. Immunoblotting of RIPK2 revealed comparable ubiquitination of RIPK2 in VCP-silenced and control cells upon MDP stimulation (Fig 4-22).

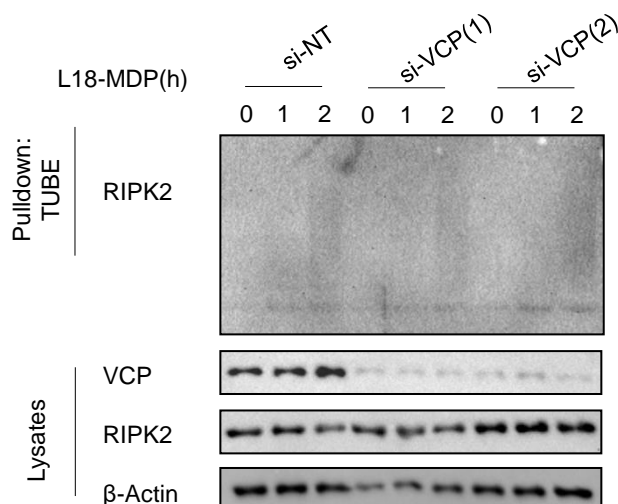


Figure 4-22 Evaluation of RIPK2 ubiquitination in VCP knockdown HCT116 cells upon MDP stimulation. Representative immunoblotting (n = 2) of HCT116 cells transfected with si-NT or si-VCP and stimulated with L18-MDP (200 ng/ml) for 0 h, 1 h, and 2 h.

Furthermore, VCP has been implicated in regulating alternative NF-κB pathway by mediating processing of NF-κB p100 subunit into p52 subunit [137, 138]. Immunoblotting revealed increased phosphorylation of P100 upon L18-MDP stimulation in VCP knockdown cells. Moreover, compromised P100 phosphorylation observed in *NOD2* KO cell was suggestive of NOD2 dependent mechanism (Fig 4-23).

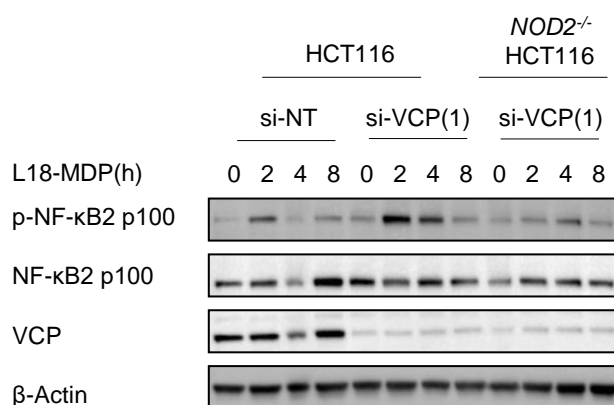


Figure 4-23 Enhanced activation of alternative NF-κB pathway in VCP knockdown HCT116 cells upon MDP stimulation. Representative immunoblotting (n = 3) of HCT116 cells transfected with si-NT or si-VCP upon L18-MDP stimulation (1 μg/ml) for the 0 h, 2 h, 4 h, and 8 h.

4.5.5.2. Evaluating ER stress in VCP-silenced cells upon L18-MDP stimulation

Previously, VCP knockdown or inhibition has been proposed to induce ER stress and UPR [182, 183]. ER stress responses are mediated by three ER transmembrane sensors, IRE1, PERK, and ATF6. Upon ER stress, these sensors are activated and initiate downstream signaling pathways. For example, activated IRE1 α splices X-box binding protein 1 (XBP1) mRNA which acts as a transcription factor and subsequently leads to upregulation of UPR target genes. Similar to IRE1, ATF6 activation results in production of UPR regulators like CHOP, PDI, and EDEM1 [66, 184]. To investigate ER stress upon L18-MDP stimulation, XBP1 splicing and CHOP transcriptional level were evaluated in VCP-silenced HCT116 cells. RT-PCR and subsequent DNA electrophoresis revealed increased XBP1 splicing upon MDP stimulation in VCP knockdown cells compared with control cells (Fig 4-24, B). Correspondingly, CHOP mRNA level was significantly increased in cells transfected with VCP si-RNA upon L18-MDP stimulation (Fig 4-24, A).

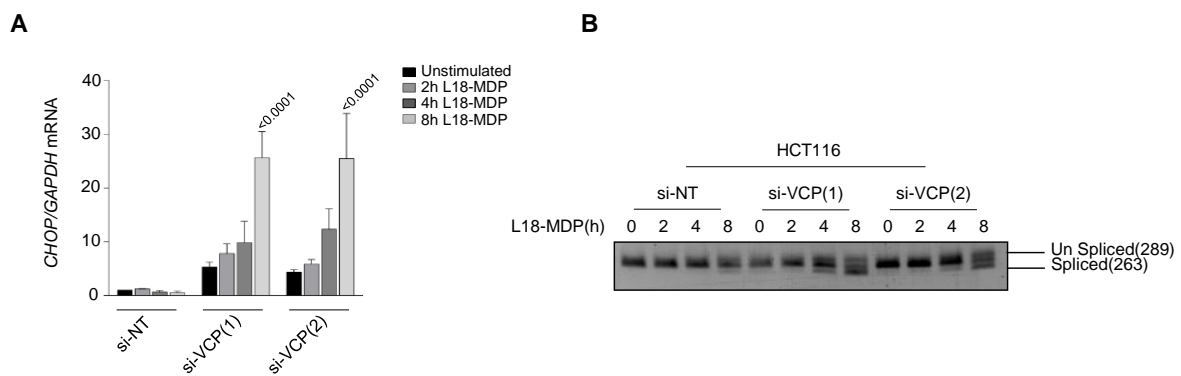


Figure 4-24 Evaluation of ER stress in VCP-silenced cells upon MDP stimulation. (A) CHOP quantitative RT-PCR analysis (n=3) and (B) XBP1 RT-PCR (n=3) in HCT116 cells transfected with si-NT or si-VCP and stimulated with L18-MDP (1 μ g/ml) for 0 h, 2 h, 4 h, and 8 h. The amplicon size of the unspliced XBP1 isoform (inactive) is 289 bp and the spliced isoform (active) is 263 bp. Upon MDP stimulation in VCP-silenced cells, there was an increase in the intensity of the PCR band related to spliced isoform. In panel A data are represented as mean \pm SEM.

Next, to test the function of NOD2 in L18-MDP-induced ER stress in VCP-silenced cells, the assay was repeated in *NOD2* KO cells. The experiment revealed that MDP-induced ER stress in VCP knockdown cells was independent of NOD2 as *NOD2* KO cells also showed an increased level of CHOP mRNA after MDP stimulation (Fig 4-25).

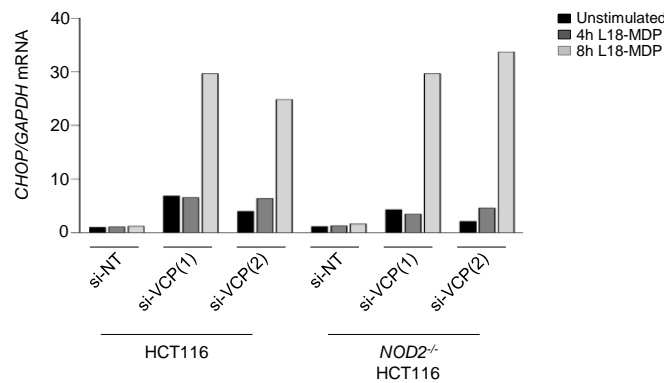


Figure 4-25 Evaluation of ER stress in VCP-silenced *NOD2* KO HCT116 cells upon MDP stimulation. CHOP quantitative RT-PCR analysis in HCT116 cells and *NOD2* KO HCT116 cells transfected with si-NT or si-VCP upon L18-MDP (1 μ g/ml) treatment for the indicated times.

4.5.5.3. Evaluating tunicamycin-induced NOD2 signaling in VCP-silenced HCT116 cells

Next, the inflammatory responses induced during ER stress were assessed by treatment of VCP-silenced HCT116 cells with tunicamycin and evaluating IL-8 mRNA level using qPCR. *NOD2* KO and lentiviral reconstituted *NOD2* WT HCT116 cells were transfected with non-targeting or VCP siRNAs and stimulated with tunicamycin for 8 and 24 h. IL-8 mRNA level was significantly increased in VCP-silenced cells overexpressing WT *NOD2* but not in the KOs (Fig 4-26, A). VCP knockdown has been reported to induce ER stress and UPR response [182, 183]. To test whether the altered response between *NOD2* WT and KO cells is caused by different levels of ER stress,

CHOP mRNA level was measured by qPCR. Consistent with the previous studies, CHOP mRNA level was significantly increased in VCP-silenced cells which was independent of NOD2 expression (Fig 4-26, B).

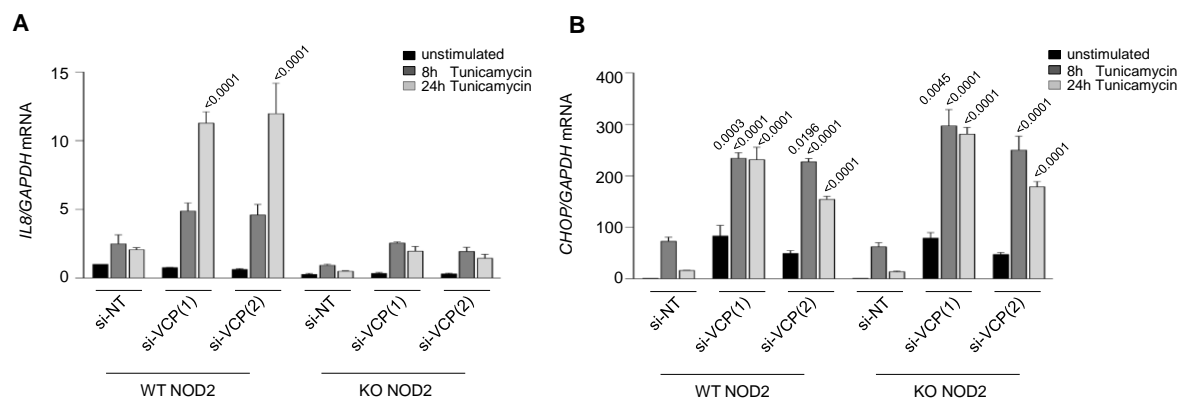


Figure 4-26 induced proinflammation in VCP-silenced HCT116 cells upon tunicamycin stimulation. (A) IL-8 (n=3) and (B) CHOP (n=3) q-PCR analysis in NOD2 WT reconstituted and NOD2 KO HCT116 cells transfected with si-NT or si-VCP and stimulated with tunicamycin (5 μ g/ml) for the 0 h, 8 h, and 24 h. Data are represented as mean \pm SEM.

Next, DAPI/Annexin V staining was analyzed to assess whether the enhanced proinflammation can be attributed to higher cell death. However, no differences were observed concerning cell death upon tunicamycin treatment between NOD2 KO and WT reconstituted cells (Fig 4-27).

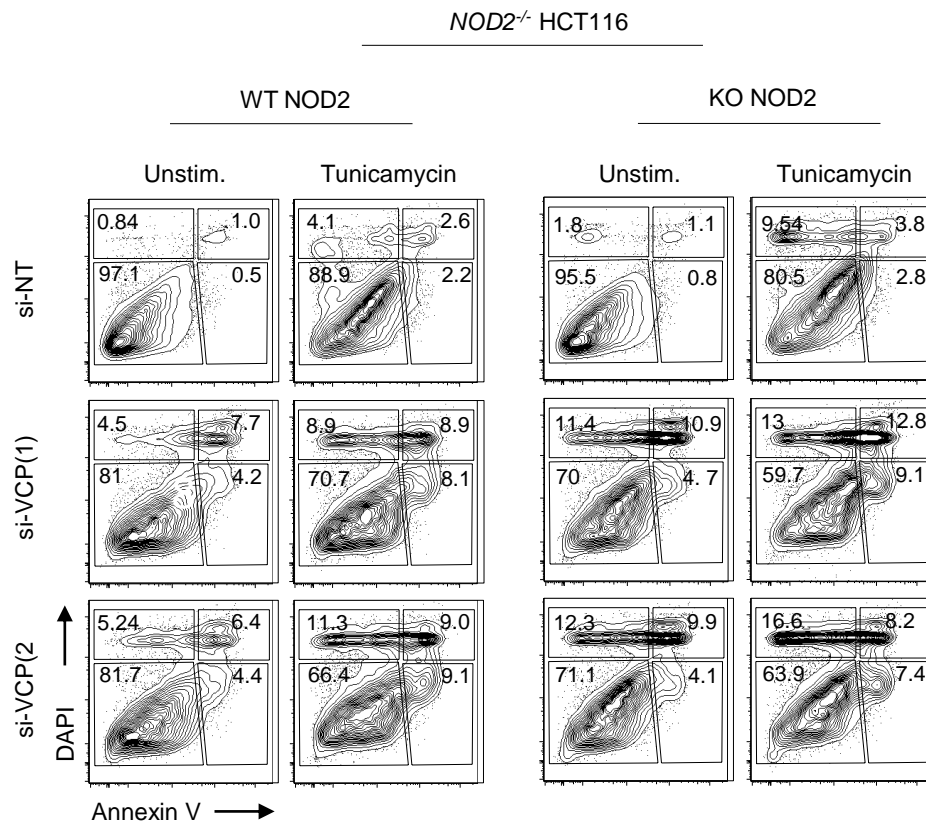


Figure 4-27 Evaluation of cell death in VCP-silenced HCT116 cells upon tunicamycin stimulation. Representative FACS analysis (n=2) of Annexin V/DAPI staining in *NOD2* KO and lentiviral reconstituted *NOD2* WT HCT116 cells transfected with si-NT or si-VCP stimulated with tunicamycin for 24 h.

In addition to the analysis of IL-8 transcriptional level, NF- κ B signaling was evaluated using immunoblotting in VCP knockdown HCT116 cells treated with tunicamycin. In contrast to increased IL-8 mRNA level, VCP silenced cells exhibited a reduced level of NF- κ B p65 subunit (Ser536) phosphorylation upon tunicamycin treatment as compared with control cells (Fig 4-28).

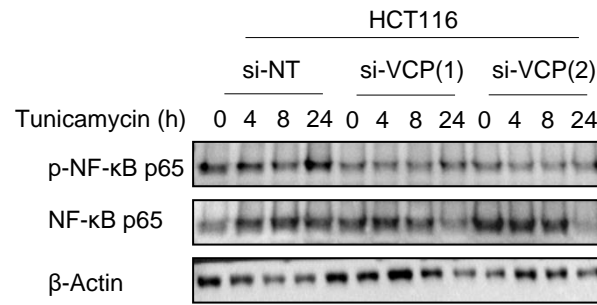


Figure 4-28 Evaluation of canonical NF-κB pathway in VCP knockdown HCT116 cells upon tunicamycin stimulation. Representative immunoblotting (n = 3) of HCT116 cells transfected with si-NT or si-VCP and stimulated with tunicamycin for the indicated times.

5. Discussion

As a cytosolic sensor of bacterial peptidoglycan derived from both commensal and pathogenic microbes [185, 186], NOD2 is one of the most studied and critical susceptibility factors for CD and its signaling has been affected in many other inflammatory diseases like Blau syndrome, early-onset sarcoidosis and autoimmunity [17]. Investigating the molecular function and characterization of rare mutations in key proteins like NOD2 will not only improve our understanding of the pathomechanism of the mutated protein but also aids in identifying molecular components that are important for regulating NOD2-related signaling pathway.

5.1. NOD2, a key player in intestinal homeostasis

Using genome-wide linkage strategies, Hugot et al. mapped the first susceptibility locus for IBD (IBD1) in chromosome 16 [187]. Further investigations unveiled *NOD2/CARD15* within the IBD1 interval and revealed an association of its polymorphism to the development of CD [72, 74]. From then on, several studies identified more *NOD2* polymorphisms linked to CD and other inflammatory disorders. CD, as one of the major clinical types of inflammatory bowel disease, is a multifactorial disease that arises from the contribution of both genetic and environmental elements. Considering the host-microbiome as one of the most critical environmental determinants [188] and in light of several studies supporting NOD2 function in sensing microbial fragments, it is not surprising that NOD2 polymorphisms might lead to impaired response to commensal or invading pathogens and thus result in uncontrolled inflammation [9, 88]. Several hypotheses have been suggested regarding the pathomechanism of NOD2 variants in the development of CD, from abrogated bacterial

detection, diminished expression of α -defensins, impaired autophagy and bacterial handling, and dysregulated TLR signaling.

The contribution of disturbed NOD2-mediated signaling in intestinal immunity and promoting CD has been verified by additional studies in a murine model. *Nod2* deficient mice appeared healthy without any symptoms of intestinal inflammation and no significantly higher susceptibility to DSS-induced colitis [91]. The KOs exhibited comparable composition of hematopoietic cells with WT animals [91]. However, *Nod2*^{-/-} mice displayed increased intestinal permeability and enhanced susceptibility to infection with various pathogens [62, 91, 189, 190]. It is noteworthy that *Nod2* deletion in SAMP mice (SAMP1Yit/Fc strain) alleviated the intestinal inflammation and also restrains DSS-triggered colitis [191]. The microbial dysbiosis reported by some other studies in *Nod2* KO mice might also explain the higher risk of colitis [92, 93, 110]. Furthermore, *Nod2* has been shown to be highly expressed in Lgr5+ stem cells and protects against stress upon MDP stimulation [27].

5.2. Identification of biallelic missense mutation in *NOD2*

Since the first identification of *NOD2* using linkage mapping in association with CD [80, 81], several studies were conducted to decipher the magnitude of association of this innate immune receptor with CD in different populations [192, 193]. The contribution of *NOD2* polymorphism in the etiology of CD varies between populations. While three main *NOD2* variants (R702W, G908R, and 1007fs) displayed an association with CD in many Caucasian populations, studies on some other populations like Japanese revealed no association [83, 194-196]. Further studies unveiled the role of *NOD2* in the pathogenesis of other inflammatory disorders including Blau syndrome, *NOD2*-associated autoinflammatory disease (NAID), asthma, and allergy [102, 103, 197-199].

In the current thesis, whole exome sequencing on a cohort of patients diagnosed with inflammatory bowel disease or primary immune deficiencies, unveiled a biallelic missense mutation in the first CARD domain of NOD2 protein (E54K) in a patient presenting with self-limiting diarrhea, recurrent perianal candida dermatitis responsive to topical antifungal treatment, recurrent hemophagocytic lymphohistiocytosis (HLH), and prolonged Norovirus infection. Later analysis revealed another possible causative variant in STXBP2. Mutations in STXBP2 have been previously reported in patients with Familial hemophagocytic lymphohistiocytosis (FHL) [175]. However, *in silico* analysis of both variants using SIFT and PolyPhen-2 disclosed *NOD2* variant as deleterious and STXBP2 variant as a benign one.

Most of the CD-associated NOD2 polymorphisms are located in or near the LRR domain of the protein leading to impaired response to NOD2 stimulation. Whereas in Blau syndrome and early-onset sarcoidosis, mutations are considered as gain of function and are mainly located in the NBD domain [17]. Given the distinct location of the identified NOD2 mutation affecting the RIPK2-interacting CARD domain, further functional investigations were conducted on the NOD2 variant.

5.3. Characterization of a biallelic missense mutation in *NOD2*

5.3.1. PGN- dependent signaling

NOD2 has been shown to induce the expression of several proinflammatory cytokines including TNF α , IL-1 β , IL-6, and IL-8 through activation of NF-kB and MAPK pathways. Monocytes of patients carrying the frameshift mutation showed impaired production of proinflammatory cytokines [88, 200]. In agreement with previous studies, we observed in a patient harboring NOD2 variant E54K that TNF α production was abrogated in monocytes in response to L18-MDP stimulation compared with healthy donors. Correspondingly, both PBMCs and neutrophils from the patient showed impaired

activation of NF- κ B and MAPK pathways implicated by defective phosphorylation of key proteins of the signaling pathways like p65, ERK, and p38. Neutrophils constitute essential elements of the innate immune system which recognize invading pathogens through pattern recognition receptors [201]. Owing to the fact that NOD2 has been shown to be expressed and functional in human neutrophils [20], it became of interest to study the etiology of the identified mutation in patient's neutrophils. Investigating CD62L shedding as an activation marker revealed impaired activation of the patient's neutrophils upon treatment with L18-MDP compared with healthy donor cells.

NOD2 has been shown to be highly expressed in hematopoietic cells, notably macrophages, neutrophils, and dendritic cells but also in intestinal epithelial cells and Paneth cells [41]. Previous analysis of NOD2 signaling verified impaired signaling in the hematopoietic compartment; however, to clarify the pathomechanism of the NOD2 variant E54K in the intestinal background, colon-carcinoma HCT116 cells were engineered using the CRISPR/Cas9 system to generate *NOD2* KO cells. MDP challenge of *NOD2* KO HCT116 cells lentivirally reconstituted with NOD2 variant E54K revealed impaired production of proinflammatory cytokine IL-8 compared with WT *NOD2* expressing cells. IL-8 (CXCL8) is a pleiotropic chemoattractant cytokine produced by various cell types and has been shown to be expressed in the gastrointestinal tract upon induction of the NF- κ B pathway [202, 203]. Increased activity of NF- κ B and IL-8 expression has been reported in inflamed intestinal tissue of IBD patients [204-206]. However, in line with the observed phenotype in the index patient, several studies observed impaired MDP-induced IL-8 production in cells from CD patients carrying *NOD2* mutations [88, 202].

5.3.2. PGN-independent signaling

Several subsets of cellular processes have been identified to play a major role in maintaining homeostasis in the gut and breakdown in these processes might lead to inflammation. One of these pathways is ER stress and subsequently UPR which is elicited by the accumulation of unfolded or misfolded proteins in the organelle [207]. UPR supports the preservation of functional highly secretory cells in the gut such as Paneth cells and goblet cells. The bulk of studies have linked polymorphisms within ER stress and UPR genes such as XBP1 and AGR2 to IBD [208, 209]. Mice lacking Xbp1 in their intestinal epithelial cells display an elevated level of ER stress and develop enteritis spontaneously [208]. Further functional studies revealed an increased level of ER stress in biopsies from CD patients demonstrated by higher expression of chaperone proteins Gp96 and GRP78 (BIP) [210-212].

It has been shown that ER stress employs NOD1/NOD2 to trigger inflammatory responses [64]. This function of NOD1/NOD2 has been depicted to be mediated through interaction with TRAF2 and RIPK2. However, the mechanism of NOD1/NOD2 activation by ER stress was not determined in this study. It's worthy to be noted that, no experimental evidences have been provided so far about the consequence of NOD2 polymorphisms during ER stress. Using the heterologous HCT116 cellular model, we here demonstrated the NOD2 function in mediating inflammation triggered through ER stress was measured by tunicamycin stimulation and evaluation of IL-8 mRNA. Interestingly, cells reconstituted with NOD2 WT or CD-associated variants L1007fsinsC showed increased expression of IL-8 upon tunicamycin treatment which was not observed in cells overexpressing NOD2 variant E54K. These findings suggested that both PGN-dependent and PGN-independent signaling of NOD2 is affected by the mutant E54K. However, the underlying genotype-specific mechanisms

of different inflammatory responses triggered by ER stress need to be elucidated in future studies.

5.3.3 Investigating RIPK2 interaction and post-translational modification

Recruitment of NOD2 downstream adaptor protein, RIPK2 to the complex occurs through CARD domain interactions of proteins. In light of the fact that the identified mutation resides in the first CARD domain of NOD2 protein, we analyzed the interaction between NOD2 and RIPK2 by co-immunoprecipitation experiments in HEK293 cells ectopically expressing NOD2 WT or mutants (E54K and L1007fsinsC) along with RIPK2. Consistent with previous studies [179], we observed that the NOD2 variant L1007fsinsC interacted with RIPK2 while the interaction was abrogated for the NOD2 variant E54K. Previously Parkhouse and Monie et al. studied MDP response and the ability of RIPK2 to bind to 50 CD-associated NOD2 polymorphisms [179]. They identified only two polymorphisms R38M and R138Q that lead to impaired interaction with RIPK2. However, In the gnomAD database, no homozygous mutant alleles of *NOD2* were reported for those variants.

In addition to the recruitment of RIPK2 to the NOD2 complex, activation of the signaling depends on polyubiquitination of RIPK2 by different E3 ubiquitin ligases [45, 47, 48, 180, 181]. Purification of endogenous ubiquitin conjugates using tandem ubiquitin-binding entities (TUBEs) revealed impaired ubiquitination of RIPK2 upon MDP stimulation in both NOD2 variants E54K and L1007fsinsC. Ubiquitination of RIPK2 plays a critical function in signal propagation since the ubiquitinated RIPK2 acts as a scaffold for other proteins that are recruited to the complex leading to activation of NF- κ B and MAPK signaling [42, 43, 49].

Taken together, these findings imply that RIPK2 interaction and ubiquitination are key events in signal transduction and defective ubiquitination of RIPK2 observed in NOD2

mutants E54K and L1007fsinsC might be postulated to cause abrogated MDP-induced NF- κ B activation. In support of this, reduced RIPK2 ubiquitination in XIAP deficient cells has been shown to cause blunted NOD2 signaling [48].

5.4. Investigating interaction network of mutated NOD2 protein (E54K)

In light of the relevant function of NOD2 in innate immunity, it is not surprising that the pathway is tightly regulated. Various approaches such as whole-genome RNAi screening, yeast-two-hybrid assays, and immunoprecipitation experiments have been employed to discover the regulatory mechanisms of this pathway [69, 213, 214].

Several NOD2 interacting proteins have been characterized in the context of NOD2 common mutations [213, 214]. Immunoprecipitation on HEK293 cells followed by mass spectrometry unveiled Carbamoyl phosphate synthetase/aspartate transcarbamylase/dihydroorotase (CAD) as a novel negative regulator of NOD2. Further investigations revealed increased MDP-triggered NF- κ B activity of the cells overexpressing CD-associated NOD2 variants (R702W, G908R, and 1007fs) upon CAD inhibition. Notably, the interaction of CAD with NOD2 was not disturbed in cells overexpressing NOD2 risk variants [214]. Another study employing yeast-two-hybrid screens unveiled eight novel NOD2 interacting proteins exhibiting impaired interaction with common CD-associated NOD2 variants.[213].

Because of the fact that the E54K variant resulted in the abrogation of both PGN-dependent and -independent NOD2 signaling, it became of great interest to study the NOD2 interaction network for this variant. The interaction network was investigated by conducting immunoprecipitation experiments in HEK293T cells with ectopic expression of NOD2 WT or E54K and L1007fsinsC variants. Immunoprecipitation-coupled mass spectrometry (LC-MS/MS) revealed Valosin-containing protein (VCP)

and AAA-domain-containing protein 3A (ATAD3A) as novel NOD2 interacting proteins. VCP is a 97 kDa evolutionary conserved ATPase that showed impaired interaction with the two NOD2 variants E54K and L1007fsinsC. ATAD3A is a 66 kD mitochondrial protein that showed interaction with NOD2 WT and both variants.

5.5. The role of ATAD3A in the NOD2 signaling pathway

Disturbed mitochondrial function has been reported in some patients suffering from IBD [215]. *NOD2* is the first and still strongest genetic loci associated with IBD [80, 81] and some studies have suggested NOD2 involvement in mitochondrial function [216-218]. MDP stimulation of skeletal muscle cells has been reported to induce mitochondrial dysfunction [218]. Murine NOD2 (*Nod2*) has also been demonstrated to interact with mitochondrial antiviral signaling (MAVS) during infection with respiratory syncytial virus which leads to activation of IRF3 and its subsequent translocation into the nucleus where it binds IFN-stimulated response elements (ISRE) and induce expression of interferon inducible genes [62].

In this study among the identified NOD2 interacting proteins in LC-MS/MS screening some mitochondrial proteins were listed, from which ATAD3A was selected and the interaction confirmed by immunoblotting. ATAD3A is a AAA domains ATPase mitochondrial residing protein encoded in the nucleus that is involved in controlling mitochondrial dynamics [150]. Knockdown of ATAD3A in cancer cell line increases mitochondrial fragmentation and reduces mitochondria and ER communication [150, 164]. In humans, *ATAD3A* mutations and biallelic deletions have been shown to be associated with neurological disorders [160, 161, 219].

To elucidate the function of ATAD3A in the NOD2 signaling pathway, *ATAD3A* CRISPR/Cas9 KO HCT116 cells were stimulated with MDP or tunicamycin and the

transcriptional level of IL-8 was measured by qPCR. MDP treatment significantly increased IL-8 mRNA level in *ATAD3A* KO cells compared with WT cells. Consistent with this finding, Saxena et al. showed that induced mitochondrial dysfunction of colon-derived epithelial cell lines leads to increased production of IL-8 upon treatment with commensal *E. coli*. They observed enhanced IL-8 production in *NOD2*-depleted cells challenged with dinitrophenol (DNP) and *E. coli* [216]. To determine whether the MDP response of identified and common *NOD2* variants is altered upon *ATAD3A* depletion, further investigations need to be employed.

One possible hypothesis to explain the observed negative regulatory function of *ATAD3A* in the MDP response of colon carcinoma cells could be through controlling the steady-state levels of *NOD2* or its direct interaction partner *RIPK2*. To test this possibility, HEK293T cells were transiently co-transfected with *ATAD3A* together with *RIPK2* and/or *NOD2*. The ectopic expression of *ATAD3A*, reduced the protein level of *NOD2* and *RIPK2* which could not be rescued by pretreatment with the proteasomal inhibitor MG132. Investigating the observed finding in the doxycycline-inducible system revealed the effect of *ATAD3A* overexpression is not specific for the *NOD2* protein but also resulted in a reduced level of *VCP* and *RASGRP1* proteins. One possible assumption for this observation of induced reduction in protein level might be attributed to the higher rate of cell death. Annexin V/ DAPI staining revealed higher cell death in cells overexpressing *ATAD3A* compared with control cells.

Next, the role of *ATAD3A* in *NOD2*-induced inflammation upon tunicamycin stimulation was investigated. Interestingly, *ATAD3A* KO cells responded to tunicamycin similar to the control cell line.

Taken together, in this present study *ATAD3A* was identified as a novel *NOD2* interacting protein. The knockout of *ATAD3A* leads to higher IL-8 production upon MDP stimulation. The importance of intestinal epithelial mitochondrial function in

establishing immune response to commensal bacteria has already been demonstrated before [216]. However, to determine whether *ATAD3A* KO derives a higher MDP response is due to general mitochondrial dysfunction or its specific regulatory role in the NOD2 signaling pathway needs to be further investigated.

5.6. The role of VCP in NOD2 signaling pathway

VCP is a ubiquitously expressed chaperone that regulates a myriad of cellular processes through interaction with different interacting proteins [220]. In this study, VCP has been identified as a novel NOD2 interacting protein that exhibited compromised interaction with NOD2 variants E54K and L1007fsinsC. Previous yeast-two-hybrid screening discovered VCP in one of their three screenings and listed VCP as a potential NOD2 interaction partner but no functional studies was conducted to confirm interaction or regulatory function of VCP in NOD2 signaling [213]. Proteomic studies performed on HEK293T cells overexpressing NOD2 WT or the L1007fsinsC variant mentioned VCP in a group of proteins differentially expressed in cells overexpressing the frameshift variant L1007fsinsC compared with WT NOD2 [221]. These studies support the finding that NOD2 and VCP are interacting however, the functional relevance of this interaction warrants further investigations.

To understand the function of VCP in NOD2 signaling pathways, MDP and tunicamycin responses of HCT116 cells were evaluated in the context of VCP knockdown. MDP stimulation of VCP-silenced HCT116 cells revealed diminished NF- κ B activity and IL-8 production compared with cells transfected with non-targeting siRNA. Previously Li et al. demonstrated that VCP knockdown leads to impaired TNF α and IL1 β -induced NF- κ B activation [135]. The authors suggested impaired degradation of ubiquitinated I κ B α , as an underlying mechanism. Investigating the possibility of a similar

pathomechanism, Immunoblotting on VCP knockdown HCT116 cells upon MDP stimulation revealed altered kinetics of I κ B α activity with sustained phosphorylation of (Ser32) after four hours however no protein accumulation was observed.

Since VCP plays a critical function in post ubiquitination regulation of interacting proteins, one could assume disturbed RIPK2 ubiquitination as an underlying mechanism for impaired NF- κ B activity in VCP-silenced cells. However, TUBE pull-down assays on VCP knockdown HCT116 cells uncovered proper ubiquitination of RIPK2 upon MDP stimulation, suggesting an alternate regulatory mechanism.

A similar role of VCP in the non-canonical NF- κ B pathway has been demonstrated through regulating proteolysis of NF- κ B precursors p100/p105 and generation of p50 and p52 [137, 138]. P100 phosphorylation and total protein level were examined in VCP knockdown HCT116 cells upon MDP treatment by immunoblotting. Interestingly, MDP stimulation induced a higher level of P100 phosphorylation in VCP knockdown HCT116 cells which was NOD2 dependent as in *NOD2* KO HCT116 cells it was not induced. However, no accumulation of p100 protein was observed in VCP-silenced cells upon MDP stimulation. These data indicate VCP as a possible negative regulator of NOD2 function in the non-canonical NF- κ B pathway as its knockdown leads to increased phosphorylation of p100 upon MDP treatment. It would be of particular interest to determine the cellular consequences of such gain of function effect.

VCP has a crucial function in ERAD (Endoplasmic-reticulum-associated protein degradation) through mediating proteasomal degradation of ubiquitinated proteins [220]. Several lines of inquiry have demonstrated VCP as an essential element in the maintenance of efficient ER activity [113]. Disturbed ER homeostasis and activation of inflammatory pathways triggered by UPR have been associated with several inflammatory conditions [222]. Mutations in several UPR pathway mediators like XBP1 have been associated with IBD [208]. Given the NOD2 pivotal function connecting ER

stress with inflammatory responses and VCP regulatory role in ERAD, it became of interest to study the interplay between NOD2 and VCP during ER stress in inducing inflammation in VCP-silenced colon carcinoma cells. HCT116 cells transfected with VCP-targeting siRNAs showed a significantly higher level of IL-8 mRNA upon tunicamycin stimulation. Further investigation revealed that the VCP function in regulating IL-8 production during ER stress is NOD2-dependent. Previous studies have demonstrated that VCP inhibitors or its knockdown induces ER stress and leads to an unresolved unfolded protein response [182, 183]. Evaluation of CHOP mRNA level as an ER stress marker revealed enhanced expression of CHOP in VCP-silenced cells, which was independent of NOD2. One possible explanation for the higher IL-8 level induced by tunicamycin in VCP-silenced cells could be due to an add-on effect of VCP knockdown to tunicamycin stimulation which can subsequently result in higher NF- κ B activity and IL-8 production in NOD2 expressing cells. Immunoblotting was performed to investigate whether increased activation of the NF- κ B pathway is the underlying mechanism. Unexpectedly, HCT116 cells transfected with VCP siRNAs showed reduced phosphorylation of NF- κ B p65 subunit (Ser536) upon tunicamycin stimulation indicating that other mechanisms rather than NF- κ B pathway mediate the higher levels of IL-8 in VCP silenced cells overexpressing NOD2.

Collectively, the results of my thesis identify VCP as a novel interaction partner and regulator of the NOD2 protein, even though the regulatory mechanism remains incompletely resolved. In the present study, VCP knockdown leads to an impaired activation of the canonical NF- κ B but increased activation of the non-canonical NF- κ B in MDP treated cells. It has also been shown that VCP regulates NOD2 function to induce inflammation upon ER stress. These findings might be explained by the fact that VCP is a multifunctional protein regulating several cellular processes through

interaction with different client proteins and therefore it is not surprising that it possibly regulates NOD2 signaling in various ways.

5.7. Perspectives

In this study, the pathomechanism of a biallelic missense mutation in *NOD2* was investigated in comparison with the CD-associated frameshift mutation which has already been reported to abrogate NOD2-mediated signaling induced by MDP. Even though both mutants displayed impaired MDP-induced NF- κ B activation, in terms of response to tunicamycin and RIPK2 interaction they behaved differently. Further investigations revealed that both variants of NOD2 failed to interact with VCP. However, the relevant role of VCP in the different mutation-specific inflammatory responses observed during ER stress has not been covered in this study and needs to be further investigated.

ATAD3A and VCP have been identified as two novel NOD2-interacting proteins in this study. Their relevant function in the NOD2-mediated pathway was determined in colon carcinoma cells deficient in ATAD3A and VCP. However, to decipher in more detail the ATAD3A function in NOD2 signaling, specific inhibition of the interaction for example via site-directed mutagenesis or deleting different protein domains might be a better strategy to overcome the general effect of its depletion in mitochondrial structure and function. The same strategy can be employed for VCP to overcome the ER stress induced by its knockdown. Furthermore, applying unbiased and high throughput approaches like RNAseq and SILAC assay can enlighten the key cellular pathways involved in the observed phenotypes.

Investigating *Vcp* or *Atad3* KO mouse models would also be a suitable way to assess the physiological relevance of NOD2 and VCP or ATAD3A interaction not only in

intestinal epithelial cells but also immune cells, particularly DCs and macrophages which express high levels of NOD2. In light of the different responses observed in *VCP* or *ATAD3A* depleted cells to MDP and tunicamycin, it is conceivable that NOD2 PGN-dependent and -independent functions are regulated distinctly, and investigating more the mechanism of action of its interaction partners can provide better insight into the biology of this key receptor of the innate immune system and open up new horizons of possible therapeutic targets.

6. Summary

Intestinal inflammation in Crohn's Disease (CD) involves dysregulated balances between commensal bacteria and genetically predisposed hosts [223, 224]. Genome-wide association studies (GWAS) have revealed several loci associated with CD, such as the intracellular receptor of bacterial peptidoglycan NOD2 [223]. Even though NOD2 has a functionally confirmed role in intestinal homeostasis, detailed mechanisms of its signaling pathway remain unclear. Here, I have studied the effects of a rare sequence variant in NOD2, identified in a patient presenting with intractable diarrhea, recurrent perianal candida dermatitis responsive to topical antifungal treatment, hemophagocytic lymphohistiocytosis (HLH), and prolonged Norovirus infection.

Functional studies on the pathomechanism of the identified mutation showed impaired PGN-dependent and -independent NOD2 signaling *in vitro*. Due to the drastic effect of the mutation on NOD2-mediated signaling, the interaction network was elucidated using immunoprecipitation-coupled mass spectrometry. Valosin-containing protein (VCP) and ATPase family AAA-domain containing protein 3A (ATAD3A) were identified as novel NOD2 interacting proteins. To study the role of VCP and ATAD3A, I generated and studied NOD2 signaling in cells with reduced VCP or ATAD3A expression. *ATAD3A* depletion resulted in a higher level of proinflammatory cytokine IL-8 production upon MDP stimulation without influencing ER stress-induced inflammation triggered upon tunicamycin stimulation of HCT116 cells. While MDP stimulation on VCP-silenced cells led to impaired canonical NF- κ B activation, tunicamycin stimulation induced more transcriptional level of IL-8 in NOD2 expressing cells. These findings are indicative of the possible regulatory role of ATAD3A and VCP

in NOD2 signaling; however, the molecular mechanisms of their function and possible role in inflammation are not fully clear and necessitate further studies.

7. References

1. Marshall, J.S., Warrington, R., Watson, W., and Kim, H.L. (2018). An introduction to immunology and immunopathology. *Allergy, Asthma & Clinical Immunology* *14*, 1-10.
2. Murphy, K., and Weaver, C. (2016). *Janeway's immunobiology*, (Garland Science).
3. Takeuchi, O., and Akira, S. (2010). Pattern recognition receptors and inflammation. *Cell* *140*, 805-820.
4. Akira, S., Uematsu, S., and Takeuchi, O. (2006). Pathogen recognition and innate immunity. *Cell* *124*, 783-801.
5. Schroder, K., and Tschopp, J. (2010). The inflammasomes. *cell* *140*, 821-832.
6. Brubaker, S.W., Bonham, K.S., Zanoni, I., and Kagan, J.C. (2015). Innate immune pattern recognition: a cell biological perspective. *Annual review of immunology* *33*, 257-290.
7. Girardin, S.E., Travassos, L.H., Hervé, M., Blanot, D., Boneca, I.G., Philpott, D.J., Sansonetti, P.J., and Mengin-Lecreulx, D. (2003). Peptidoglycan molecular requirements allowing detection by Nod1 and Nod2. *Journal of Biological Chemistry* *278*, 41702-41708.
8. Girardin, S.E., Boneca, I.G., Viala, J., Chamaillard, M., Labigne, A., Thomas, G., Philpott, D.J., and Sansonetti, P.J. (2003). Nod2 is a general sensor of peptidoglycan through muramyl dipeptide (MDP) detection. *Journal of Biological Chemistry* *278*, 8869-8872.
9. Inohara, N., Ogura, Y., Fontalba, A., Gutierrez, O., Pons, F., Crespo, J., Fukase, K., Inamura, S., Kusumoto, S., and Hashimoto, M. (2003). Host recognition of bacterial Muramyl dipeptide mediated through NOD2 IMPLICATIONS FOR CROHN' S DISEASE. *Journal of Biological Chemistry* *278*, 5509-5512.
10. Chen, G., Shaw, M.H., Kim, Y.-G., and Nuñez, G. (2009). NOD-like receptors: role in innate immunity and inflammatory disease. *Annual Review of Pathological Mechanical Disease* *4*, 365-398.
11. Caruso, R., Warner, N., Inohara, N., and Núñez, G. (2014). NOD1 and NOD2: signaling, host defense, and inflammatory disease. *Immunity* *41*, 898-908.
12. Tattoli, I., Travassos, L.H., Carneiro, L.A., Magalhaes, J.G., and Girardin, S.E. (2007). The Nodosome: Nod1 and Nod2 control bacterial infections and inflammation. In *Seminars in immunopathology*, Volume 29. (Springer), p. 289.
13. Chin, A.I., Dempsey, P.W., Bruhn, K., Miller, J.F., Xu, Y., and Cheng, G. (2002). Involvement of receptor-interacting protein 2 in innate and adaptive immune responses. *Nature* *416*, 190.
14. Inohara, N., Koseki, T., del Peso, L., Hu, Y., Yee, C., Chen, S., Carrio, R., Merino, J., Liu, D., and Ni, J. (1999). Nod1, an Apaf-1-like activator of caspase-9 and nuclear factor- κ B. *Journal of Biological Chemistry* *274*, 14560-14567.
15. Ogura, Y., Inohara, N., Benito, A., Chen, F.F., Yamaoka, S., and Núñez, G. (2001). Nod2, a Nod1/Apaf-1 family member that is restricted to monocytes and activates NF- κ B. *Journal of Biological Chemistry* *276*, 4812-4818.
16. Park, J.-H., Kim, Y.-G., McDonald, C., Kanneganti, T.-D., Hasegawa, M., Body-Malapel, M., Inohara, N., and Nunez, G. (2007). RICK/RIP2 mediates innate immune responses induced through Nod1 and Nod2 but not TLRs. *The Journal of Immunology* *178*, 2380-2386.

17. Philpott, D.J., Sorbara, M.T., Robertson, S.J., Croitoru, K., and Girardin, S.E. (2014). NOD proteins: regulators of inflammation in health and disease. *Nature Reviews Immunology* *14*, 9-23.
18. Shaw, M.H., Reimer, T., Sánchez-Valdepeñas, C., Warner, N., Kim, Y.-G., Fresno, M., and Nuñez, G. (2009). T cell–intrinsic role of Nod2 in promoting type 1 immunity to *Toxoplasma gondii*. *Nature immunology* *10*, 1267.
19. Petterson, T., Jendholm, J., Månsson, A., Bjartell, A., Riesbeck, K., and Cardell, L.O. (2011). Effects of NOD-like receptors in human B lymphocytes and crosstalk between NOD1/NOD2 and Toll-like receptors. *Journal of leukocyte biology* *89*, 177-187.
20. Ekman, A.K., and Cardell, L.O. (2010). The expression and function of Nod-like receptors in neutrophils. *Immunology* *130*, 55-63.
21. Hedl, M., Li, J., Cho, J.H., and Abraham, C. (2007). Chronic stimulation of Nod2 mediates tolerance to bacterial products. *Proceedings of the National Academy of Sciences* *104*, 19440-19445.
22. Cooney, R., Baker, J., Brain, O., Danis, B., Pichulik, T., Allan, P., Ferguson, D.J., Campbell, B.J., Jewell, D., and Simmons, A. (2010). NOD2 stimulation induces autophagy in dendritic cells influencing bacterial handling and antigen presentation. *Nature medicine* *16*, 90.
23. Okumura, S., Yuki, K., Kobayashi, R., Okamura, S., Ohmori, K., Saito, H., Ra, C., and Okayama, Y. (2009). Hyperexpression of NOD2 in intestinal mast cells of Crohn's disease patients: preferential expression of inflammatory cell-recruiting molecules via NOD2 in mast cells. *Clinical Immunology* *130*, 175-185.
24. Ogura, Y., Lala, S., Xin, W., Smith, E., Dowds, T., Chen, F., Zimmermann, E., Tretiakova, M., Cho, J., and Hart, J. (2003). Expression of NOD2 in Paneth cells: a possible link to Crohn's ileitis. *Gut* *52*, 1591-1597.
25. Ramanan, D., San Tang, M., Bowcutt, R., and Cadwell, K. (2014). Bacterial sensor Nod2 prevents inflammation of the small intestine by restricting the expansion of the commensal *Bacteroides vulgatus*. *Immunity* *41*, 311-324.
26. Hisamatsu, T., Suzuki, M., Reinecker, H.-C., Nadeau, W.J., McCormick, B.A., and Podolsky, D.K. (2003). CARD15/NOD2 functions as an antibacterial factor in human intestinal epithelial cells. *Gastroenterology* *124*, 993-1000.
27. Nigro, G., Rossi, R., Commere, P.-H., Jay, P., and Sansonetti, P.J. (2014). The cytosolic bacterial peptidoglycan sensor Nod2 affords stem cell protection and links microbes to gut epithelial regeneration. *Cell host & microbe* *15*, 792-798.
28. Rosenstiel, P., Fantini, M., Bräutigam, K., Kühbacher, T., Waetzig, G.H., Seegert, D., and Schreiber, S. (2003). TNF- α and IFN- γ regulate the expression of the NOD2 (CARD15) gene in human intestinal epithelial cells. *Gastroenterology* *124*, 1001-1009.
29. Wang, T.-T., Dabbas, B., Laperriere, D., Bitton, A.J., Soualhine, H., Tavera-Mendoza, L.E., Dionne, S., Servant, M.J., Bitton, A., and Seidman, E.G. (2010). Direct and indirect induction by 1, 25-dihydroxyvitamin D3 of the NOD2/CARD15-defensin β 2 innate immune pathway defective in Crohn disease. *Journal of Biological Chemistry* *285*, 2227-2231.
30. Leung, C.H., Lam, W., Ma, D.L., Gullen, E.A., and Cheng, Y.C. (2009). Butyrate mediates nucleotide-binding and oligomerisation domain (NOD) 2-dependent mucosal immune responses against peptidoglycan. *European journal of immunology* *39*, 3529-3537.
31. TAKAHASHI, Y., ISUZUGAWA, K., MURASE, Y., IMAI, M., YAMAMOTO, S., IIZUKA, M., AKIRA, S., BAHR, G.M., MOMOTANI, E.-i., and HORI, M. (2006). Up-regulation of NOD1 and NOD2 through TLR4 and TNF- α in LPS-treated murine macrophages. *Journal of veterinary medical science* *68*, 471-478.

32. Kim, Y.-G., Park, J.-H., Reimer, T., Baker, D.P., Kawai, T., Kumar, H., Akira, S., Wobus, C., and Núñez, G. (2011). Viral infection augments Nod1/2 signaling to potentiate lethality associated with secondary bacterial infections. *Cell host & microbe* 9, 496-507.
33. Philpott, D.J., and Girardin, S.E. (2010). Nod-like receptors: sentinels at host membranes. *Current opinion in immunology* 22, 428-434.
34. Lipinski, S., Grabe, N., Jacobs, G., Billmann-Born, S., Till, A., Häsler, R., Aden, K., Paulsen, M., Arlt, A., and Kraemer, L. (2012). RNAi screening identifies mediators of NOD2 signaling: implications for spatial specificity of MDP recognition. *Proceedings of the National Academy of Sciences* 109, 21426-21431.
35. Stenzel, N., Fetzer, C.P., Heumann, R., and Erdmann, K.S. (2009). PDZ-domain-directed basolateral targeting of the peripheral membrane protein FRMPD2 in epithelial cells. *Journal of cell science* 122, 3374-3384.
36. McDonald, C., Chen, F.F., Ollendorff, V., Ogura, Y., Marchetto, S., Lécine, P., Borg, J.-P., and Nuñez, G. (2005). A role for Erbin in the regulation of Nod2-dependent NF- κ B signaling. *Journal of Biological Chemistry* 280, 40301-40309.
37. Lee, J., Tattoli, I., Wojtal, K.A., Vavricka, S.R., Philpott, D.J., and Girardin, S.E. (2009). pH-dependent internalization of muramyl peptides from early endosomes enables Nod1 and Nod2 signaling. *Journal of Biological Chemistry* 284, 23818-23829.
38. Thay, B., Damm, A., Kufer, T.A., Wai, S.N., and Oscarsson, J. (2014). *Aggregatibacter actinomycetemcomitans* outer membrane vesicles are internalized in human host cells and trigger NOD1- and NOD2-dependent NF- κ B activation. *Infection and immunity* 82, 4034-4046.
39. Nakamura, N., Lill, J.R., Phung, Q., Jiang, Z., Bakalarski, C., de Maziere, A., Klumperman, J., Schlatter, M., Delamarre, L., and Mellman, I. (2014). Endosomes are specialized platforms for bacterial sensing and NOD2 signalling. *Nature* 509, 240.
40. Vavricka, S.R., Musch, M.W., Chang, J.E., Nakagawa, Y., Phanvijhitsiri, K., Waypa, T.S., Merlin, D., Schneewind, O., and Chang, E.B. (2004). hPepT1 transports muramyl dipeptide, activating NF- κ B and stimulating IL-8 secretion in human colonic Caco2/bbe cells. *Gastroenterology* 127, 1401-1409.
41. Al Nabhani, Z., Dietrich, G., Hugot, J.-P., and Barreau, F. (2017). Nod2: The intestinal gate keeper. *PLoS pathogens* 13, e1006177.
42. Hasegawa, M., Fujimoto, Y., Lucas, P.C., Nakano, H., Fukase, K., Núñez, G., and Inohara, N. (2008). A critical role of RICK/RIP2 polyubiquitination in Nod-induced NF- κ B activation. *The EMBO journal* 27, 373-383.
43. Yang, Y., Yin, C., Pandey, A., Abbott, D., Sasseti, C., and Kelliher, M.A. (2007). NOD2 pathway activation by MDP or Mycobacterium tuberculosis infection involves the stable polyubiquitination of Rip2. *Journal of Biological Chemistry* 282, 36223-36229.
44. Tigno-Aranjuez, J.T., Asara, J.M., and Abbott, D.W. (2010). Inhibition of RIP2's tyrosine kinase activity limits NOD2-driven cytokine responses. *Genes & development* 24, 2666-2677.
45. Bertrand, M.J., Doiron, K., Labbé, K., Korneluk, R.G., Barker, P.A., and Saleh, M. (2009). Cellular inhibitors of apoptosis cIAP1 and cIAP2 are required for innate immunity signaling by the pattern recognition receptors NOD1 and NOD2. *Immunity* 30, 789-801.
46. Tao, M., Scacheri, P.C., Marinis, J.M., Harhaj, E.W., Matesic, L.E., and Abbott, D.W. (2009). ITC1 K63-ubiquitinates the NOD2 binding protein, RIP2, to influence inflammatory signaling pathways. *Current Biology* 19, 1255-1263.
47. Yang, S., Wang, B., Humphries, F., Jackson, R., Healy, M.E., Bergin, R., Aviello, G., Hall, B., McNamara, D., and Darby, T. (2013). Pellino3 ubiquitinates RIP2 and

- mediates Nod2-induced signaling and protective effects in colitis. *Nature immunology* *14*, 927.
48. Damgaard, R.B., Nachbur, U., Yabal, M., Wong, W.W.-L., Fiil, B.K., Kastirr, M., Rieser, E., Rickard, J.A., Bankovacki, A., and Peschel, C. (2012). The ubiquitin ligase XIAP recruits LUBAC for NOD2 signaling in inflammation and innate immunity. *Molecular cell* *46*, 746-758.
 49. Inohara, N., Koseki, T., Lin, J., Del Peso, L., Lucas, P.C., Chen, F.F., Ogura, Y., and Núñez, G. (2000). An induced proximity model for NF- κ B activation in the Nod1/RICK and RIP signaling pathways. *Journal of Biological Chemistry* *275*, 27823-27831.
 50. Zhong, Y., Kinio, A., and Saleh, M. (2013). Functions of NOD-like receptors in human diseases. *Frontiers in immunology* *4*, 333.
 51. Kim, Y.-G., Park, J.-H., Daignault, S., Fukase, K., and Núñez, G. (2008). Cross-tolerization between Nod1 and Nod2 signaling results in reduced refractoriness to bacterial infection in Nod2-deficient macrophages. *The Journal of Immunology* *181*, 4340-4346.
 52. Lee, K.-H., Biswas, A., Liu, Y.-J., and Kobayashi, K.S. (2012). Proteasomal degradation of Nod2 protein mediates tolerance to bacterial cell wall components. *Journal of Biological Chemistry* *287*, 39800-39811.
 53. Travassos, L.H., Carneiro, L.A., Ramjeet, M., Hussey, S., Kim, Y.-G., Magalhães, J.G., Yuan, L., Soares, F., Chea, E., and Le Bourhis, L. (2010). Nod1 and Nod2 direct autophagy by recruiting ATG16L1 to the plasma membrane at the site of bacterial entry. *Nature immunology* *11*, 55.
 54. Meinzer, U., Barreau, F., Esmiol-Welterlin, S., Jung, C., Villard, C., Léger, T., Ben-Mkaddem, S., Berrebi, D., Dussillant, M., and Alnabhani, Z. (2012). *Yersinia pseudotuberculosis* effector YopJ subverts the Nod2/RICK/TAK1 pathway and activates caspase-1 to induce intestinal barrier dysfunction. *Cell host & microbe* *11*, 337-351.
 55. Mizushima, N., Levine, B., Cuervo, A.M., and Klionsky, D.J. (2008). Autophagy fights disease through cellular self-digestion. *Nature* *451*, 1069.
 56. Levine, B., and Kroemer, G. (2008). Autophagy in the pathogenesis of disease. *Cell* *132*, 27-42.
 57. Van de Veerdonk, F.L., Netea, M.G., Dinarello, C.A., and Joosten, L.A. (2011). Inflammasome activation and IL-1 β and IL-18 processing during infection. *Trends in immunology* *32*, 110-116.
 58. Netea, M., Ferwerda, G., De Jong, D., Girardin, S., Kullberg, B., and van der Meer, J. (2005). NOD2 3020insC mutation and the pathogenesis of Crohn's disease: impaired IL-1 β production points to a loss-of-function phenotype.
 59. Ferwerda, G., Kramer, M., de Jong, D., Piccini, A., Joosten, L.A., DevesaGiner, I., Girardin, S.E., Adema, G.J., van der Meer, J.W., and Kullberg, B.J. (2008). Engagement of NOD2 has a dual effect on proIL-1 β mRNA transcription and secretion of bioactive IL-1 β . *European journal of immunology* *38*, 184-191.
 60. Hsu, L.-C., Ali, S.R., McGillivray, S., Tseng, P.-H., Mariathasan, S., Humke, E.W., Eckmann, L., Powell, J.J., Nizet, V., and Dixit, V.M. (2008). A NOD2–NALP1 complex mediates caspase-1-dependent IL-1 β secretion in response to *Bacillus anthracis* infection and muramyl dipeptide. *Proceedings of the National Academy of Sciences* *105*, 7803-7808.
 61. Keestra-Gounder, A.M., and Tsohis, R.M. (2017). NOD1 and NOD2: beyond peptidoglycan sensing. *Trends in immunology* *38*, 758-767.

62. Sabbah, A., Harnack, R., Frohlich, V., Tominaga, K., Dube, P.H., Xiang, Y., and Bose, S. (2009). Activation of innate immune antiviral responses by Nod2. *Nature immunology* *10*, 1073.
63. Finney, C.A., Lu, Z., LeBourhis, L., Philpott, D.J., and Kain, K.C. (2009). Disruption of Nod-like receptors alters inflammatory response to infection but does not confer protection in experimental cerebral malaria. *The American journal of tropical medicine and hygiene* *80*, 718-722.
64. Keestra-Gounder, A.M., Byndloss, M.X., Seyffert, N., Young, B.M., Chávez-Arroyo, A., Tsai, A.Y., Cevallos, S.A., Winter, M.G., Pham, O.H., and Tiffany, C.R. (2016). NOD1 and NOD2 signalling links ER stress with inflammation. *Nature* *532*, 394.
65. Schwarz, D.S., and Blower, M.D. (2016). The endoplasmic reticulum: structure, function and response to cellular signaling. *Cellular and Molecular Life Sciences* *73*, 79-94.
66. Hetz, C. (2012). The unfolded protein response: controlling cell fate decisions under ER stress and beyond. *Nature reviews Molecular cell biology* *13*, 89.
67. Caruso, R., and Núñez, G. (2016). Innate immunity: ER stress recruits NOD1 and NOD2 for delivery of inflammation. *Current biology* *26*, R508-R511.
68. Liu, J., Qian, C., and Cao, X. (2016). Post-translational modification control of innate immunity. *Immunity* *45*, 15-30.
69. Bist, P., Cheong, W.S., Ng, A., Dikshit, N., Kim, B.-H., Pulloor, N.K., Khameneh, H.J., Hedl, M., Shenoy, A.R., and Balamuralidhar, V. (2017). E3 Ubiquitin ligase ZNRF4 negatively regulates NOD2 signalling and induces tolerance to MDP. *Nature communications* *8*, 15865.
70. Ver Heul, A.M., Fowler, C.A., Ramaswamy, S., and Piper, R.C. (2013). Ubiquitin regulates caspase recruitment domain-mediated signaling by nucleotide-binding oligomerization domain-containing proteins NOD1 and NOD2. *Journal of Biological Chemistry* *288*, 6890-6902.
71. Magalhaes, J.G., Philpott, D.J., Nahori, M.A., Jéhanno, M., Fritz, J., Bourhis, L., Viala, J., Hugot, J.P., Giovannini, M., and Bertin, J. (2005). Murine Nod1 but not its human orthologue mediates innate immune detection of tracheal cytotoxin. *EMBO reports* *6*, 1201-1207.
72. Stevens, C., Henderson, P., Nimmo, E.R., Soares, D.C., Dogan, B., Simpson, K.W., Barrett, J.C., Wilson, D.C., Satsangi, J., and Consortium, I.I.B.D.G. (2013). The intermediate filament protein, vimentin, is a regulator of NOD2 activity. *Gut* *62*, 695-707.
73. Kalla, R., Ventham, N., Kennedy, N., Quintana, J., Nimmo, E., Buck, A., and Satsangi, J. (2015). MicroRNAs: new players in IBD. *Gut* *64*, 504-513.
74. Cao, B., Zhou, X., Ma, J., Zhou, W., Yang, W., Fan, D., and Hong, L. (2017). Role of MiRNAs in inflammatory bowel disease. *Digestive diseases and sciences* *62*, 1426-1438.
75. Pierdomenico, M., Cesi, V., Cucchiara, S., Vitali, R., Prete, E., Costanzo, M., Aloï, M., Oliva, S., and Stronati, L. (2016). NOD2 is regulated by Mir-320 in physiological conditions but this control is altered in inflamed tissues of patients with inflammatory bowel disease. *Inflammatory bowel diseases* *22*, 315-326.
76. Sartor, R.B. (2006). Mechanisms of disease: pathogenesis of Crohn's disease and ulcerative colitis. *Nature Reviews Gastroenterology & Hepatology* *3*, 390.
77. Xavier, R., and Podolsky, D. (2007). Unravelling the pathogenesis of inflammatory bowel disease. *Nature* *448*, 427.
78. Fakhoury, M., Negrulj, R., Mooranian, A., and Al-Salami, H. (2014). Inflammatory bowel disease: clinical aspects and treatments. *Journal of inflammation research* *7*, 113.

79. Khor, B., Gardet, A., and Xavier, R.J. (2011). Genetics and pathogenesis of inflammatory bowel disease. *Nature* *474*, 307.
80. Hugot, J.-P., Chamaillard, M., Zouali, H., Lesage, S., Cézard, J.-P., Belaiche, J., Almer, S., Tysk, C., O'Morain, C.A., and Gassull, M. (2001). Association of NOD2 leucine-rich repeat variants with susceptibility to Crohn's disease. *Nature* *411*, 599.
81. Ogura, Y., Bonen, D.K., Inohara, N., Nicolae, D.L., Chen, F.F., Ramos, R., Britton, H., Moran, T., Karaliuskas, R., and Duerr, R.H. (2001). A frameshift mutation in NOD2 associated with susceptibility to Crohn's disease. *Nature* *411*, 603.
82. Negroni, A., Pierdomenico, M., Cucchiara, S., and Stronati, L. (2018). NOD2 and inflammation: current insights. *Journal of inflammation research* *11*, 49.
83. Lesage, S., Zouali, H., Cézard, J.-P., Colombel, J.-F., Belaiche, J., Almer, S., Tysk, C., O'Morain, C., Gassull, M., and Binder, V. (2002). CARD15/NOD2 mutational analysis and genotype-phenotype correlation in 612 patients with inflammatory bowel disease. *The American Journal of Human Genetics* *70*, 845-857.
84. Glas, J., Seiderer, J., Tillack, C., Pfennig, S., Beigel, F., Jürgens, M., Olszak, T., Laubender, R.P., Weidinger, M., and Müller-Myhsok, B. (2010). The NOD2 single nucleotide polymorphisms rs2066843 and rs2076756 are novel and common Crohn's disease susceptibility gene variants. *PloS one* *5*.
85. Tukel, T., Present, D., Rachmilewitz, D., Mayer, L., Grant, D., Risch, N., Shalata, A., and Desnick, R.J. (2004). Crohn disease: frequency and nature of CARD15 mutations in Ashkenazi and Sephardi/Oriental Jewish families. *The American Journal of Human Genetics* *74*, 623-636.
86. Hampe, J., Cuthbert, A., Croucher, P.J., Mirza, M.M., Mascheretti, S., Fisher, S., Frenzel, H., King, K., Hasselmeyer, A., and MacPherson, A.J. (2001). Association between insertion mutation in NOD2 gene and Crohn's disease in German and British populations. *The Lancet* *357*, 1925-1928.
87. Hugot, J.-P., Zaccaria, I., Cavanaugh, J., Yang, H., Vermeire, S., Lappalainen, M., Schreiber, S., Annese, V., Jewell, D.P., and Fowler, E.V. (2007). Prevalence of CARD15/NOD2 mutations in Caucasian healthy people. *The American journal of gastroenterology* *102*, 1259.
88. van Heel, D.A., Ghosh, S., Butler, M., Hunt, K.A., Lundberg, A.M., Ahmad, T., McGovern, D.P., Onnie, C., Negoro, K., and Goldthorpe, S. (2005). Muramyl dipeptide and toll-like receptor sensitivity in NOD2-associated Crohn's disease. *The Lancet* *365*, 1794-1796.
89. Wehkamp, J., Harder, J., Weichenthal, M., Schwab, M., Schäffeler, E., Schlee, M., Herrlinger, K., Stallmach, A., Noack, F., and Fritz, P. (2004). NOD2 (CARD15) mutations in Crohn's disease are associated with diminished mucosal α -defensin expression. *Gut* *53*, 1658-1664.
90. Homer, C.R., Richmond, A.L., Rebert, N.A., Achkar, J.P., and McDonald, C. (2010). ATG16L1 and NOD2 interact in an autophagy-dependent antibacterial pathway implicated in Crohn's disease pathogenesis. *Gastroenterology* *139*, 1630-1641. e1632.
91. Kobayashi, K.S., Chamaillard, M., Ogura, Y., Henegariu, O., Inohara, N., Nunez, G., and Flavell, R.A. (2005). Nod2-dependent regulation of innate and adaptive immunity in the intestinal tract. *Science* *307*, 731-734.
92. Petnicki-Ocwieja, T., Hrnčir, T., Liu, Y.-J., Biswas, A., Hudcovic, T., Tlaskalova-Hogenova, H., and Kobayashi, K.S. (2009). Nod2 is required for the regulation of commensal microbiota in the intestine. *Proceedings of the National Academy of Sciences* *106*, 15813-15818.
93. Rehman, A., Sina, C., Gavrilova, O., Häsler, R., Ott, S., Baines, J.F., Schreiber, S., and Rosenstiel, P. (2011). Nod2 is essential for temporal development of intestinal microbial communities. *Gut* *60*, 1354-1362.

94. Robertson, S.J., Zhou, J.Y., Geddes, K., Rubino, S.J., Cho, J.H., Girardin, S.E., and Philpott, D.J. (2013). Nod1 and Nod2 signaling does not alter the composition of intestinal bacterial communities at homeostasis. *Gut microbes* 4, 222-231.
95. Shanahan, M.T., Carroll, I.M., Grossniklaus, E., White, A., von Furstenberg, R.J., Barner, R., Fodor, A.A., Henning, S.J., Sartor, R.B., and Gulati, A.S. (2014). Mouse Paneth cell antimicrobial function is independent of Nod2. *Gut* 63, 903-910.
96. Watanabe, T., Kitani, A., Murray, P.J., and Strober, W. (2004). NOD2 is a negative regulator of Toll-like receptor 2-mediated T helper type 1 responses. *Nature immunology* 5, 800.
97. Watanabe, T., Kitani, A., Murray, P.J., Wakatsuki, Y., Fuss, I.J., and Strober, W. (2006). Nucleotide binding oligomerization domain 2 deficiency leads to dysregulated TLR2 signaling and induction of antigen-specific colitis. *Immunity* 25, 473-485.
98. Kramer, M., Netea, M.G., De Jong, D.J., Kullberg, B.J., and Adema, G.J. (2006). Impaired dendritic cell function in Crohn's disease patients with NOD2 3020insC mutation. *Journal of leukocyte biology* 79, 860-866.
99. Salucci, V., Rimoldi, M., Penati, C., Sampietro, G.M., Van Duist, M.M., Matteoli, G., Saibeni, S., Vecchi, M., Ardizzone, S., and Porro, G.B. (2008). Monocyte-derived dendritic cells from Crohn patients show differential NOD2/CARD15-dependent immune responses to bacteria. *Inflammatory bowel diseases* 14, 812-818.
100. Philip Smith, J.S., Pearson, R., Holway, N., Shaxted, M., Butler, M., Clark, N., Jamontt, J., Watson, R.P., Sanmugalingam, D., and Parkinson, S.J. (2012). Host genetics and environmental factors regulate ecological succession of the mouse colon tissue-associated microbiota. *PloS one* 7.
101. Miceli-Richard, C., Lesage, S., Rybojad, M., Prieur, A.-M., Manouvrier-Hanu, S., Häfner, R., Chamaillard, M., Zouali, H., Thomas, G., and Hugot, J.-P. (2001). CARD15 mutations in Blau syndrome. *Nature genetics* 29, 19.
102. Weidinger, S., Klopp, N., Rümmler, L., Wagenpfeil, S., Baurecht, H., Gauger, A., Darsow, U., Jakob, T., Novak, N., and Schäfer, T. (2005). Association of CARD15 polymorphisms with atopy-related traits in a population-based cohort of Caucasian adults. *Clinical & Experimental Allergy* 35, 866-872.
103. Kabesch, M., Peters, W., Carr, D., Leupold, W., Weiland, S.K., and von Mutius, E. (2003). Association between polymorphisms in caspase recruitment domain containing protein 15 and allergy in two German populations. *Journal of allergy and clinical immunology* 111, 813-817.
104. Daley, D., Lemire, M., Akhabir, L., Chan-Yeung, M., He, J.Q., McDonald, T., Sandford, A., Stefanowicz, D., Tripp, B., and Zamar, D. (2009). Analyses of associations with asthma in four asthma population samples from Canada and Australia. *Human genetics* 125, 445-459.
105. De Jager, P.L., Graham, R., Farwell, L., Sawcer, S., Richardson, A., Behrens, T., Compston, A., Hafler, D., Kere, J., and Vyse, T.J. (2006). The role of inflammatory bowel disease susceptibility loci in multiple sclerosis and systemic lupus erythematosus. *Genes & Immunity* 7, 327-334.
106. Laukens, D., Peeters, H., Marichal, D., Vander Cruyssen, B., Mielants, H., Elewaut, D., Demetter, P., Cuvelier, C., Van Den Berghe, M., and Rottiers, P. (2005). CARD15 gene polymorphisms in patients with spondyloarthropathies identify a specific phenotype previously related to Crohn's disease. *Annals of the rheumatic diseases* 64, 930-935.
107. Peeters, H., Vander Cruyssen, B., Laukens, D., Coucke, P., Marichal, D., Van Den Berghe, M., Cuvelier, C., Remaut, E., Mielants, H., and De Keyser, F. (2004). Radiological sacroiliitis, a hallmark of spondylitis, is linked with CARD15 gene

- polymorphisms in patients with Crohn's disease. *Annals of the rheumatic diseases* 63, 1131-1134.
108. Kanazawa, N., Okafuji, I., Kambe, N., Nishikomori, R., Nakata-Hizume, M., Nagai, S., Fuji, A., Yuasa, T., Manki, A., and Sakurai, Y. (2005). Early-onset sarcoidosis and CARD15 mutations with constitutive nuclear factor- κ B activation: common genetic etiology with Blau syndrome. *Blood* 105, 1195-1197.
 109. Chamailard, M., Philpott, D., Girardin, S.E., Zouali, H., Lesage, S., Chareyre, F., Giovannini, M., Zaehring, U., Penard-Lacronique, V., and Sansonetti, P.J. (2003). Gene-environment interaction modulated by allelic heterogeneity in inflammatory diseases. *Proceedings of the National Academy of Sciences* 100, 3455-3460.
 110. Couturier-Maillard, A., Secher, T., Rehman, A., Normand, S., De Arcangelis, A., Haesler, R., Huot, L., Grandjean, T., Bressenot, A., and Delanoye-Crespin, A. (2013). NOD2-mediated dysbiosis predisposes mice to transmissible colitis and colorectal cancer. *The Journal of clinical investigation* 123.
 111. Companioni, O., Bonet, C., Muñoz, X., Weiderpass, E., Panico, S., Tumino, R., Palli, D., Agnoli, C., Vineis, P., and Boutron-Ruault, M.C. (2014). Polymorphisms of *Helicobacter pylori* signaling pathway genes and gastric cancer risk in the European prospective investigation into cancer-eurgast cohort. *International journal of cancer* 134, 92-101.
 112. Rosenstiel, P., Hellmig, S., Hampe, J., Ott, S., Till, A., Fischbach, W., Sahly, H., Lucius, R., Fölsch, U.R., and Philpott, D. (2006). Influence of polymorphisms in the NOD1/CARD4 and NOD2/CARD15 genes on the clinical outcome of *Helicobacter pylori* infection. *Cellular microbiology* 8, 1188-1198.
 113. Xia, D., Tang, W.K., and Ye, Y. (2016). Structure and function of the AAA+ ATPase p97/Cdc48p. *Gene* 583, 64-77.
 114. DeLaBarre, B., and Brunger, A.T. (2003). Complete structure of p97/valosin-containing protein reveals communication between nucleotide domains. *Nature Structural & Molecular Biology* 10, 856.
 115. Erzberger, J.P., and Berger, J.M. (2006). Evolutionary relationships and structural mechanisms of AAA+ proteins. *Annu. Rev. Biophys. Biomol. Struct.* 35, 93-114.
 116. DeLaBarre, B., and Brunger, A.T. (2005). Nucleotide dependent motion and mechanism of action of p97/VCP. *Journal of molecular biology* 347, 437-452.
 117. Rouiller, I., DeLaBarre, B., May, A.P., Weis, W.I., Brunger, A.T., Milligan, R.A., and Wilson-Kubalek, E.M. (2002). Conformational changes of the multifunction p97 AAA ATPase during its ATPase cycle. *Nature Structural & Molecular Biology* 9, 950.
 118. Acharya, U., Jacobs, R., Peters, J.-M., Watson, N., Farquhar, M.G., and Malhotra, V. (1995). The formation of Golgi stacks from vesiculated Golgi membranes requires two distinct fusion events. *Cell* 82, 895-904.
 119. Latterich, M., Fröhlich, K.-U., and Schekman, R. (1995). Membrane fusion and the cell cycle: Cdc48p participates in the fusion of ER membranes. *Cell* 82, 885-893.
 120. Rabouille, C., Levine, T.P., Peters, J.-M., and Warren, G. (1995). An NSF-like ATPase, p97, and NSF mediate cisternal regrowth from mitotic Golgi fragments. *Cell* 82, 905-914.
 121. Guo, X., Sun, X., Hu, D., Wang, Y.-J., Fujioka, H., Vyas, R., Chakrapani, S., Joshi, A.U., Luo, Y., and Mochly-Rosen, D. (2016). VCP recruitment to mitochondria causes mitophagy impairment and neurodegeneration in models of Huntington's disease. *Nature communications* 7, 12646.
 122. Madeo, F., Schlauer, J., Zischka, H., Mecke, D., and Frohlich, K.-U. (1998). Tyrosine phosphorylation regulates cell cycle-dependent nuclear localization of Cdc48p. *Molecular biology of the cell* 9, 131-141.

123. Meyer, H., and Weihl, C.C. (2014). The VCP/p97 system at a glance: connecting cellular function to disease pathogenesis. (The Company of Biologists Ltd).
124. Buchberger, A., Schindelin, H., and Hänzelmann, P. (2015). Control of p97 function by cofactor binding. *FEBS letters* 589, 2578-2589.
125. Yeung, H.O., Klopsteck, P., Niwa, H., Isaacson, R.L., Matthews, S., Zhang, X., and Freemont, P.S. (2008). Insights into adaptor binding to the AAA protein p97. (Portland Press Ltd.).
126. Ye, Y., Tang, W.K., Zhang, T., and Xia, D. (2017). A mighty “protein extractor” of the cell: structure and function of the p97/CDC48 ATPase. *Frontiers in molecular biosciences* 4, 39.
127. Meyer, H., Bug, M., and Bremer, S. (2012). Emerging functions of the VCP/p97 AAA-ATPase in the ubiquitin system. *Nature cell biology* 14, 117.
128. Ju, J.-S., and Weihl, C.C. (2010). p97/VCP at the intersection of the autophagy and the ubiquitin proteasome system. *Autophagy* 6, 283-285.
129. Tresse, E., Salomons, F.A., Vesa, J., Bott, L.C., Kimonis, V., Yao, T.-P., Dantuma, N.P., and Taylor, J.P. (2010). VCP/p97 is essential for maturation of ubiquitin-containing autophagosomes and this function is impaired by mutations that cause IBMPFD. *Autophagy* 6, 217-227.
130. Shirogane, T., Fukada, T., Muller, J.M., Shima, D.T., Hibi, M., and Hirano, T. (1999). Synergistic roles for Pim-1 and c-Myc in STAT3-mediated cell cycle progression and antiapoptosis. *Immunity* 11, 709-719.
131. Braun, R.J., and Zischka, H. (2008). Mechanisms of Cdc48/VCP-mediated cell death—from yeast apoptosis to human disease. *Biochimica et Biophysica Acta (BBA)-Molecular Cell Research* 1783, 1418-1435.
132. Vaz, B., Halder, S., and Ramadan, K. (2013). Role of p97/VCP (Cdc48) in genome stability. *Frontiers in genetics* 4, 60.
133. Ramanathan, H.N., and Ye, Y. (2012). The p97 ATPase associates with EEA1 to regulate the size of early endosomes. *Cell research* 22, 346.
134. Pleasure, I.T., Black, M.M., and Keen, J.H. (1993). Valosin-containing protein, VCP, is a ubiquitous clathrin-binding protein. *Nature* 365, 459.
135. Li, J.-M., Wu, H., Zhang, W., Blackburn, M.R., and Jin, J. (2014). The p97-UFD1L-NPL4 protein complex mediates cytokine-induced I κ B α proteolysis. *Molecular and cellular biology* 34, 335-347.
136. Alexandru, G., Graumann, J., Smith, G.T., Kolawa, N.J., Fang, R., and Deshaies, R.J. (2008). UBXD7 binds multiple ubiquitin ligases and implicates p97 in HIF1 α turnover. *Cell* 134, 804-816.
137. Yılmaz, Z.B., Kofahl, B., Beaudette, P., Baum, K., Ipenberg, I., Weih, F., Wolf, J., Dittmar, G., and Scheidereit, C. (2014). Quantitative dissection and modeling of the NF- κ B p100-p105 module reveals interdependent precursor proteolysis. *Cell reports* 9, 1756-1769.
138. Zhang, Z., Wang, Y., Li, C., Shi, Z., Hao, Q., Wang, W., Song, X., Zhao, Y., Jiao, S., and Zhou, Z. (2015). The transitional endoplasmic reticulum ATPase p97 regulates the alternative nuclear factor NF- κ B signaling via partial degradation of the NF- κ B subunit p100. *Journal of Biological Chemistry* 290, 19558-19568.
139. Ju, J.-S., Fuentealba, R.A., Miller, S.E., Jackson, E., Piwnica-Worms, D., Baloh, R.H., and Weihl, C.C. (2009). Valosin-containing protein (VCP) is required for autophagy and is disrupted in VCP disease. *The Journal of cell biology* 187, 875-888.
140. Badadani, M., Nalbandian, A., Watts, G.D., Vesa, J., Kitazawa, M., Su, H., Tanaja, J., Dec, E., Wallace, D.C., and Mukherjee, J. (2010). VCP associated inclusion body myopathy and paget disease of bone knock-in mouse model exhibits tissue pathology typical of human disease. *PloS one* 5, e13183.

141. Custer, S.K., Neumann, M., Lu, H., Wright, A.C., and Taylor, J.P. (2010). Transgenic mice expressing mutant forms VCP/p97 recapitulate the full spectrum of IBMPFD including degeneration in muscle, brain and bone. *Human molecular genetics* *19*, 1741-1755.
142. Krick, R., Bremer, S., Welter, E., Schlotterhose, P., Muehe, Y., Eskelinen, E.-L., and Thumm, M. (2010). Cdc48/p97 and Shp1/p47 regulate autophagosome biogenesis in concert with ubiquitin-like Atg8. *The Journal of cell biology* *190*, 965-973.
143. Müller, J., Deinhardt, K., Rosewell, I., Warren, G., and Shima, D. (2007). Targeted deletion of p97 (VCP/CDC48) in mouse results in early embryonic lethality. *Biochemical and biophysical research communications* *354*, 459-465.
144. Watts, G.D., Wymer, J., Kovach, M.J., Mehta, S.G., Mumm, S., Darvish, D., Pestronk, A., Whyte, M.P., and Kimonis, V.E. (2004). Inclusion body myopathy associated with Paget disease of bone and frontotemporal dementia is caused by mutant valosin-containing protein. *Nature genetics* *36*, 377.
145. Johnson, J.O., Mandrioli, J., Benatar, M., Abramzon, Y., Van Deerlin, V.M., Trojanowski, J.Q., Gibbs, J.R., Brunetti, M., Gronka, S., and Wu, J. (2010). Exome sequencing reveals VCP mutations as a cause of familial ALS. *Neuron* *68*, 857-864.
146. Asai, T., Tomita, Y., Nakatsuka, S.i., Hoshida, Y., Myoui, A., Yoshikawa, H., and Aozasa, K. (2002). VCP (p97) regulates NFκB signaling pathway, which is important for metastasis of osteosarcoma cell line. *Japanese journal of cancer research* *93*, 296-304.
147. Kaistha, B., Schimanski, S., Gress, T., and Buchholz, M. (2017). VCP/p97 is upregulated in pancreatic cancer and promotes proliferation and cell cycle progression in cancer cells. *Zeitschrift für Gastroenterologie* *55*, KV 182.
148. Fu, Q., Jiang, Y., Zhang, D., Liu, X., Guo, J., and Zhao, J. (2016). Valosin-containing protein (VCP) promotes the growth, invasion, and metastasis of colorectal cancer through activation of STAT3 signaling. *Molecular and cellular biochemistry* *418*, 189-198.
149. Yamamoto, S., Tomita, Y., Uruno, T., Hoshida, Y., Qiu, Y., Iizuka, N., Nakamichi, I., Miyauchi, A., and Aozasa, K. (2005). Increased expression of valosin-containing protein (p97) is correlated with disease recurrence in follicular thyroid cancer. *Annals of surgical oncology* *12*, 925-934.
150. Gilquin, B., Taillebourg, E., Cherradi, N., Hubstenberger, A., Gay, O., Merle, N., Assard, N., Fauvarque, M.-O., Tomohiro, S., and Kuge, O. (2010). The AAA+ ATPase ATAD3A controls mitochondrial dynamics at the interface of the inner and outer membranes. *Molecular and cellular biology* *30*, 1984-1996.
151. Li, S., Lamarche, F., Charton, R., Delphin, C., Gires, O., Hubstenberger, A., Schlattner, U., and Rousseau, D. (2014). Expression analysis of ATAD3 isoforms in rodent and human cell lines and tissues. *Gene* *535*, 60-69.
152. Goller, T., Seibold, U.K., Kremmer, E., Voos, W., and Kolanus, W. (2013). Atad3 function is essential for early post-implantation development in the mouse. *PLoS one* *8*, e54799.
153. Hubstenberger, A., Labourdette, G., Baudier, J., and Rousseau, D. (2008). ATAD 3A and ATAD 3B are distal 1p-located genes differentially expressed in human glioma cell lines and present in vitro anti-oncogenic and chemoresistant properties. *Experimental cell research* *314*, 2870-2883.
154. Peralta, S., Goffart, S., Williams, S.L., Diaz, F., Garcia, S., Nissanka, N., Area-Gomez, E., Pohjoismäki, J., and Moraes, C.T. (2018). ATAD3 controls mitochondrial cristae structure in mouse muscle, influencing mtDNA replication and cholesterol levels. *J Cell Sci* *131*, jcs217075.

155. Snider, J., Thibault, G., and Houry, W.A. (2008). The AAA+ superfamily of functionally diverse proteins. *Genome biology* 9, 216.
156. Frickey, T., and Lupas, A.N. (2004). Phylogenetic analysis of AAA proteins. *Journal of structural biology* 146, 2-10.
157. He, J., Cooper, H., Reyes, A., Di Re, M., Sembongi, H., Litwin, T., Gao, J., Neuman, K., Fearnley, I.M., and Spinazzola, A. (2012). Mitochondrial nucleoid interacting proteins support mitochondrial protein synthesis. *Nucleic acids research* 40, 6109-6121.
158. Issop, L., Fan, J., Lee, S., Rone, M.B., Basu, K., Mui, J., and Papadopoulos, V. (2015). Mitochondria-associated membrane formation in hormone-stimulated Leydig cell steroidogenesis: role of ATAD3. *Endocrinology* 156, 334-345.
159. Rone, M.B., Midzak, A.S., Issop, L., Rammouz, G., Jagannathan, S., Fan, J., Ye, X., Blonder, J., Veenstra, T., and Papadopoulos, V. (2012). Identification of a dynamic mitochondrial protein complex driving cholesterol import, trafficking, and metabolism to steroid hormones. *Molecular endocrinology* 26, 1868-1882.
160. Harel, T., Yoon, W.H., Garone, C., Gu, S., Coban-Akdemir, Z., Eldomery, M.K., Posey, J.E., Jhangiani, S.N., Rosenfeld, J.A., and Cho, M.T. (2016). Recurrent de novo and biallelic variation of ATAD3A, encoding a mitochondrial membrane protein, results in distinct neurological syndromes. *The American Journal of Human Genetics* 99, 831-845.
161. Cooper, H.M., Yang, Y., Ylikallio, E., Khairullin, R., Woldegebriel, R., Lin, K.-L., Euro, L., Palin, E., Wolf, A., and Trokovic, R. (2017). ATPase-deficient mitochondrial inner membrane protein ATAD3A disturbs mitochondrial dynamics in dominant hereditary spastic paraplegia. *Human molecular genetics* 26, 1432-1443.
162. You, W.-C., Chiou, S.-H., Huang, C.-Y., Chiang, S.-F., Yang, C.-L., Sudhakar, J.N., Lin, T.-Y., Chiang, I.-P., Shen, C.-C., and Cheng, W.-Y. (2013). Mitochondrial protein ATPase family, AAA domain containing 3A correlates with radioresistance in glioblastoma. *Neuro-oncology* 15, 1342-1352.
163. Teng, Y., Ren, X., Li, H., Shull, A., Kim, J., and Cowell, J.K. (2016). Mitochondrial ATAD3A combines with GRP78 to regulate the WASF3 metastasis-promoting protein. *Oncogene* 35, 333.
164. Fang, H.-Y., Chang, C.-L., Hsu, S.-H., Huang, C.-Y., Chiang, S.-F., Chiou, S.-H., Huang, C.-H., Hsiao, Y.-T., Lin, T.-Y., and Chiang, I.-P. (2010). ATPase family AAA domain-containing 3A is a novel anti-apoptotic factor in lung adenocarcinoma cells. *J Cell Sci* 123, 1171-1180.
165. Chen, T.-C., Hung, Y.-C., Lin, T.-Y., Chang, H.-W., Chiang, I., Chen, Y.-Y., and Chow, K.-C. (2011). Human papillomavirus infection and expression of ATPase family AAA domain containing 3A, a novel anti-autophagy factor, in uterine cervical cancer. *International journal of molecular medicine* 28, 689-696.
166. Huang, K.-H., Chow, K.-C., Chang, H.-W., Lin, T.-Y., and Lee, M.-C. (2011). ATPase family AAA domain containing 3A is an anti-apoptotic factor and a secretion regulator of PSA in prostate cancer. *International journal of molecular medicine* 28, 9-15.
167. McKenna, A., Hanna, M., Banks, E., Sivachenko, A., Cibulskis, K., Kernytsky, A., Garimella, K., Altshuler, D., Gabriel, S., and Daly, M. (2010). The Genome Analysis Toolkit: a MapReduce framework for analyzing next-generation DNA sequencing data. *Genome research* 20, 1297-1303.
168. McLaren, W., Gil, L., Hunt, S.E., Riat, H.S., Ritchie, G.R., Thormann, A., Flicek, P., and Cunningham, F. (2016). The ensembl variant effect predictor. *Genome biology* 17, 122.

169. Lek, M., Karczewski, K., Minikel, E., Samocha, K., Banks, E., Fennell, T., O'Donnell-Luria, A., Ware, J., Hill, A., and Cummings, B. Analysis of protein-coding genetic variation in 60,706 humans. *bioRxiv*. 2015. DOI 10, 030338.
170. Karczewski, K.J., Francioli, L.C., Tiao, G., Cummings, B.B., Alföldi, J., Wang, Q., Collins, R.L., Laricchia, K.M., Ganna, A., and Birnbaum, D.P. (2019). Variation across 141,456 human exomes and genomes reveals the spectrum of loss-of-function intolerance across human protein-coding genes. *BioRxiv*, 531210.
171. Magnaghi, P., D'alessio, R., Valsasina, B., Avanzi, N., Rizzi, S., Asa, D., Gasparri, F., Cozzi, L., Cucchi, U., and Orrenius, C. (2013). Covalent and allosteric inhibitors of the ATPase VCP/p97 induce cancer cell death. *Nature chemical biology* 9, 548.
172. Tyanova, S., Temu, T., and Cox, J. (2016). The MaxQuant computational platform for mass spectrometry-based shotgun proteomics. *Nature protocols* 11, 2301.
173. Sim, N.-L., Kumar, P., Hu, J., Henikoff, S., Schneider, G., and Ng, P.C. (2012). SIFT web server: predicting effects of amino acid substitutions on proteins. *Nucleic acids research* 40, W452-W457.
174. Adzhubei, I.A., Schmidt, S., Peshkin, L., Ramensky, V.E., Gerasimova, A., Bork, P., Kondrashov, A.S., and Sunyaev, S.R. (2010). A method and server for predicting damaging missense mutations. *Nature methods* 7, 248.
175. Rohr, J., Beutel, K., Maul-Pavicic, A., Vraetz, T., Thiel, J., Warnatz, K., Bondzio, I., Gross-Wieltsch, U., Schündeln, M., and Schütz, B. (2010). Atypical familial hemophagocytic lymphohistiocytosis due to mutations in UNC13D and STXBP2 overlaps with primary immunodeficiency diseases. *Haematologica* 95, 2080-2087.
176. Griffin, J.D., Spertini, O., Ernst, T., Belvin, M., Levine, H., Kanakura, Y., and Tedder, T. (1990). Granulocyte-macrophage colony-stimulating factor and other cytokines regulate surface expression of the leukocyte adhesion molecule-1 on human neutrophils, monocytes, and their precursors. *The Journal of Immunology* 145, 576-584.
177. Spertini, O., Freedman, A., Belvin, M., Penta, A., Griffin, J., and Tedder, T. (1991). Regulation of leukocyte adhesion molecule-1 (TQ1, Leu-8) expression and shedding by normal and malignant cells. *Leukemia* 5, 300-308.
178. Zhao, L.-C., Edgar, J.B., and Dailey, M.O. (2001). Characterization of the rapid proteolytic shedding of murine L-selectin. *Journal of Immunology Research* 8, 267-277.
179. Parkhouse, R., and Monie, T.P. (2015). Dysfunctional Crohn's disease-associated NOD2 polymorphisms cannot be reliably predicted on the basis of RIPK2-binding or membrane association. *Frontiers in immunology* 6, 521.
180. Warner, N., Burberry, A., Franchi, L., Kim, Y.-G., McDonald, C., Sartor, M.A., and Nunez, G. (2013). A genome-wide siRNA screen reveals positive and negative regulators of the NOD2 and NF- κ B signaling pathways. *Sci. Signal.* 6, rs3-rs3.
181. Fiil, B.K., Damgaard, R.B., Wagner, S.A., Keusekotten, K., Fritsch, M., Bekker-Jensen, S., Mailand, N., Choudhary, C., Komander, D., and Gyrd-Hansen, M. (2013). OTULIN restricts Met1-linked ubiquitination to control innate immune signaling. *Molecular cell* 50, 818-830.
182. Wójcik, C., Rowicka, M., Kudlicki, A., Nowis, D., McConnell, E., Kujawa, M., and DeMartino, G.N. (2006). Valosin-containing protein (p97) is a regulator of endoplasmic reticulum stress and of the degradation of N-end rule and ubiquitin-fusion degradation pathway substrates in mammalian cells. *Molecular biology of the cell* 17, 4606-4618.
183. Bastola, P., Neums, L., Schoenen, F.J., and Chien, J. (2016). VCP inhibitors induce endoplasmic reticulum stress, cause cell cycle arrest, trigger caspase-mediated cell

- death and synergistically kill ovarian cancer cells in combination with Salubrinal. *Molecular oncology* *10*, 1559-1574.
184. Osowski, C.M., and Urano, F. (2011). Measuring ER stress and the unfolded protein response using mammalian tissue culture system. In *Methods in enzymology*, Volume 490. (Elsevier), pp. 71-92.
185. Grimes, C.L., Ariyananda, L.D.Z., Melnyk, J.E., and O'Shea, E.K. (2012). The innate immune protein Nod2 binds directly to MDP, a bacterial cell wall fragment. *Journal of the American Chemical Society* *134*, 13535-13537.
186. Mo, J., Boyle, J.P., Howard, C.B., Monie, T.P., Davis, B.K., and Duncan, J.A. (2012). Pathogen sensing by nucleotide-binding oligomerization domain-containing protein 2 (NOD2) is mediated by direct binding to muramyl dipeptide and ATP. *Journal of Biological Chemistry* *287*, 23057-23067.
187. Hugot, J.-P., Laurent-Puig, P., Gower-Rousseau, C., Olson, J.M., Lee, J.C., Beaugier, L., Naom, I., Dupas, J.-L., Van Gossum, A., and Orholm, M. (1996). Mapping of a susceptibility locus for Crohn's disease on chromosome 16. *Nature* *379*, 821-823.
188. Jostins, L., Ripke, S., Weersma, R.K., Duerr, R.H., McGovern, D.P., Hui, K.Y., Lee, J.C., Schumm, L.P., Sharma, Y., and Anderson, C.A. (2012). Host-microbe interactions have shaped the genetic architecture of inflammatory bowel disease. *Nature* *491*, 119-124.
189. Barreau, F., Meinzer, U., Chareyre, F., Berrebi, D., Niwa-Kawakita, M., Dussailant, M., Foligne, B., Ollendorff, V., Heyman, M., and Bonacorsi, S. (2007). CARD15/NOD2 is required for Peyer's patches homeostasis in mice. *PloS one* *2*.
190. Shimada, K., Chen, S., Dempsey, P.W., Sorrentino, R., Alsabeh, R., Slepkin, A.V., Peterson, E., Doherty, T.M., Underhill, D., and Crother, T.R. (2009). The NOD/RIP2 pathway is essential for host defenses against *Chlamydomydia pneumoniae* lung infection. *PLoS pathogens* *5*.
191. Corridoni, D., Rodriguez-Palacios, A., Di Stefano, G., Di Martino, L., Antonopoulos, D., Chang, E., Arseneau, K., Pizarro, T., and Cominelli, F. (2017). Genetic deletion of the bacterial sensor NOD2 improves murine Crohn's disease-like ileitis independent of functional dysbiosis. *Mucosal immunology* *10*, 971-982.
192. Lappalainen, M., Paavola-Sakki, P., Halme, L., Turunen, U., Färkkilä, M., Repo, H., and Kontula, K. (2008). Novel CARD15/NOD2 mutations in Finnish patients with Crohn's disease and their relation to phenotypic variation in vitro and in vivo. *Inflammatory bowel diseases* *14*, 176-185.
193. Sugimura, K., Taylor, K.D., Lin, Y.-c., Hang, T., Wang, D., Tang, Y.-M., Fischel-Ghodsian, N., Targan, S.R., Rotter, J.I., and Yang, H. (2003). A novel NOD2/CARD15 haplotype conferring risk for Crohn disease in Ashkenazi Jews. *The American Journal of Human Genetics* *72*, 509-518.
194. Cuthbert, A.P., Fisher, S.A., Mirza, M.M., King, K., Hampe, J., Croucher, P.J., Mascheretti, S., Sanderson, J., Forbes, A., and Mansfield, J. (2002). The contribution of NOD2 gene mutations to the risk and site of disease in inflammatory bowel disease. *Gastroenterology* *122*, 867-874.
195. Sugimura, M., Kinouchi, Y., Takahashi, S., Aihara, H., Takagi, S., Negoro, K., Obana, N., Kojima, Y., Matsumoto, K., and Kikuchi, T. (2003). CARD15/NOD2 mutational analysis in Japanese patients with Crohn's disease. *Clinical genetics* *63*, 160-162.
196. Inoue, N., Tamura, K., Kinouchi, Y., Fukuda, Y., Takahashi, S., Ogura, Y., Inohara, N., Núñez, G., Kishi, Y., and Koike, Y. (2002). Lack of common NOD2 variants in Japanese patients with Crohn's disease. *Gastroenterology* *123*, 86-91.
197. Miceli-Richard, C., Lesage, S., Rybojad, M., Prieur, A.-M., Manouvrier-Hanu, S., Häfner, R., Chamaillard, M., Zouali, H., Thomas, G., and Hugot, J.-P. (2001). CARD15 mutations in Blau syndrome. *Nature genetics* *29*, 19-20.

198. Yao, Q., Zhou, L., Cusumano, P., Bose, N., Piliang, M., Jayakar, B., Su, L.-C., and Shen, B. (2011). A new category of autoinflammatory disease associated with NOD2 gene mutations. *Arthritis research & therapy* *13*, R148.
199. Yao, Q., Shen, M., McDonald, C., Lacbawan, F., Moran, R., and Shen, B. (2015). NOD2-associated autoinflammatory disease: a large cohort study. *Rheumatology* *54*, 1904-1912.
200. Netea, M.G., Kullberg, B.J., De Jong, D.J., Franke, B., Sprong, T., Naber, T.H., Drenth, J.P., and Van der Meer, J.W. (2004). NOD2 mediates anti-inflammatory signals induced by TLR2 ligands: implications for Crohn's disease. *European journal of immunology* *34*, 2052-2059.
201. Ley, K., Hoffman, H.M., Kubes, P., Cassatella, M.A., Zychlinsky, A., Hedrick, C.C., and Catz, S.D. (2018). Neutrophils: New insights and open questions. *Science immunology* *3*, eaat4579.
202. Shahzad, A., Knapp, M., Lang, I., and Köhler, G. (2010). Interleukin 8 (IL-8)-a universal biomarker? *International archives of medicine* *3*, 11.
203. Cotton, J.A., Platnich, J.M., Muruve, D.A., Jijon, H.B., Buret, A.G., and Beck, P.L. (2016). Interleukin-8 in gastrointestinal inflammation and malignancy: induction and clinical consequences. *International Journal of Interferon, Cytokine and Mediator Research* *8*, 13.
204. Grimm, M., Elsbury, S., Pavli, P., and Doe, W. (1996). Interleukin 8: cells of origin in inflammatory bowel disease. *Gut* *38*, 90-98.
205. Rogler, G., Brand, K., Vogl, D., Page, S., Hofmeister, R., Andus, T., Knuechel, R., Baeuerle, P.A., Schölmerich, J., and Gross, V. (1998). Nuclear factor κ B is activated in macrophages and epithelial cells of inflamed intestinal mucosa. *Gastroenterology* *115*, 357-369.
206. Nielsen, O., Rüdiger, N., Gaustadnes, M., and Horn, T. (1997). Intestinal interleukin-8 concentration and gene expression in inflammatory bowel disease. *Scandinavian journal of gastroenterology* *32*, 1028-1034.
207. Hooper, K.M., Barlow, P.G., Henderson, P., and Stevens, C. (2019). Interactions between autophagy and the unfolded protein response: implications for inflammatory bowel disease. *Inflammatory bowel diseases* *25*, 661-671.
208. Kaser, A., Lee, A.-H., Franke, A., Glickman, J.N., Zeissig, S., Tilg, H., Nieuwenhuis, E.E., Higgins, D.E., Schreiber, S., and Glimcher, L.H. (2008). XBP1 links ER stress to intestinal inflammation and confers genetic risk for human inflammatory bowel disease. *Cell* *134*, 743-756.
209. Zheng, W., Rosenstiel, P., Huse, K., Sina, C., Valentonyte, R., Mah, N., Zeitlmann, L., Grosse, J., Ruf, N., and Nürnberg, P. (2006). Evaluation of AGR2 and AGR3 as candidate genes for inflammatory bowel disease. *Genes & Immunity* *7*, 11-18.
210. Rolhion, N., Barnich, N., Bringer, M.-A., Glasser, A.-L., Ranc, J., Hébuterne, X., Hofman, P., and Darfeuille-Michaud, A. (2010). Abnormally expressed ER stress response chaperone Gp96 in CD favours adherent-invasive Escherichia coli invasion. *Gut* *59*, 1355-1362.
211. Deuring, J.J., de Haar, C., Koelewijn, C.L., Kuipers, E.J., Peppelenbosch, M.P., and van der Woude, C.J. (2012). Absence of ABCG2-mediated mucosal detoxification in patients with active inflammatory bowel disease is due to impeded protein folding. *Biochemical Journal* *441*, 87-93.
212. Shkoda, A., Ruiz, P.A., Daniel, H., Kim, S.C., Rogler, G., Sartor, R.B., and Haller, D. (2007). Interleukin-10 blocked endoplasmic reticulum stress in intestinal epithelial cells: impact on chronic inflammation. *Gastroenterology* *132*, 190-207.

213. Thiébaud, R., Esmiol, S., Lecine, P., Mahfouz, B., Hermant, A., Nicoletti, C., Parnis, S., Perroy, J., Borg, J.-P., and Pascoe, L. (2016). Characterization and genetic analyses of new genes coding for NOD2 interacting proteins. *PloS one* *11*, e0165420.
214. Richmond, A.L., Kabi, A., Homer, C.R., Marina-García, N., Nickerson, K.P., Nesvizhskii, A.I., Sreekumar, A., Chinnaiyan, A.M., Nuñez, G., and McDonald, C. (2012). The nucleotide synthesis enzyme CAD inhibits NOD2 antibacterial function in human intestinal epithelial cells. *Gastroenterology* *142*, 1483-1492. e1486.
215. Novak, E.A., and Mollen, K.P. (2015). Mitochondrial dysfunction in inflammatory bowel disease. *Frontiers in cell and developmental biology* *3*, 62.
216. Saxena, A., Lopes, F., and McKay, D.M. (2018). Reduced intestinal epithelial mitochondrial function enhances in vitro interleukin-8 production in response to commensal *Escherichia coli*. *Inflammation Research* *67*, 829-837.
217. Saxena, A., Lopes, F., Poon, K.K., and McKay, D.M. (2017). Absence of the NOD2 protein renders epithelia more susceptible to barrier dysfunction due to mitochondrial dysfunction. *American Journal of Physiology-Gastrointestinal and Liver Physiology* *313*, G26-G38.
218. Maurya, C.K., Arha, D., Rai, A.K., Kumar, S.K., Pandey, J., Avisetti, D.R., Kalivendi, S.V., Klip, A., and Tamrakar, A.K. (2015). NOD2 activation induces oxidative stress contributing to mitochondrial dysfunction and insulin resistance in skeletal muscle cells. *Free Radical Biology and Medicine* *89*, 158-169.
219. Peralta, S., González-Quintana, A., Ybarra, M., Delmiro, A., Pérez-Pérez, R., Docampo, J., Arenas, J., Blázquez, A., Ugalde, C., and Martín, M.A. (2019). Novel ATAD3A recessive mutation associated to fatal cerebellar hypoplasia with multiorgan involvement and mitochondrial structural abnormalities. *Molecular genetics and metabolism* *128*, 452-462.
220. van den Boom, J., and Meyer, H. (2018). VCP/p97-mediated unfolding as a principle in protein homeostasis and signaling. *Molecular cell* *69*, 182-194.
221. Weichart, D., Gobom, J., Klopffleisch, S., Häslér, R., Gustavsson, N., Billmann, S., Lehrach, H., Seegert, D., Schreiber, S., and Rosenstiel, P. (2006). Analysis of NOD2-mediated proteome response to muramyl dipeptide in HEK293 cells. *Journal of Biological Chemistry* *281*, 2380-2389.
222. Kaser, A., Adolph, T.E., and Blumberg, R.S. (2013). The unfolded protein response and gastrointestinal disease. In *Seminars in immunopathology*, Volume 35. (Springer), pp. 307-319.
223. McGovern, D.P., Kugathasan, S., and Cho, J.H. (2015). Genetics of inflammatory bowel diseases. *Gastroenterology* *149*, 1163-1176. e1162.
224. Liu, T.-C., and Stappenbeck, T.S. (2016). Genetics and pathogenesis of inflammatory bowel disease. *Annual Review of Pathology: Mechanisms of Disease* *11*, 127-148.

8. List of Figures

Figure 1-1 Schematic illustration of NOD2 protein domains [17].	3
Figure 1-2 Mechanisms of bacterial recognition by NOD2 and downstream signaling.	7
Figure 1-3 NOD1/NOD2-mediated signaling.	9
Figure 1-4 VCP cellular functions.	15
Figure 3-1 Schematic representation of NOD2 cloning strategy	36
Figure 4-1 Confirmation of NOD2 and STXBP2 variants segregation in the family.	53
Figure 4-2 Immunophenotyping of B cells.	55
Figure 4-3 B cell proliferation and plasmablasts differentiation.	56
Figure 4-4 Immune phenotyping of T cells and monocytes.	57
Figure 4-5 Impaired MDP responses of patient-derived monocytes.	58
Figure 4-6 Impaired nuclear factor-κB (NF-κB) and mitogen-activated protein kinase (MAPK) signaling in patient 's primary cells upon stimulation with MDP.	59
Figure 4-7 impaired CD62L shedding on neutrophils upon MDP simulation.	60
Figure 4-8 Impaired NF-κB activation upon L18-MDP stimulation.	61
Figure 4-9 Screening NOD2 KO HCT116 cells using NF-κB luciferase reporter assay.	62
Figure 4-10 Impaired NOD2-mediated signaling upon MDP or tunicamycin stimulation.	63
Figure 4-11 Impaired RIPK2 interaction.	64
Figure 4-12 Impaired RIPK2 ubiquitination upon MDP stimulation.	65

Figure 4-13 Different pattern of protein bands in cells overexpressing WT NOD2 compared with E54K variant.	66
Figure 4-14 Identification of VCP and ATAD3A as novel NOD2 interacting proteins.....	67
Figure 4-15 Confirmation of ATAD3A Knock out in HCT116 cells.....	67
Figure 4-16 ATAD3A Knock out resulted in enhanced interleukin-8 production in HCT116 cells upon MDP stimulation.....	68
Figure 4-17 ATAD3A overexpression promoted NOD2 and RIPK2 degradation in HEK293T cells.	69
Figure 4-18 ATAD3A overexpression promoted NOD2, VCP and RASGRP1 degradation in HEK293T cells.....	70
Figure 4-19 Screening possible VCP KO clones and optimizing VCP-targeting siRNAs concentrations in HCT116 cells.	71
Figure 4-20 Impaired MDP-mediated NOD2 signaling in VCP knockdown cells.	72
Figure 4-21 Normal turn over of IκBα in VCP knockdown HCT116 cells upon MDP stimulation.	73
Figure 4-22 Evaluation of RIPK2 ubiquitination in VCP knockdown HCT116 cells upon MDP stimulation.....	74
Figure 4-23 Enhanced activation of alternative NF-κB pathway in VCP knockdown HCT116 cells upon MDP stimulation.	74
Figure 4-24 Evaluation of ER stress in VCP-silenced cells upon MDP stimulation.	75
Figure 4-25 Evaluation of ER stress in VCP-silenced NOD2 KO HCT116 cells upon MDP stimulation..	76

Figure 4-26 induced proinflammation in VCP-silenced HCT116 cells upon tunicamycin stimulation. 77

Figure 4-27 Evaluation of cell death in VCP-silenced HCT116 cells upon tunicamycin stimulation. 78

Figure 4-28 Evaluation of canonical NF- κ B pathway in VCP knockdown HCT116 cells upon tunicamycin stimulation. 79

9. List of Tables

Table 1-1 Pattern-recognition receptor Families	2
Table 3-1The list of reagents	19
Table 3-2 The list of mediums and supplements	20
Table 3-3 The list of constructs generated in this thesis	23
Table 3-4 The list of the qPCR primers	23
Table 3-5 The list of Primers used for Sanger sequencing, cloning and site directed mutagenesis.....	25
Table 3-6 the list of the siRNA and sgRNA target sequences	26
Table 3-7 The list of antibodies used for immunoblotting	27
Table 3-8 The list of antibodies used for Flow cytometry	29
Table 3-9 The list of the restriction enzymes used in this study.....	30
Table 3-10 Standard PCR program	33
Table 3-11 recommended number of cells and DNA amount for different cell culture plates	41

10. Abbreviations

°C	° Celsius
sgRNA	single guide RNA
ALRs	AIM2-like receptors
AMP	ampicillin
APCs	antigen-presenting cells
ATAD3A	ATPase family AAA-domain containing protein 3A
ATF6	Activating Transcription Factor 6
ATF6	Activating Transcription Factor 6
ATG16L1	Autophagy Related 16 Like 1
ATG5	autophagy-related protein-5
BIR	baculovirus inhibitor repeat
CARD	caspase recruitment domain
CD	Crohn's disease
CFSE	Carboxyfluorescein succinimidyl ester
CHOP	CCAAT/Enhancer-Binding Protein Homologous Protein
ciAP1	cellular inhibitor of apoptosis 1
CLRs	C-type lectin receptors
Cyt D	cytochalasin D
DAMPs	damage- associated molecular patterns
DMEM	Dulbecco's Modified Eagle Medium
dNTP	deoxyribonucleotide triphosphate
ECOVA	E. coli expressing OVA peptide
EDEM1	ER Degradation Enhancing Alpha-Mannosidase Like Protein 1

Abbreviations

EDTA	Ethylenediaminetetraacetic acid
ER	endoplasmic reticulum
ERAD	ER-associated degradation
FACS	fluorescence-activated cell sorting
FBS	fetal bovine serum
FHL	Familial haemophagocytic lymphohistiocytosis
HIF1a	Hypoxia Inducible Factor 1 Subunit Alpha
HLH	hemophagocytic lymphohystiocytosis
IBD	Inflammatory bowel diseases
IBMPFD	Inclusion body myopathy with early-onset Paget disease and frontotemporal dementia
IFNs	type I interferon
IFN γ	interferon- γ
IkB α	Nuclear Factor of Kappa Light Chain Gene Enhancer In B-Cells
<i>IL6</i>	Interleukin 6
IL-8	Interleukin 8
IMDM	Iscove's Modified Dulbecco's Medium
IRE1a	inositol-requiring enzyme 1
IRF3	interferon regulatory factor-3
KD	Kilo Dalton
KO	Knock-out
LB	Luria Broth
LPS	lipopolysaccharide
LUBAC	linear ubiquitin chain assembly complex
MAPK	mitogen activated protein kinase

Abbreviations

MAVS	mitochondrial antiviral signaling
MDP	muramyl dipeptide
MFI	mean fluorescence intensity
NALP1	NLR Family Pyrin Domain Containing 1
NBD	Nucleotide binding domain
NF- κ B	nuclear factor "kappa-light-chain-enhancer" of activated B-cells
NLRs	NOD-like receptors
NOD2	Nucleotide-binding oligomerization domain 2
OVA	ovalbumin
PAMPs	pathogen-associated molecular patterns
PBMCs	Peripheral blood mononuclear cells
PBS	Phosphate-Buffered Saline
PCR	Polymerase chain reaction
PDI	Protein Disulfide Isomerase
PEI	Polyethylenimine
PERK	PKR-like ER kinase
PGN	peptidoglycan
PRRs	Pattern recognition receptors
PYD	pyrin domain
qPCR	Quantitative PCR
RASGRP	RAS Guanyl Releasing Protein 1
RIPK2	receptor-interacting protein 2
RLRs	RIG-I-like receptors
SDS	sodium dodecyl sulfate
siRNAs	small interfering RNA

SLC15A3	solute carrier family 15 member 3
ssRNA	single-stranded RNA
STXBP2	Syntaxin Binding Protein 2
TAB1	Transforming Growth Factor Beta-Activated Kinase-Binding Protein 1
TAK1	Transforming Growth Factor-Beta-Activated Kinase 1
TBE	Tris-Borate-EDTA
TLRs	Toll-like receptors
TNF	tumor necrosis factor
TRAF2	TNF Receptor Associated Factor 2
TUBE	Tandem Ubiquitin Binding Entity
UC	ulcerative colitis
UPR	unfolded protein response
VCP	Valosin-containing protein
WT	Wild type
XBP1	X-Box Binding Protein 1
XIAP	X-linked inhibitor of apoptosis protein
ZNRF4	Zinc and Ring Finger 4
β -ME	β -mercaptoethanol